DATA-DRIVEN CONTROLLER TUNING USING THE CORRELATION APPROACH

THÈSE N^{O} 3536 (2006)

PRÉSENTÉE LE 1ER SEPTEMBRE 2006

À LA FACULTÉ SCIENCES ET TECHNIQUES DE L'INGÉNIEUR

Laboratoire d'Automatique

SECTION DE GÉNIE MÉCANIQUE

ÉCOLE POLYTECHNIQUE FÉDÉRALE DE LAUSANNE

POUR L'OBTENTION DU GRADE DE DOCTEUR ÈS SCIENCES

PAR

Ljubisa MISKOVIC

M.Sc. in Electrical Engineering, University of Belgrade, Yougoslavie
de nationalité serbe et monténégrine

acceptée sur proposition du jury:

Prof. P. Xirouchakis, président du jury
Prof. D. Bonvin, Dr A. Karimi, directeurs de thèse
Prof. M. Campi, rapporteur
Prof. M. Gevers, rapporteur
Prof. P. Vandergheynst, rapporteur

ÉCOLE POLYTECHNIQUE
FÉDÉRALE DE LAUSANNE

Lausanne, EPFL
2006

Acknowledgments

Several persons have contributed to this thesis. First and foremost I would like to mention my co-advisors Professor Dominique Bonvin and Dr Alireza Karimi who have introduced me to the subject and who have been an invaluable source of inspiration during the course of this work. Special thanks are owed to Alireza for his encouragement and insightful guidance. It was always a pleasure to discuss a variety of subjects with him. I would also like to thank my other co-author Professor Michel Gevers for interesting discussions and helpful advice.

It was an honor and pleasure to have, as the members of my Thesis Committee, Professor Paul Xirouchakis, Professor Dominique Bonvin, Dr Alireza Karimi, Professor Michel Gevers, Professor Marco Campi and Professor Pierre Vandergheynst. I am grateful to them for accepting to read and evaluate the contents of this thesis.

My gratitude also belongs to the people with whom I collaborated in the organization of the European Journal of Control benchmark problem on the design and optimization of restricted-complexity controllers: Professor Ioan-Dore Landau, Dr Alireza Karimi and Dr Hynek Prochazka. I would also like to thank my co-workers on the "Main Axes Control of the Overwhelmingly Large Telescope (OWL)" project funded by European Southern Observatory (ESO): Dr Babak Sedghi, Dr Alireza Karimi, Dr Martin Dimmler and Professor Roland Longchamp.

I would like to express my deep gratitude to Professor Jean-Claude Badoux, former EPFL President, for offering me a three-year scholarship that financed a part of my studies. The financial support for the remainder of my studies came from the Swiss National Foundation for Scientific Research, and is gratefully acknowledged.

I would like to thank Professor Roland Longhchamp, Professor Dominique Bonvin and Dr. Denis Gillet for letting me join the Laboratoire

d'Automatique. Many thanks to all the colleagues at the LA for providing an enjoyable and stimulating working atmosphere. In particular, I am grateful to the "équipe du secrétariat": Marie-Claire, Ruth, Francine, Carole, Rana and Homeira for their help on numerous occasions. My gratitude also goes to Philippe, Marc and Christophe for helping me with computer related problems. It was a real pleasure to share my office with Babak, Greg and Levente. I am grateful to them, not only for having very interesting discussions over various topics, but also for their support and patience. I would like to thank to Daniel and Benoît for correcting the "Version abrégée" of this thesis.

These acknowledgments would not be complete without thanking all the friends that made my stay in Lausanne very fun and enjoyable. Special acknowledgments go to my neighbors Boki, Jelena, Iggy, Deki and Mina for all the moments we spent together. My gratitude also goes to Ljubica, Maja, Despot, Cane, Miljan, Chantale, Ivan, Dragana, Dave, Natacha, Sergio and Barbara for their friendship and support.

I would like to thank my parents Milija and Stojanka, and my brother Nebojša and his family for their unconditional support, love and encouragement.

Most of all, my profound gratitude and love goes to my wife Bojana and my daughter Mila. I would like to thank them for all the joy and happiness they brought into my life. This thesis is dedicated to them.

Abstract

The essential ingredients of control design procedures include the acquisition of process knowledge and its efficient integration into the controller. In many practical control applications, a reliable mathematical description of the plant is difficult or impossible to obtain, and the controller has to be designed on the basis of measurements. This thesis proposes a new data-driven method labeled Correlation-based Tuning (CbT). The underlying idea is inspired by the well-known correlation approach in system identification. The controller parameters are tuned iteratively either to decorrelate the closed-loop output error between designed and achieved closed-loop systems with the external reference signal (decorrelation procedure) or to reduce this correlation (correlation reduction). Ideally, the resulting closed-loop output error contains only the contribution of the noise and perfect model-following can be achieved. By the very nature of the control design criterion, the controller parameters are asymptotically insensitive to noise.

Both theoretical and implementation aspects of CbT are treated. For the decorrelation procedure, a correlation equation is solved using the stochastic approximation method. The iterative procedure converges to the solution of the correlation equation even in the case when an approximate gradient of the closed-loop output error with respect to controller parameters is used. The asymptotic distribution of the resulting controller parameter estimates is analyzed. When perfect decorrelation is not possible, the correlation reduction method can be used. That is, instead of solving the correlation equation, the norm of a cross-correlation function is minimized. A frequency domain analysis of the criterion shows that the algorithm minimizes the two-norm of the difference between the achieved and designed closed-loop systems.With the correlation reduction method, an unbiased estimate of the gradient of the closed-loop output error is necessary to guarantee convergence of the algorithm to a local minimum of the criterion. Furthermore,

this criterion can be generalized to allow handling the mixed sensitivity specifications.

An extension of this method for the tuning of linear time-invariant multivariable controllers is proposed for both procedures. CbT allows tuning some of the elements of the controller transfer function matrix to satisfy the desired closed-loop performance, while the other elements are tuned to mutually decouple the closed-loop outputs. The tuning of all decouplers and controllers can be made by performing only one experiment per iteration regardless of the number of inputs and outputs since all reference signals can be excited simultaneously. However, due to the fact that decoupling is imposed as a design criterion, simultaneous excitation of all references brings a negative impact on the variance of the estimated controller parameters. In fact, one must choose between low experimental cost (simultaneous excitation) and better accuracy of the estimated parameters (sequential excitation).

The CbT algorithm has been tested on numerous simulation examples and implemented experimentally on a magnetic suspension system and the active suspension system benchmark problem proposed for a special issue of European Journal of Control on the design and optimization of restricted-complexity controllers.

Keywords: controller tuning, correlation, data-driven control.

Version abrégée

La conception de schémes de commande performants passe par une bonne connaisance des processus mis en jeux et l'intégration de cette connaisance au sein des régulateurs. Dans beacoup d'applications pratiques, il est difficile, voire même impossible, de formuler un modèle mathématique suffisamment précis du procédé, et il devient alors nécessaire de concevoir le régulateur en se basant sur des mesures. Cette thèse propose une nouvelle méthodologie basée sur les mesures, appelée Correlation-based Tuning (CbT). Elle s'inspire de l'approche bien connue de corrélation, qui est utilisée dans le cadre de l'identification des systèmes. Les paramètres du régulateur sont ajustés itérativement de manière à soit décorreler l'erreur de sortie en boucle fermée du signal de référence externe ("decorrelation procedure"), ou réduire cette correlation ("correlation reduction"). Dans le meilleurs des cas, l'erreur de sortie en boucle fermée contient uniquement la contribution relative au bruit, et une poursuite parfaite des trajectiories peut alors être réalisée. D'autre part, le choix du critère de synthèse pour la commande assure que la sensibilité des paramètres du régulateur vis-à-vis du bruit tend vers zéro.

À la fois des aspects théoriques et de mise en oeuvre pratique sont traités. Concernant la procédure de décorrelation, une équation de corrélation est résolue par une méthode d'approximation stochastique. Le processus itératif converge vers la solution de l'équation, même lorsque le gradient de l'erreur de sortie en boucle fermée (par rapport aux paramètres de régulateur) est approché. Une analyse de la distribution asymptotique des paramètres estimés est effectuée. Quand la décorrelation totale ne peut pas être obtenue, la méthode de réduction de corrélation est utilisée. L'analyse du critère dans le domain fréquentiel révèle que l'algorithme revient alors à minimiser la norme-2 de l'écart entre les systèmes en boucle fermée specifié et observé. Avec cette approche, une estimée non-biasée du gradient de l'erreur

en boucle fermée est toutefois nécessaire pour garantir la convergence de l'algorithme vers un minimum local du critère. En outre, il est possible de généraliser ce critère afin de traiter les cas où les spécifications sont définies en termes de fonctions de sensibilité.

Par la suite, une extension de cette méthodologie à l'ajustement des régulateurs multivariables linéares est proposée dans les 2 cas. L'approche CbT permet d'ajuster certains éléments de la matrice de fonctions de transfert du régulateur de manière à ce que les performances désirées soient satisfaites en boucle fermée; les autres éléments sont ajustés afin que les sorties en boucle fermée soient mutuellement découplées. L'ajustement de l'ensemble des régulateurs et découpleurs peut s'effectuer sur la base d'une seule expérience par itération, indépendament du nombre d'entrées et de sorties, étant donné que tous les signaux de référence peuvent être excités simultanément. Néanmoins, l'excitation simultanée de toutes les signaux de référence augmente la variance des paramètres estimés du régulateur puisque la découplage est ici imposé comme critère de synthèse. Il existe en fait un compromis entre la réduction du coût experimental (excitation simultanée) et la précision des paramètres estimés (excitation séquentielle).

Cette méthodologie a été testée sur de nombreux exemples en simulation numérique, et appliquée à un système expérimental de sustentation magnétique. Elle a egalement été appliquée à un problème de référence, relatif à un système de suspension active, proposé lors d'une édition spéciale de la revue "European Journal of Control" sur la conception et l'optimisation de régulateurs de complexité réduite.

Mot-clés: ajustement de régulateurs, corrélation, commande basée sur les mesures

Contents

1 Introduction **1**

1.1 Historical background 1
1.2 Motivation 3
1.3 Related work 4
1.4 The basic concept of correlation-based controller tuning . . . 8
1.5 Contribution of the thesis 11
1.6 Outline 14

2 Preliminaries **17**

2.1 Basic notations and system description 17
2.2 Estimation of $\partial y/\partial \rho$ using a model 20
2.3 Robbins-Monro procedure 21
2.4 The correlation approach in system identification 25
2.5 Iterative feedback tuning 26

3 Decorrelation Procedure **29**

3.1 The control design criterion 31
3.2 Iterative solution using the Robbins-Monro procedure 32
3.2.1 Assumptions 32
3.2.2 Convergence 34
3.2.3 Choice of instrumental variables 34
3.2.4 Fixed terms in the controller 36
3.2.5 Algorithm 37
3.2.6 2DOF controllers 38
3.2.7 Sufficient condition for positive-definiteness of $Q(\rho)$. 38
3.2.8 Asymptotic accuracy when i tends to infinity 42
3.3 Iterative solution using the Newton-Raphson algorithm . . . 44

3.3.1 Newton-Raphson algorithm 44
3.3.2 Relation to standard IFT 46
3.3.3 Asymptotic accuracy when N tends to infinity 49
3.3.4 Algorithm 61
3.3.5 Simulation example 61
3.4 Application to a magnetic suspension system 64
3.4.1 The magnetic suspension system 64
3.4.2 Experimental results 66
3.5 Conclusions 69

4 Correlation Reduction **71**
4.1 Introduction 71
4.2 The control design criterion 73
4.3 Iterative solution 74
4.3.1 Robbins-Monro procedure 74
4.3.2 Gauss-Newton algorithm 75
4.4 Frequency-domain analysis of the control design criterion . . 76
4.5 Generalized correlation criterion 82
4.6 Stopping condition 89
4.7 Algorithm 92
4.8 Correlation-reduction method for the disturbance rejection problem 93
4.9 Application to an active suspension system 95
4.9.1 System description 95
4.9.2 Experimental results 96
4.10 Conclusions 101

5 Correlation-based tuning of linear decoupling multivariable controllers **103**
5.1 Introduction 103
5.2 Notations and system description 105
5.3 CbT for MIMO systems 107
5.3.1 Idea of multivariable correlation-based tuning 107
5.3.2 Cross-correlation function 109
5.3.3 Decorrelation procedure for MIMO systems 110
5.3.4 Correlation reduction for MIMO systems 119

5.3.5 Iterative solution using deterministic methods 122
5.4 Simulation Results 123
5.4.1 Decorrelation procedure vs. correlation reduction . . 123
5.4.2 Correlation-reduction CbT vs. IFT 125
5.5 Conclusion 128

6 Conclusions **131**
6.1 Summary 131
6.2 Perspectives 133

Bibliography **135**

Curriculum Vitae and List of Publications **145**

Notation Glossary

Abbreviations

ARMAX	AutoRegressive MovingAverage with eXogeneous input
ARX	AutoRegressive with eXogeneous input
BJ	Box-Jenkins
CbT	Correlation-based Tuning
FIR	Finite Impulse Response
IFT	Iterative Feedback Tuning
IV	Instrumental Variables
LMI	Linear Matrix Inequality
LQG	Linear Quadratic Gaussian
LS	Least squares
LTI	Linear Time Invariant
MIMO	Multi-Input Multi-Output
MRAC	Model-Reference Adaptive Control
OE	Output Error
PE	Prediction Error
PID	Proportional-Integral-Derivative controller
PRBS	Pseudo Random Binary Sequence
RST	Type of two-degree-of-freedom controller
SISO	Single-Input Single-Output
SPR	Strictly Positive Real
SPSA	Simultaneous Perturbation Stochastic Approximation control
STR	Self-Tuning Regulation
VRFT	Virtual Reference Feeback Tuning
w.p.	With probability

Operators

$\arg\min_x f(x)$	Minimizing argument of $f(x)$
$\langle x, y \rangle$	Inner product of two vectors x and y
A^*	Complex conjugate transpose of matrix A
A^T	Transpose of matrix A
A^{-1}	Inverse of matrix A
$E\{x\}$	Mathematical expectation of the random variable x
q^{-1}	Delay operator: $u(t-1) = q^{-1}u(t)$

Symbols

$\phi(\rho, t)$	Regressor vector
$\psi(\rho, t)$	Derivative of $y(\rho, t)$ with respect to ρ
ρ	Controller parameters vector
ρ°	Solution of the correlation equation $f(\rho) = 0$
$\tilde{\rho}$	Controller parameters vector with a different ordering of the elements
$\tilde{\rho}^\circ$	Solution of the correlation equation $f(\tilde{\rho}) = 0$
$\varepsilon_{ie}(\rho, t)$	Closed-loop input error
$\varepsilon_{oe}(\rho, t)$	Closed-loop output error
$\zeta(\rho, t)$	Instrumental variables vector
$A_c(q^{-1})$	Characteristic polynomial
$e(\rho, t)$	Control error $y(\rho, t) - r(t)$
$G(q^{-1})$	Transfer function (matrix) of the "true plant
$G_d(q^{-1})$	Plant model
$H(q^{-1})$	Noise model
$K(q^{-1})$	Linear feedback controller
$K^\circ(q^{-1})$	Decorrelating controller
$K_d(q^{-1})$	Initial controller based on G_d
$r(t)$	External reference signal
$u(\rho, t)$	Controller output
$v(t)$	Measurement noise
$x(t) \overset{f}{\sim} y(t)$	$x(t)$ is a function of $y(t)$
$x_N \in As\mathcal{N}(m, P)$	N-dimensional sequence of random variables x_N that converges in distribution to the normal dis-

	tribution with mean m and covariance matrix P
$y(\rho, t)$	Measured output
$y_d(t)$	Desired output
$f(\rho)$	Cross-correlation function between $\varepsilon_{oe}(\rho, t)$ and $\zeta(\rho, t)$
$\bar{f}(\rho)$	Estimate of $f(\rho)$ based on N data samples
$g(\rho)$	Cross-correlation function between $\varepsilon_{ie}(\rho, t)$ and $\zeta(\rho, t)$
$\bar{g}(\rho)$	Estimate of $g(\rho)$ based on N data samples
$A(q^{-1})$	Denominator of $G(q^{-1})$
$A_d(q^{-1})$	Denominator of $G_d(q^{-1})$
$B(q^{-1})$	Numerator of $G(q^{-1})$
$B_d(q^{-1})$	Numerator of $G_d(q^{-1})$
$Q(\rho)$	Jacobian matrix of $f(\rho)$
$\bar{Q}(\rho)$	Analogous to $Q(\rho)$
$\bar{Q}^{+}(\rho)$	Pseudo-inverse of $\bar{Q}(\rho)$
$\mathcal{R}$	Space of real numbers
$\mathcal{R}^k$	Space of real k-dimensional vectors
$\mathcal{R}^{j\times k}$	Space of real $j \times k$ matrices
R	Pole polynomial of RST controller
S	Feedback polyomial of RST controller
T	Feedforward polynomial of RST controller
$\mathcal{S}(q^{-1})$	Output sensitivity function
$\mathcal{T}(q^{-1})$	Complementary sensitivity function
$\mathcal{U}(q^{-1})$	Input sensitivity function
$\Phi_{xy}(\omega)$	Cross-spectrum between $x(t)$ and $y(t)$
$\Phi_x(\omega)$	Spectrum of $x(t)$
$R_{xy}(\tau)$	Fourrier transform of $\Phi_{xy}(\omega)$
$R_x(\tau)$	Fourrier transform of $\Phi_x(\omega)$
Var x	Variance matrix of the random variable x
γ_i	Positive step size

List of Figures

1.1 Model-following problem 9

2.1 Block diagram of the achieved and designed closed-loop systems 19
2.2 Robbins-Monro procedure: the idea 22
2.3 Open-loop identification problem 25
2.4 IFT: gradient experiment 28

3.1 Criterion J averaged over 100 noise realizations for IFT (thick line) and CbT (thin line) over 400 iterations 48
3.2 Criterion J averaged over 500 noise realizations for IFT (solid) and CbT (dashed) over 9 iterations 49
3.3 Closed-loop output error resulting from a comparison of the achieved and designed closed-loop systems 51
3.4 Confidence interval around $\tilde{\rho}^\circ$ for $n_{\tilde{\rho}} = 1$ 54
3.5 Closed-loop step responses: designed (solid), initial (dashed), obtained with the decorrelation procedure after 8 iterations (dash-dot) 62
3.6 Parametric distance versus iteration number 63
3.7 Magnetic suspension system 65
3.8 Closed-loop response achieved with the initial RST controller (solid) and designed response (dashed) 67
3.9 Closed-loop response achieved with the IFT after 8 iterations (solid), and designed response (dashed) 68
3.10 Closed-loop response achieved with the CbT after 6 iterations (solid), and designed response (dashed) 68

4.1 Bode plots of $G(e^{j\omega T_s})$ (dash-dot) and $G_d(e^{j\omega T_s})$ (solid) . . . 79

4.2 Magnitude plots of the complementary sensitivity functions: designed $\mathcal{T}_d(e^{j\omega T_s})$ (solid), initial $\mathcal{T}(e^{j\omega T_s}, K_d, G)$ (dashed) and final $\mathcal{T}(e^{j\omega T_s}, K(\rho), G)$ (dash-dot) 80
4.3 Magnitude plots of the output sensitivity functions: designed $\mathcal{S}_d(e^{j\omega T_s})$ (solid), initial $\mathcal{S}(e^{j\omega T_s}, K_d, G)$ (dashed) and final $\mathcal{S}(e^{j\omega T_s}, K(\rho), G)$ (dash-dot) 81
4.4 Magnitude plots of the input sensitivity functions: designed $\mathcal{U}_d(e^{j\omega T_s})$ (solid), initial $\mathcal{U}(e^{j\omega T_s}, K_d, G)$ (dashed) and final $\mathcal{U}(e^{j\omega T_s}, K(\rho), G)$ (dash-dot) 81
4.5 Closed-loop input error resulting from a comparison of the achieved and designed closed-loop systems 83
4.6 Output sensitivity functions: designed $\mathcal{S}_d(e^{j\omega})$ (solid), initial $\mathcal{S}(e^{j\omega}, K_d, G)$ (dashed) and final $\mathcal{S}(e^{j\omega}, K(\rho), G)$ (dash-dot) for $(k_{oe}, k_{ie}) = (1, 0)$ 85
4.7 Input sensitivity functions: designed $\mathcal{U}_d(e^{j\omega})$ (solid), initial $\mathcal{U}(e^{j\omega}, K_d, G)$ (dashed) and final $\mathcal{U}(e^{j\omega}, K(\rho), G)$ (dash-dot) for $(k_{oe}, k_{ie}) = (1, 0)$ 85
4.8 Output sensitivity functions: designed $\mathcal{S}_d(e^{j\omega})$ (solid), initial $\mathcal{S}(e^{j\omega}, K_d, G)$ (dashed) and final $\mathcal{S}(e^{j\omega}, K(\rho), G)$ (dash-dot) for $(k_{oe}, k_{ie}) = (0, 1)$ 86
4.9 Input sensitivity functions: designed $\mathcal{U}_d(e^{j\omega})$ (solid), initial $\mathcal{U}(e^{j\omega}, K_d, G)$ (dashed) and final $\mathcal{U}(e^{j\omega}, K(\rho), G)$ (dash-dot) for $(k_{oe}, k_{ie}) = (0, 1)$ 87
4.10 Output sensitivity functions: designed $\mathcal{S}_d(e^{j\omega})$ (solid), initial $\mathcal{S}(e^{j\omega}, K_d, G)$ (dashed) and final $\mathcal{S}(e^{j\omega}, K(\rho), G)$ (dash-dot) for $(k_{oe}, k_{ie}) = (0.5, 0.5)$ 87
4.11 Input sensitivity functions: designed $\mathcal{U}_d(e^{j\omega})$ (solid), initial $\mathcal{U}(e^{j\omega}, K_d, G)$ (dashed) and final $\mathcal{U}(e^{j\omega}, K(\rho), G)$ (dash-dot) for $(k_{oe}, k_{ie}) = (0.5, 0.5)$ 88
4.12 Closed-loop step responses: designed (solid), initial (dashed), obtained with the correlation-reduction method after 3 iterations (dash-dot) 91
4.13 Output sensitivity functions: designed $\mathcal{S}_d(e^{j\omega})$ (solid), initial $\mathcal{S}(e^{j\omega}, K_d, G)$ (dashed) and final $\mathcal{S}(e^{j\omega}, K(\rho), G)$ (dash-dot) . 91

4.14 Controlled plant with the measured disturbance v_1 and the measurement noise v_2 93
4.15 The schematic diagram of the active suspension system . . . 96
4.16 Block diagram of the active suspension system 97
4.17 Magnitudes of $C_r(e^{-j\omega})/D_r(e^{-j\omega})$ (dashed), $W_r(e^{-j\omega})$ (dash-dot), and aggregate weighting $W_r(e^{-j\omega})C_r(e^{-j\omega})/D_r(e^{-j\omega})$ (solid) used in (4.38) 97
4.18 Incorporating fixed terms in the secondary path 98
4.19 Output and input sensitivity functions of the closed-loop system: before tuning (dash-dot), after 3 iterations (dashed), after 8 iterations (thick solid line), and constraints (thin solid line) 100
4.20 Closed-loop output and input sensitivity functions estimated from data collected on the experimental setup with the final controller (thick line) and constraints (thin line) 100

5.1 Achieved multivariable closed-loop system and its reference model M_d 106
5.2 Multivariable 2×2 controller 109
5.3 Decorrelation procedure vs. correlation reduction. Reference signals (dash-dot) and desired responses (dotted). Achieved responses: the initial controller (dashed), final controller obtained by decorrelation procedure (thin solid line) and final controller obtained by correlation reduction (thick solid line). The references are changed in a step-like manner at 0 and 2.5s (for r_1) and 5s (for r_2). 124
5.4 Correlation-reduction CbT: Closed-loop responses in a noisy environment. Reference signals (dash-dot), desired responses (dotted), achieved responses with the initial controller (dashed) and final controller (solid). The references are changed in a step-like manner at 0 and 5s (for r_1) and 10s (for r_2). 126
5.5 Correlation-reduction CbT vs. IFT controller in a noise-free context. Reference signals (dash-dot), desired responses (dotted), closed-loop response with the CbT controller (solid) and IFT controller (dashed) 127

Chapter 1

Introduction

Automatic control is the scientific discipline that employs methods from mathematics and engineering in order to force dynamical systems to behave in a desired fashion. The first application of feedback control goes as far back as the invention of a float regulator by the Greek Ktesibos in the times of antiquity [52]. Since then, mankind has witnessed a tremendous development of this field that has closely followed advances in technology. In recent years, the increase in the demand for higher accuracy, economical benefits, increased safety, reduced energy consumption, and so on, has made feedback loops inevitable in almost every part of our daily lives. Typical examples of systems that use feedback loops are vehicles, consumer electronics, aircraft, power plants and chemical processes.

1.1 Historical background

In the early days of automatic control, the control design was based mainly on engineering intuition without any established methodology. The first systematic methods based on the use of Bode and Nyquist plots were developed and applied to the design of amplifiers in the 1930s and 1940s [67, 6]. In 1960, Kalman published his seminal papers that introduced state-space methods along with the design equations for the linear quadratic regulator and the discrete Kalman filter [39, 40]. These papers set the stage for an extraordinary development of model-based control design methods. A few years later, in the field of system identification, the paper [3] appeared that sparked the development of the prediction error (PE) framework [54]. These identification techniques provided reliable models allowing the applicability

of model-based control design to a wide range of dynamical systems and processes.

For a long time, identification and control design were considered separately within the framework of model-based control. The dominant idea was to identify the best possible model and then design the controller on the basis of that model. However, when implementing this controller on the real system, performance degradation occurred because of modeling errors. Then, the paradigm "goal-oriented identification" emerged in the system identification community [19, 85]. Namely, it was understood that the model was an approximation of the "true system" and that the quality of the model should reflect the intended model application.

Based on this observation, a new research topic named "iterative identification and control" started to develop around 1990. In this line of research, identification and control design have been considered as a joint design problem. An iterative scheme is used to solve this problem by means of separate identification and control design. In each identification step, the previously designed controller is used to obtain new data from the plant. Then, the controller is designed on the basis of the model obtained in the identification step. If the resulting closed-loop system does not meet the specifications, one continues to iterate. It was recognized that the identification criterion should match the control design criterion, which led to the result that a model identified in closed loop should be used for controller design [33, 13]. Methods of iterative identification and control have blossomed in the 1990s. Practical applications have shown that these schemes improve the closed-loop performance, especially in the first few iterations. However, there are also examples where the divergence of these schemes is observed. It is demonstrated in [36] that identification for control schemes does not necessarily converge to a local minimum of the design objective in the presence of modeling errors. In addition, it should be noted that all steps of model identification including data acquisition, order selection, parametric identification, model validation, uncertainty bound estimation as well as robust controller design should be redone at each iteration. For more details about this research area the reader is referred to [82, 84, 32, 17].

1.2 Motivation

Iterative identification and control is appealing to process engineers because it is not necessary to open the loop in order to identify a model and subsequently to design a controller. However, reliable models of industrial plants are often difficult or impossible to obtain due to the high complexity of the plants. In addition, the cost of modelling in some cases can be excessive. It is argued in the literature that obtaining the process model is the single most time consuming task in the application of model-based control [68].

A straightforward idea to circumvent the aforementioned problems is to use the information collected on the plant *directly* for controller update, i.e. without the intermediary of a plant model. The methods featuring this idea, so-called data-driven methods, bring benefits compared to model-based control design methods. Within this framework, besides the obvious reduction of the control design cost, the complexity of the controller is not dependent on that of the model as it is, for instance, for iterative identification and control schemes. Consequently, the design of low-complexity controllers naturally appears as the primary application field of data-driven methods. In practice, low-order controllers are usually preferred because the controller size may be limited by hardware and/or computational requirements. Moreover, simple controllers are easier to understand, implement and maintain – the typical example being the PID controller. Considering that PID controllers still operate in more than 90% of the installed industrial loops [4], it is clear that data-driven methods have wide potential.

Although direct optimization of the control objective over the controller parameters is much simpler than identification and control re-design at each iteration and the convergence to a local minimum can be guaranteed, it requires more experiments on the real plant. There are several questions that arise in this context. The first and rather obvious question is whether the increased experimental cost is acceptable to industry and how to reduce it. When is it appropriate to use an iterative approach and when is it better to apply a method using a single set of measurements? An another question is how to address the robustness issues of the closed-loop system. In fact, it is very difficult to speak about the robustness of the closed-loop system for a model-free approach where the controller parameters are tuned to

improve time-domain performances. However, the robustness of the system can be taken into account with a judicious choice of the criterion (with some a priori information about the plant) and an appropriate selection of the excitation signal.

A question of great importance is how to cope with the noise that necessarily corrupts the measurements and therefore also affects the closed-loop performance. In a model-based approach, the influence of noise is treated in the identification step and may be taken into account as model uncertainty in the control design step. On the other hand, for a data-driven approach that minimizes a norm of some error signal, satisfying model-following objectives is not obvious because the estimated controller parameters are affected by noise. In particular, in a high-noise setting, tracking performance can be poor since the resulting controllers tend to minimum-variance controllers. In this thesis, a new control design objective is proposed in an attempt to address this and the other aforementioned questions.

1.3 Related work

The idea to directly update the controller parameters using data collected in closed loop is not new. In fact, it emerged in the 1950s in the area of direct adaptive control. In particular, it is worth mentioning Model Reference Adaptive Control (MRAC) and direct Self Tuning Regulation (STR) methods [2]. In that period, many of the parameter adjustment mechanisms were gradient-based. The crucial problem was how does one compute the gradient of the criterion with respect to the controller parameters assuming that the plant and disturbance dynamics are not known. In addition to the well-known gradient approximation used in the MIT rule [69] and its variations, the efforts for gradient computation have been pursued in two directions.

The first group of methods relies on finite-difference approximations of the gradient. The idea is to evaluate the criterion for different perturbed values of the controller parameters and then to compute the gradient numerically. The basic difficulty with this approach is that, in general, all perturbed parameters affect each signal, which hinders successful gradient approximation since it is impossible to distinguish individual contributions

of the perturbed parameters to the changes in the measured signals. To overcome this problem, it was proposed to alter the parameters sequentially [1, 80, 14]. The number of experiments needed to approximate the gradient is proportional to the number of parameters, which for the case of Multi-Input Multi-Output (MIMO) systems is often unacceptably large. In [55], it is proposed to perturb the various parameters at different frequencies in order to determine independently the variations in the criterion due to changes in each parameter.

The second research direction consisted of computing the partial derivatives of a performance criterion with respect to adjustable parameters by filtering signals measured during system operation either by a model of the system or by the system itself. An approximate Wiener filter has been designed in [63] where the gradient of the performance criterion (defined as the mean square error between the output of the filter and a desired output) has been computed using the signals collected on the filter itself. The same publication proposes for the design of an optimal feedback control system to use a model of the closed-loop system to generate the signals needed to compute the sensitivities. This idea is developed further in [64] where the gradient of the performance criterion is computed using the system itself as a model. In order to obtain an estimate of the gradient, the error signal is delayed and fed back to the input via an outer loop. In [81] an identified model of the plant is used to compute the gradient.

The data-driven methods have been brought back into focus in the mid-1990s. Simultaneous Perturbation Stochastic Approximation control (SPSA) appeared in this context [78]. SPSA belongs to the class of stochastic approximation algorithms that are typically used for finding roots in the presence of noisy measurements. Usually these algorithms rely on the finite-difference approach and therefore the number of experiments required depends on the number of parameters to be adjusted. In an effort to reduce the experimental cost, it has been proposed in [77] to perturb all parameters simultaneously. This method turned out to be much more efficient than the finite-difference stochastic approximation algorithms, in particular SPSA requires only one or two experiments per iteration. However, the number of iterations required to reach a minimum can be important with this method. The parametric convergence of this method has also been proven.

The idea of computing the gradient of the performance criterion using the system itself appeared again in [35]. This gradient-based method for the iterative optimization of the performance criterion over the controller parameters has been called Iterative Feedback Tuning (IFT). IFT allows computing an unbiased estimate of the gradient of the control objective using signals acquired on the closed-loop system. With the resulting estimate of the gradient, the minimization of the criterion is performed iteratively using a Gauss-Newton scheme. To compute the gradient, three experiments per iteration are needed in the case of two-degree-of-freedom controllers. Here, the only "special" experiment is the second one, where the output measured during the first experiment is fed back to the reference input. During the first and third experiments data may be collected under normal operating conditions where the same reference signal is used in both experiments. The third experiment is necessary to ensure the unbiasedness property of the gradient estimate. For tuning a one-degree-of-freedom controller, the first two experiments suffice. Assuming that the closed-loop signals remain bounded, it can be proven using ideas from stochastic approximation procedures that this algorithm converges to a local minimum as the number of iterations goes to infinity [26, 28]. Due to its simplicity and attraction, IFT has gained popularity in the control community and a number of papers have appeared on this topic. The possibility of using IFT for the control of nonlinear systems has been presented in [27]. IFT has also been used for tuning a multivariable controller in [29]. An overview of this method is given in [31].

An interesting approach to controller design is the unfalsified control concept proposed in [71]. In this paper, with no assumption about the plant, the candidate controllers are evaluated based solely on experimental data. Controllers that are found to be incapable of meeting the required performance specifications are eliminated from a class of admissible control laws. This idea is used for controller tuning in [50]. An interesting feature of these methods is that candidate controllers are falsified before they are implemented in the feedback loop. However, note that in both aforementioned references noise-free systems are considered.

Virtual Reference Feedback Tuning (VRFT) is yet another data-driven method that appeared recently. The original concept behind VRFT is intro-

duced in [23]. This concept is further developed in [9], where implementation aspects have been addressed and a data prefilter has been designed in order to match the VRFT and model-following criteria. This approach aims at solving a model reference control problem without iteration, i.e. by using a single set of measurements. The idea of VRFT is very interesting. Let a set of input-output data, say (u_m, y_m), be measured on a noise-free system (it does not matter whether data are collected in open-loop or closed-loop operation) and assume that a reference model is defined. A reference signal that would give the measured output y_m if applied to the reference model can be constructed. This reference signal is called "virtual" because it is not used in the actual generation of the output y_m. Moreover, it is possible to compute the virtual tracking error defined as the difference between the virtual reference and y_m. The idea is to compute a controller that generates u_m when fed by the virtual tracking error. By suitable filtering of the virtual tracking error and u_m, the transfer function of the feedback loop consisting of the calculated controller and the unknown plant is equal to the given reference model, provided that the controller is of appropriate order. Observe that the task of calculating the controller reduces to a simple identification problem. VRFT uses an instrumental variable method to counteract the effect of the noise. An interesting application of this one-shot method consists of providing initial controllers for iterative algorithms intended to perform the "fine-tuning" of the controllers.

The method presented in this thesis is closely related to the well-known correlation approach in system identification [74, 75, 54]. The main incentive for introducing this approach in system identification is to ensure the unbiasedness properties of the estimated parameters. Correlation techniques have not been used much in control outside of the field of system identification. The rare exceptions are [63, 46, 47], where these techniques have been used for the computation of parameter sensitivities. Another example is the correlation-based auto-tuning technique developed in [25]. In that paper, the cross-correlation of a small pseudo-random-binary-sequence (PRBS) test signal and the process output is used to compute the process impulse response, which is then numerically transformed into its frequency response to extract the ultimate gain and period for use in the Ziegler-Nichols formula.

In gradient-based controller tuning schemes, there is a necessity to verify whether the controller calculated iteratively will stabilize the closed-loop system or whether the controller computed in subsequent iteration will provide a better closed-loop performance than the previously computed controllers. Therefore, controller validation is an important issue that is treated in a number of papers. The unfalsified control concept in [8] has been used to directly validate closed-loop controller performance from open-loop data, or from closed-loop data acquired while another controller was in the feedback loop. Another approach to control validation is given in [18]. In that paper, based on the knowledge that the true system belongs to a constructed uncertainty set with a certain probability, it is proposed to validate the controller that stabilizes all models in the uncertainty set. Therefore, this particular controller also stabilizes the true system with at least the same probability. In a similar fashion, controllers can also be validated for closed-loop performance. If a plant model is not available, the stability test based on the Vinnicombe gap between two successive controllers can be performed using closed-loop data [41]. In this thesis, the closed-loop stability and performance are verified using simply an identified model, and no method adapted to the approach proposed here has been developed.

1.4 The basic concept of correlation-based controller tuning

In a standard approach to the model-following problem, the controller parameters are adjusted so that a norm of the closed-loop output error, defined as the output error between the achieved closed-loop system and a reference model (or a designed closed-loop system), is minimized. Several observations that followed an analysis of these approaches initiated the development of the method presented here:

- Observe first that perfect model-following is not attainable due to the very nature of the criterion. That is, in the presence of noisy measurements, there is always a trade-off between model-following and noise attenuation. In other words, the estimated controller parameters are affected by noise and do not converge to the values that provide perfect

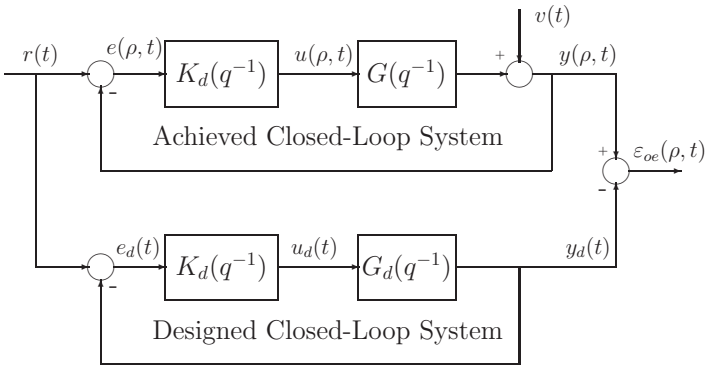

Figure 1.1: Model-following problem

matching between achieved and designed closed-loop systems.

- The second observation is that, when perfect-following is not achieved, the closed-loop output error consists of a part due to modeling errors and a contribution originating from the disturbance $v(t)$. To clarify this observation, let us consider the model-following problem shown in Fig. 1.1. Suppose that the controller K_d is designed using the plant model G_d and then applied to the real plant G. Let the system be excited by the reference signal $r(t)$. From this figure, the closed-loop output error can be computed as:

$$\begin{aligned}
\varepsilon_{oe}(\rho,t) &= y(\rho,t) - y_d(t) \\
&= \left\{(1+GK_d)^{-1}GK_d - (1+G_dK_d)^{-1}G_dK_d\right\} r(t) \\
&\quad -(1+GK_d)^{-1}v(t) \\
&= \left\{(1+GK_d)^{-1}K_d(1+G_dK_d)^{-1}\right\}\{G-G_d\}\, r(t) \\
&\quad -(1+GK_d)^{-1}v(t)
\end{aligned}$$

It is obvious that the closed-loop output error contains a contribution due to the difference between G and G_d (modeling errors) and another contribution containing the measurement noise $v(t)$ filtered by the achieved closed-loop system.

- Finally, observe that the contribution due to the difference between

the achieved and designed closed-loop systems is correlated with the reference signal $r(t)$.

Under the realistic assumption that the measurement noise and, by the same reasoning, the contribution due to this noise are not correlated with the reference signal, the control objective can be modified as follows. Instead of minimizing a quadratic criterion, say the 2-norm of the closed-loop output error, tune the controller parameters to decorrelate the closed-loop output error $\varepsilon_{oe}(\rho, t)$ with the external reference signal $r(t)$. The motivation for introducing such a control objective is clear. If the closed-loop output error between designed and achieved closed-loop systems is not correlated with the reference signal, this means that the resulting controller is updated to compensate the effect of modeling errors only. In other words, the achieved closed-loop system has captured the dynamics of the designed one, and the closed-loop output error contains only the contribution due to measurement noise. Therefore, perfect model-following is achieved regardless of the presence of the disturbance $v(t)$. This feature is the founding block of this thesis.

Note that the effect of noise on the closed-loop output is not minimized in this approach. One may argue that this insensitivity to noise implies that this method, called Correlation-based Tuning (CbT), is not appropriate for disturbance rejection. However, one can consider that, in an ideal case, the loop transfer functions of the resulting and designed closed-loop systems are equal. Hence, by imposing some disturbance rejection specifications on the desired output sensitivity function, it is possible to handle the disturbances indirectly. In other words, the designed closed-loop system is typically more complex than a simple reference model for tracking since it indirectly defines all design specifications for tracking, disturbance and noise attenuation. Hence, the objective for the achieved closed-loop system is to approximate the designed one, independently of the noise characteristics. As a result, the robustness properties of the designed closed-loop system will be preserved, but the performance with respect to noise attenuation will normally not change.

The ideas presented above can be expressed mathematically in the form of the cross-correlation function defined as the mathematical expectation between the closed-loop output error and a vector of instrumental vari-

ables. The instrumental variables are chosen so as to be correlated with the reference signal and independent of the noise. Based on assumptions regarding the complexity of the controller with respect to the plant, two ways of computing the controller parameters can be distinguished. When the controller is of sufficiently high order to perfectly decorrelate the closed-loop output error from the reference signal, the controller parameters can be calculated as the roots of the cross-correlation function. This approach and the corresponding controller are called respectively "decorrelation procedure" and "decorrelating controller". The approach where the controller parameters are computed to minimize a norm of this function is labeled "correlation reduction".

1.5 Contribution of the thesis

This thesis introduces the correlation approach in control design. More specifically, the concept of instrumental variable methods is used to tune the parameters of a linear time-invariant controller using the data acquired in closed-loop operation. To the best knowledge of the author, this is the first time in control literature that correlation appears as a control design objective.

The contribution of this thesis can roughly be divided in three parts.

1. The first part analyzes the features of the decorrelation procedure.

    - For a finite number of data, the roots of the cross-correlation function are computed by using an iterative stochastic approximation scheme of the Robbins-Monro type [70]. Provided that the parameterized set of controllers contains a decorrelating controller and that the signals in closed loop remain bounded, it can be proven that, under relatively mild conditions, the controllers obtained by the iterative algorithm converge toward the decorrelating controller as the number of iterations tends toward infinity [45]. The most important part in this proof is to give conditions under which the gradient of the closed-loop error with respect to the controller parameters is positive definite in the vicinity of the solution. It is shown that this gradient is positive definite provided that an SPR

(strictly positive real) condition on some transfer function is satisfied. Using the latter result, an appropriate choice of instrumental variables is given. An important observation is that a single experiment per iteration is required to evaluate the cross-correlation function and no gradient evaluation is needed. The required number of experiments per iteration is the same regardless of whether one-degree-of-freedom or two-degree-of-freedom controllers are tuned.

- An explicit expression for the variance of the estimated controller parameters around the solution is derived [45]. This expression, which is asymptotic in the number of iterations, is useful for choosing design parameters such as instrumental variables, number of data, the form of the reference signal, etc.
- In practical situations where it is possible to collect a large number of data, noise does not greatly affect the cross-correlation function. Hence, the Newton-Raphson algorithm, as a typical representative of gradient-based deterministic schemes, can be employed to compute the controller parameters. The Newton-Raphson algorithm converges much faster than the Robbins-Monro procedure but requires an estimate of the gradient. Closed-loop data are used to evaluate the cross-correlation function and, at the same time, to identify a plant model that is subsequently used to estimate the gradient. For a finite number of data, this algorithm converges toward a set whose center is at the solution of the cross-correlation equation. The asymptotic accuracy of the controller parameter estimates as a function of the number of data is analyzed. The expression for the asymptotic variance of the controller parameter estimates allows one to construct the confidence interval around the decorrelating controller, which is, in turn, used to develop the stopping condition for the iterative procedure [59].
- The decorrelation procedure has been implemented on an experimental magnetic suspension system where a two-degree-of-freedom controller has been tuned. Excellent performance using only a few real-time experiments is achieved [44].

2. The second part treats theoretical and practical aspects of the correla-

tion reduction method. Considering that industrial plants can be very complex, it is not a rare situation that the decorrelating controller does not exist or does not belong to the selected controller class. In these situations, instead of finding the roots of the cross-correlation function, a norm of this function is minimized.

- Again, for a finite number of data, the Robbins-Monro procedure is used. This algorithm converges to a local minimum of the performance criterion provided that an unbiased estimate of the gradient is available. The gradient can be estimated by using either a full-order plant model or an additional closed-loop experiment as is done in IFT. A frequency-domain analysis of the criterion shows that the noise has asymptotically no effect on the controller parameters. In addition, it is shown that the achieved closed-loop system approaches iteratively the designed one, with the difference between the two closed-loop systems being weighted by the square of the power spectrum of the reference signal [43].
- The proposed performance criterion can be generalized so that the mixed sensitivity specifications can be handled. That is, by adding in the performance criterion the term consisting of the cross-correlation between the reference signal and the input closed-loop error (defined analogously to the closed-loop output error), the specifications expressed in terms of output and input sensitivity functions can be met [58].
- An adaptation of the correlation reduction method for the disturbance rejection problem has been proposed [57]. It is shown that, when the disturbance signal can be measured or a known signal can be injected as a "test" disturbance, this method can be used. This idea has been successfully applied to the active suspension benchmark problem posed for a special issue of the European Journal of Control on the design and optimization of restricted-complexity controllers. The controller with CbT has been ranked among the five best controllers with acceptable complexity and performance on the underlying real system [51].
- When a large number of data is available, the Gauss-Newton algo-

rithm can be used for correlation reduction. In this case, an accurate estimate of the gradient is needed to guarantee local convergence. A stopping condition for the correlation reduction method has been developed [57].

3. The idea of CbT has also been proposed for the tuning of linear time-invariant multivariable controllers.

   - Some elements of the controller transfer function matrix are tuned to satisfy the performance specifications, while others are tuned to be decouplers. Both variants of CbT, i.e. the decorrelation procedure and the correlation reduction method, can be employed. Comparing CbT to the other data-driven methods based on the minimization of some error signal, one can immediately notice advantages that CbT offers for the tuning of MIMO controllers. First of all, CbT offers perfect decoupling by decorrelating a given reference with the noncorresponding outputs, while this is not possible with the other methods. The second advantage is that all controllers and decouplers can be tuned using a single experiment per iteration regardless of the number of inputs n_u and outputs n_y. In the other methods, the number of experiments required per iteration increases typically with n_u and n_y [56, 60].
   - However, the analysis performed in this thesis reveals that simultaneous excitation of all reference inputs negatively affects the accuracy of the estimated controller parameters due to the imposed decoupling specifications. One can obtain more accurate estimates by performing n_y experiments per iteration. Actually, there is a user choice between low experimental cost and better accuracy of the estimated parameters [62, 60].

1.6 Outline

This thesis is organized as follows.

Chapter 2: Preliminaries. To facilitate the reading of the material presented in this thesis, some basic facts from control and identification

theory are recalled in this chapter. In addition, some details about IFT and the Robbins-Monro procedure are given.

Chapter 3: Decorrelation procedure. The CbT variant, where the controller parameters are calculated as the roots of the cross-correlation function, is treated from a theoretical and practical point of view in this chapter. The application of this method to an experimental setup is presented as well.

Chapter 4: Correlation reduction. In this chapter, the controller parameters are updated by minimizing the cross-correlation function. Existing extensions of this variant and the application to an active suspension system are documented.

Chapter 5: Correlation-based tuning of linear decoupling multivariable controllers. This chapter deals with the tuning of linear time-invariant multivariable controllers. Apart from performance specifications, decoupling specifications are imposed as well.

Chapter 6: Conclusions. Concluding remarks are given and some possible further research topics are proposed in this chapter.

Chapter 2

Preliminaries

The aim of this chapter is to introduce some of the definitions and concepts that are required in later chapters to follow the presentation or to prove some of the theoretical results. In addition, in order to provide an objective account of the proposed method, the features of CbT are occasionally compared with those of the closely related IFT scheme. For this purpose, a brief introduction to the IFT method is also given.

2.1 Basic notations and system description

Let the output of an Single-Input Single-Output (SISO) linear time-invariant true plant be described by the following discrete-time model

$$y(t) = G(q^{-1})u(t) + v(t) \tag{2.1}$$

where $u(t)$ is the plant input and $v(t)$ represents a zero-mean weakly stationary random process. The unknown transfer operator $G(q^{-1})$ is defined as

$$G(q^{-1}) = \frac{B(q^{-1})}{A(q^{-1})} \tag{2.2}$$

where $B(q^{-1})$ and $A(q^{-1})$ are polynomials in the backward-shift operator q^{-1}. The plant is controlled by the following one-degree-of-freedom controller

$$K(q^{-1}, \rho) = \frac{S(q^{-1}, \rho)}{R(q^{-1}, \rho)} \tag{2.3}$$

where

$$R(q^{-1},\rho) = 1 + r^{(1)}q^{-1} + \cdots + r^{(n_r)}q^{-n_r} \tag{2.4}$$

$$S(q^{-1},\rho) = s^{(0)} + s^{(1)}q^{-1} + \cdots + s^{(n_s)}q^{-n_s} \tag{2.5}$$

and the controller parameter vector ρ of dimension $n_\rho = n_r + n_s + 1$ is defined as

$$\rho^T = [r^{(1)} \cdots r^{(n_r)}, s^{(0)} \cdots s^{(n_s)}] \tag{2.6}$$

The control law can be presented in regression form

$$\begin{aligned} u(\rho,t) &= \left(1 - R(q^{-1},\rho)\right) u(\rho,t) + S(q^{-1},\rho)e(\rho,t) \\ &= \phi^T(\rho,t)\rho \end{aligned} \tag{2.7}$$

where $e(\rho,t) = r(t) - y(\rho,t)$, $r(t)$ is the closed-loop reference signal and $y(\rho,t)$ is the plant output in closed-loop operation. The regressor vector $\phi(\rho,t)$ is defined as follows

$$\phi^T(\rho,t) = [-u(\rho,t-1), \cdots, -u(\rho,t-n_r), e(\rho,t), \cdots, e(\rho,t-n_s)] \tag{2.8}$$

The controller parameters are tuned by an iterative algorithm. Thus, the controller at the i-th iteration is denoted by $K(\rho_i, q^{-1})$ and other signals, vectors, matrices and closed-loop transfer functions that depend on the operation of this controller will carry the argument ρ_i. The argument q^{-1} will be omitted when appropriate.

Fig. 2.1 shows the block diagram of the closed-loop system which is usually used in the context of iterative identification and controller design. The upper part presents the achieved closed-loop system and the lower part shows the designed closed-loop system containing the reduced-order model of the plant (designed model)

$$G_d(q^{-1}) = \frac{B_d(q^{-1})}{A_d(q^{-1})} \tag{2.9}$$

and the designed controller $K_d(q^{-1})$. The controller $K_d(q^{-1})$ is designed using the plant model $G_d(q^{-1})$ so that the designed closed-loop system satisfies all the specifications for tracking and noise attenuation. If needed, specifications for control signal limitation can be included as well.

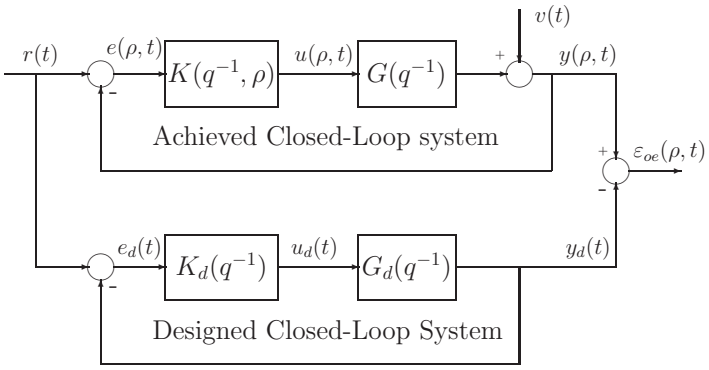

Figure 2.1: Block diagram of the achieved and designed closed-loop systems

The closed-loop output error is defined as

$$\varepsilon_{oe}(\rho,t) = y(\rho,t) - y_d(t) \tag{2.10}$$

where $y_d(t)$ is the output of the designed closed-loop system or the desired output, and the closed-loop input error is

$$\varepsilon_{ie}(\rho,t) = u(\rho,t) - u_d(t) \tag{2.11}$$

where $u_d(t)$ is the controller output in the designed closed-loop system.

The closed-loop sensitivity functions are defined as follows

- Output sensitivity function

$$\mathcal{S}(K(\rho),G) = \frac{1}{1+GK(\rho)} = \frac{AR(\rho)}{A_c(K(\rho),G)} \tag{2.12}$$

- Complementary sensitivity function

$$\mathcal{T}(K(\rho),G) = \frac{GK(\rho)}{1+GK(\rho)} = \frac{BS(\rho)}{A_c(K(\rho),G)} \tag{2.13}$$

- Input sensitivity function

$$\mathcal{U}(K(\rho),G) = \frac{K(\rho)}{1+GK(\rho)} = \frac{AS(\rho)}{A_c(K(\rho),G)} \tag{2.14}$$

where $A_c(K(\rho), G) = AR(\rho) + BS(\rho)$ is the characteristic polynomial of the closed-loop system. The corresponding sensitivity functions for the desired closed-loop systems are

$$\mathcal{S}_d = \mathcal{S}(K_d, G_d) = \frac{1}{1 + G_d K_d} \tag{2.15}$$

$$\mathcal{T}_d = \mathcal{T}(K_d, G_d) = \frac{G_d K_d}{1 + G_d K_d} \tag{2.16}$$

$$\mathcal{U}_d = \mathcal{U}(K_d, G_d) = \frac{K_d}{1 + G_d K_d} \tag{2.17}$$

2.2 Estimation of $\partial y/\partial \rho$ using a model

As explained in the introductory section, the method proposed in this thesis is gradient based. The principal components of the gradient of the proposed performance criterion with respect to ρ are the derivatives $\frac{\partial y}{\partial \rho}$. Since these sensitivity derivatives are unknown, a way to compute their estimates using a model is presented in this section.

Note that the input and output of the plant in the closed-loop system can be described as

$$\begin{aligned} y(\rho, t) &= \mathcal{T}(K(\rho), G) r(t) + \mathcal{S}(K(\rho), G) v(t) \\ &= \frac{B(q^{-1}) S(q^{-1})}{A_c(q^{-1}, K(\rho), G)} r(t) + \frac{A(q^{-1}) R(q^{-1})}{A_c(q^{-1}, K(\rho), G)} v(t) \end{aligned} \tag{2.18}$$

$$\begin{aligned} u(\rho, t) &= \mathcal{U}(K(\rho), G) \left(r(t) - v(t) \right) \\ &= \frac{A(q^{-1}) S(q^{-1})}{A_c(q^{-1}, K(\rho), G)} \left(r(t) - v(t) \right) \end{aligned} \tag{2.19}$$

and that

$$e(\rho, t) = \mathcal{S}(K(\rho), G) \left(r(t) - v(t) \right) = \frac{A(q^{-1}) R(q^{-1})}{A_c(q^{-1}, K(\rho), G)} \left(r(t) - v(t) \right) \tag{2.20}$$

The derivatives of y with respect to the parameters of R are computed as

follows [2]:

$$\begin{aligned}\frac{\partial y}{\partial r^{(j)}} &= \frac{-q^{-j}ABS}{A_c^2(K(\rho),G)}\,r(t) + \frac{q^{-j}AA_c(K(\rho),G) - q^{-j}AAR}{A_c^2(K(\rho),G)}\,v(t) \\ &= \frac{-Bq^{-j}}{A_c(K(\rho),G)}\left[\frac{AS}{A_c(K(\rho),G)}\,(r(t)-v(t))\right] \\ &= \frac{-B}{A_c(K(\rho),G)}\,u(t-j) \qquad j=1,\ldots,n_r \end{aligned} \tag{2.21}$$

In the same way, the derivatives of y with respect to the parameters of S can be computed:

$$\frac{\partial y}{\partial s^{(j)}} = \frac{B}{A_c(K(\rho),G)}\,e(t-j) \qquad j=0,\ldots,n_s \tag{2.22}$$

Thus, the gradient of y with respect to ρ can be represented in terms of the regressor vector ϕ filtered by B/A_c:

$$\psi^T(\rho,t) = \frac{\partial y(\rho,t)}{\partial \rho} = \frac{B}{A_c(K(\rho),G)}\phi^T(\rho,t) \tag{2.23}$$

Note that it is possible to measure the signals $e(t)$ and $u(t)$, i.e. the regressor vector $\phi(\rho,t)$ is available. Since the controller parameters are known, a model of the plant is needed to estimate $\psi(\rho,t)$. This model can be identified using the data collected on the plant operating in open or closed loop.

2.3 Robbins-Monro procedure

Stochastic approximation schemes have been developed as a response to a need for methods that can efficiently provide the roots of some function in situations where the influence of noise is not negligible compared to the required accuracy of the solution. The typical problem in this context is as follows. Let $f(\rho)$ be a monotonically increasing function. Suppose that one can observe the values of this function corrupted by measurement noise. Assume that the realization $\bar{f}(\rho_i)$ of $f(\rho_i)$ at ρ_i and time $i+1$ can be expressed as

$$\bar{f}(\rho_i) = f(\rho_i) + \xi_{i+1} \tag{2.24}$$

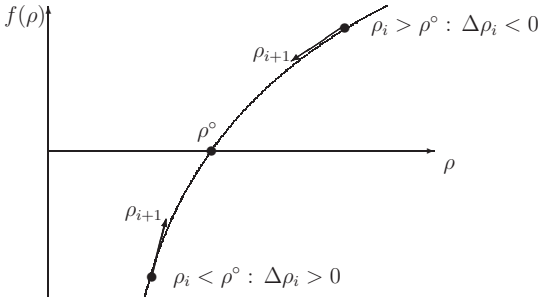

Figure 2.2: Robbins-Monro procedure: the idea

where $\xi_1, \xi_2, \ldots$ are independent zero-mean random variables. Find the solution of the equation

$$f(\rho) = 0 \tag{2.25}$$

In their pioneering work Robbins and Monro have proposed the following scheme to address this problem [70]. For a given initial point ρ_0, use the following recursion:

$$\rho_{i+1} = \rho_i - \gamma_i \bar{f}(\rho_i) \tag{2.26}$$

to solve (2.25). A sequence of positive numbers γ_i must be chosen that verifies

$$\sum_{i=1}^{\infty} \gamma_i^2 < \infty, \quad \sum_{i=1}^{\infty} \gamma_i = \infty \tag{2.27}$$

The idea is intuitively clear. The update $\Delta\rho_i = \rho_{i+1} - \rho_i$ will be positive on average for the values $\rho_i < \rho^\circ$ since its conditional expectation for a given ρ_i is as follows:

$$E\left\{\Delta\rho_i | \rho_i\right\} = -\gamma_i f(\rho_i) \tag{2.28}$$

For the values $\rho_i > \rho^\circ$ this update will be negative on average. In other words, the recursion (2.26) pushes the sequence ρ_i to approach ρ° (see

Fig. 2.2). The first condition in (2.27) ensures that the updates $\Delta\rho_i$ are "damped" throughout the recursion, otherwise the sequence ρ_i will oscillate around ρ°. The second condition in (2.27) ensures that $\Delta\rho_i$ does not decrease too fast, otherwise the sequence will not reach ρ°. Note that the random vectors ρ_i are in fact the realizations of the real variable ρ at the time i (or if the solution is sought iteratively at the iteration i).

The following result will be needed subsequently to prove the convergence of the Robbins-Monro multidimensional procedure that is extensively used in this thesis [5].

Theorem 2.1 *Let ρ be a vector in $\mathcal{R}^k$. Suppose that for each ρ there corresponds a random vector $\bar{f}(\rho) \in \mathcal{R}^k$. Let $f(\rho) = E\left\{\bar{f}(\rho)\right\}$. Now let $h(\rho)$ be a real-valued function defined on $\mathcal{R}^k$ and possessing continuous partial derivatives of the first and second order. The vector of first partial derivatives is denoted as $Q_h(\rho)$ and the matrix of second partial derivatives by $\mathcal{A}_h(\rho)$. Then, for any real number γ, by Taylor's theorem one has,*

$$\begin{aligned} h(\rho - \gamma\bar{f}(\rho)) &= h(\rho) - \gamma\langle Q_h(\rho), \bar{f}(\rho)\rangle \\ &\quad + \frac{1}{2}\gamma^2\langle \bar{f}(\rho), \mathcal{A}_h(\rho - \theta\gamma\bar{f}(\rho))\bar{f}(\rho)\rangle \end{aligned} \tag{2.29}$$

where θ is a real number with $0 \leq \theta \leq 1$. By taking expectation on both sides of (2.29) one gets

$$\begin{aligned} E\left\{h(\rho - \gamma\bar{f}(\rho))\right\} &= h(\rho) - \gamma\langle Q_h(\rho), f(\rho)\rangle \\ &\quad + \frac{1}{2}\gamma^2 E\left\{\langle \bar{f}(\rho), \mathcal{A}_h(\rho - \theta\gamma\bar{f}(\rho))\bar{f}(\rho)\rangle\right\} \end{aligned} \tag{2.30}$$

Then, let $\{\gamma_i\}$ be a sequence of positive numbers and consider the sequence of recursively defined random vectors given in (2.26). Moreover, assume $f(0) = 0$ without loss of generality and, together with (2.27), consider the following set of conditions:

(i) $h(\rho) \geq 0$

(ii) $\sup_{\epsilon < \|\rho\|} \langle Q_h(\rho), f(\rho)\rangle > 0 \quad$ *for every* $\quad \epsilon > 0$

(iii) $\inf_{\epsilon \leq \|\rho\|} \|h(\rho) - h(0)\| > 0 \quad$ *for every* $\quad \epsilon > 0$

(iv) $E\left\{\langle \bar{f}(\rho), \mathcal{A}_h(\rho - \theta\gamma\bar{f}(\rho))\bar{f}(\rho)\rangle\right\} < V_\gamma < \infty$ *and* $V_\gamma \geq 0$ *for every number* γ

Then the sequence $\{\rho_i\}$ *defined by (2.26) converges to zero almost surely.*

In Theorem 2.1 the $\langle\cdot,\cdot\rangle$ operator denotes the inner product of two vectors, while the $\|\cdot\|$ operator denotes the norm of a vector.

In addition to the convergence property of a recursive scheme, one is also interested to analyze how fast the estimates approach the solution. In other words, the behavior of the stochastic variable $\rho_i - \rho^\circ$ is of interest. The following theorem provides sufficient conditions for the asymptotic normality of the sequence $\sqrt{i}(\rho_i - \rho^\circ)$ [65].

Theorem 2.2 *Consider the process defined in (2.26) with initial condition* $\rho_0 = \rho$. *Let the sequence* γ_i *be given as* $\gamma_i = \frac{\alpha}{i}$ *where* α *is a positive constant. Suppose that the following conditions are satisfied:*

(i) The process defined in (2.26) converges to ρ° *almost surely as* $i \to \infty$ *and is a Markov process.*

(ii) The function $f(\rho)$ *may be represented by* $f(\rho) = Q(\rho^\circ)(\rho - \rho^\circ) + o(|\rho - \rho^\circ|)$, *where the matrix* $D = \frac{1}{2}I - \alpha Q(\rho^\circ)$ *is stable in the sense that its eigenvalues have a negative real part.*

(iii) All the elements of the matrix $E\left\{\left(\bar{f}(\rho_i) - f(\rho_i)\right)\left(\bar{f}(\rho_i) - f(\rho_i)\right)^T\right\}$ *are finite for* $i \geq 1$ *and* $\lim_{i\to\infty}\lim_{\rho_i\to\rho^\circ} = \lim_{i\to\infty} E\left\{\bar{f}(\rho^\circ)\bar{f}(\rho^\circ)^T\right\} = P$.

(iv) For some $\theta > 0$,

$$\lim_{\Xi\to\infty}\sup_{|\rho_i-\rho^\circ|}\sup_{i\geq 1}\int_{|\bar{f}(\rho_i)-f(\rho_i)|>\Xi}|\bar{f}(\rho_i) - f(\rho_i)|^2\mathcal{P}d\omega = 0$$

with Ξ *being a real variable and* $\mathcal{P}$ *a probability density function corresponding to* $\bar{f}(\rho_i)$.

Then, the sequence $\sqrt{i}(\rho_i - \rho^\circ) \in As\mathcal{N}(0, V)$, *i.e.* $\sqrt{i}(\rho_i - \rho^\circ)$ *converges asymptotically in distribution to a zero-mean normal distribution with covariance*

$$V = \alpha^2\int_0^\infty e^{Dx}\,P\,e^{D^Tx}dx \tag{2.31}$$

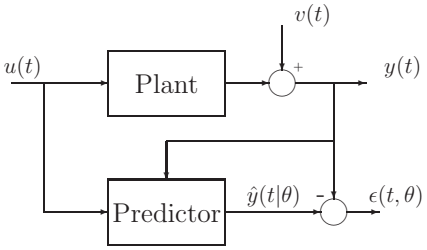

Figure 2.3: Open-loop identification problem

For more details about the stochastic approximation schemes and their features, the reader is referred to [86, 65]

2.4 The correlation approach in system identification

In this section, the idea of the correlation approach that inspired the development of CbT is presented. Consider the open-loop identification problem shown in Fig. 2.3. Suppose that the true system is given as follows:

$$y(t) = \varphi^T(t)\theta^\circ + v(t) \tag{2.32}$$

where $\varphi(t)$ is a regressor vector containing the delayed versions of input and output, and $v(t)$ is a zero-mean noise. Consider also the predictor in the form of the linear regression model:

$$\hat{y}(t|\theta) = \varphi^T(t)\hat{\theta} \tag{2.33}$$

In the correlation approach, a good model of the system is considered to be one that makes the prediction error $\epsilon(t,\theta) = y(t) - \hat{y}(t|\theta)$ uncorrelated with the input signal $u(t)$. Intuitively is clear that if $\epsilon(t,\theta)$ is correlated with $u(t)$ then all available information about $y(t)$ is not contained in $\hat{y}(t|\theta)$. This can be formulated mathematically as follows. Find the solution of the

following equation:

$$\frac{1}{N}\sum_{t=1}^{N}\zeta(t)\epsilon(t,\theta)=\frac{1}{N}\sum_{t=1}^{N}\zeta(t)\left(y(t)-\varphi^T(t)\hat{\theta}\right)=0 \tag{2.34}$$

where $\zeta(t)$ is the vector of Instrumental Variables (IV). The explicit form of the solution follows easily:

$$\hat{\theta}=\left[\frac{1}{N}\sum_{t=1}^{N}\zeta(t)\varphi^T(t)\right]^{-1}\left[\frac{1}{N}\sum_{t=1}^{N}\zeta(t)y(t)\right] \tag{2.35}$$

By replacing $y(t)$ from (2.32) in the above expression, one gets for the IV estimate:

$$\hat{\theta}=\theta^{\circ}+\left[\frac{1}{N}\sum_{t=1}^{N}\zeta(t)\varphi^T(t)\right]^{-1}\left[\frac{1}{N}\sum_{t=1}^{N}\zeta(t)v(t)\right] \tag{2.36}$$

This estimate is consistent if the following holds:

$$E\left\{\zeta(t)\varphi^T(t)\right\}\text{ has full rank} \tag{2.37}$$

$$E\left\{\zeta(t)v(t)\right\}=0 \tag{2.38}$$

Therefore, to ensure the consistency of the IV estimates, the instrumental variables should be chosen so as to be independent of the noise sequence and correlated with the regressor vector. A common choice for the instrumental variables are filtered versions of the input.

Observe that the well-known least-squares method can be obtained if one takes $\zeta(t)=\varphi(t)$. Note that, in this case, the estimate $\hat{\theta}$ will be consistent if and only if the regressor vector $\varphi(t)$ is not correlated with the noise $v(t)$. In general, the regressor vector contains samples of the output (see Fig. 2.3) and therefore, for this condition to be satisfied, $v(t)$ must be white noise which is very restrictive.

2.5 Iterative feedback tuning

As discussed before, one of the major problems in the context of gradient-based data-driven control is the computation of the gradient of the perfor-

mance criterion with respect to the controller parameters. The distinctive feature of the Iterative Feedback Tuning method is that an unbiased estimate of this gradient can be computed from signals obtained on the actual closed-loop system.

Consider the achieved and designed closed-loop systems shown in Fig. 2.1. Here, for simplicity of presentation, the minimization of the following criterion is considered:

$$J(\rho) = \frac{1}{2N} \sum_{t=1}^{N} E\left\{\varepsilon_{oe}^2(\rho, t)\right\} \tag{2.39}$$

The first derivative of the criterion (2.39) with respect to the controller parameters is:

$$\frac{\partial J}{\partial \rho} = \frac{1}{N} \sum_{t=1}^{N} E\left\{\varepsilon_{oe}(\rho, t) \frac{\partial y(\rho, t)}{\partial \rho}\right\} \tag{2.40}$$

The minimum of the criterion (2.39) is attained when the expression (2.40) is equal to zero. The roots of $\partial J/\partial \rho$ can be found by applying the Robbins-Monro stochastic approximation procedure provided that an unbiased estimate of this gradient is available.

Consider now the expression for the output $y(\rho, t)$ given in (2.18). The differentiation of $y(\rho, t)$ with respect to the i-th element of ρ gives:

$$\left.\frac{\partial y(\rho, t)}{\partial \rho_i}\right|_{\rho} = \mathcal{S}(\rho, G) G \left.\frac{\partial K(\rho)}{\partial \rho_i}\right|_{\rho} (r(t) - y(\rho, t)) \tag{2.41}$$

This expression gives an idea of how to obtain an estimate of $\partial y(\rho, t)/\partial \rho$ by performing two experiments on the actual closed-loop system. That is, perform a first experiment under normal operational conditions and collect measurements of the output $y(\rho, t)$. All signals appearing during this experiment will carry the subscript $e1$; similarly, the signals from the second experiment will have the subscript $e2$. For example, $y_{e1}(\rho, t)$ denotes the measured output during the first experiment. Then, in the second experiment, form the signal $r(t) - y_{e1}(\rho, t)$ and inject it at the process input. Then collect the output signal $y_{e2}(\rho, t)$ and filter it with the filter $\partial K(\rho)/\partial \rho$ to obtain a realization of $\partial y(\rho, t)/\partial \rho$. Illustration of this so-called gradient experiment is given in Fig. 2.4. Now, the estimate of $\partial J/\partial \rho$ is calculated

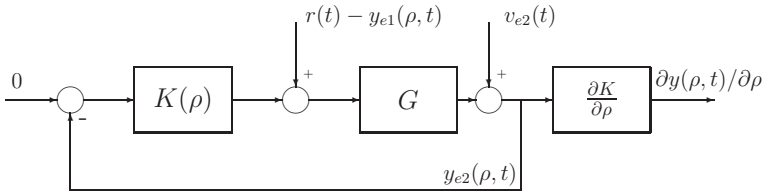

Figure 2.4: IFT: gradient experiment

as follows:

$$\widehat{\frac{\partial J}{\partial \rho}}(\rho_i) = \frac{1}{N}\sum_{t=1}^{N}\left[\frac{\partial K(\rho)}{\partial \rho} y_{e2}(\rho_i, t)\right](y_{e1}(\rho_i, t) - y_d(t)) \tag{2.42}$$

Hjalmarsson and co-workers have shown that this estimate is unbiased [34]. The controller parameters are updated using the following iterative formula:

$$\rho_{i+1} = \rho_i - \gamma_i H_i^{-1} \widehat{\frac{\partial J}{\partial \rho}}(\rho_i) \tag{2.43}$$

where H_i is some positive-definite matrix. A typical choice for this matrix might be an approximation of the Hessian, i.e.

$$H_i = \widehat{\frac{\partial^2 J}{\partial \rho^2}}(\rho_i) = \frac{1}{N}\sum_{t=1}^{N}\left[\frac{\partial K(\rho)}{\partial \rho} y_{e2}(\rho_i, t)\right]\left[\frac{\partial K(\rho)}{\partial \rho} y_{e2}(\rho_i, t)\right]^T \tag{2.44}$$

IFT offers a very nice possibility of obtaining an unbiased estimate of the gradient using only signals collected in closed loop. However, the price to pay is an increased number of experiments. For the case of two-degree-of-freedom SISO controllers, IFT requires three experiments per iteration. In the case of MIMO controllers, the number of experiments per iteration increases to $n_u \times n_y + 1$.There have been some attempts to reduce the number of experiments in the case of MIMO systems [15, 16, 38].

Chapter 3

Decorrelation Procedure

A method for iterative controller tuning using data acquired in closed-loop operation is presented in this chapter. It is assumed that a reasonable model of the plant to be controlled is at one's disposal and that it is used to design the controller. Furthermore, it is assumed that the control design is performed with all precautions to ensure that the desired specifications for tracking, disturbance rejection and control effort penalization for that model are satisfied. Very often, when such a designed controller is used, the achieved closed-loop performance is mediocre or unsatisfactory and it is desirable to improve it. To perform this task, a new data-driven method is proposed. Since the performance criterion within this method is based on the correlation approach, this scheme is coined Correlation-based Tuning (CbT). It is important to understand that the CbT approach is intended for a "fine" tuning of the controller. In other words, it is assumed that the controller obtained in model-based design procedure is in the vicinity of the controller that satisfies all design specifications for the actual system.

The basic idea of CbT is to make the output error between the designed and achieved closed-loop systems uncorrelated with the reference signal. This way the loop transfer functions of the achieved and designed closed-loop systems coincide, i.e. there remains no information about the excitation signal in the closed-loop output error. The controller parameters are calculated as the solution to a cross-correlation equation involving instrumental variables. The controller whose parameters are the solution to the cross-correlation equation is called subsequently the decorrelating controller.

Since the proposed control design objective involves mathematical ex-

pectations that are in general not known, the Robbins-Monro stochastic approximation scheme is used. One of the contributions of this chapter is to provide sufficient conditions for this iterative algorithm to converge toward the solution of the correlation equation. Convergence of this scheme depends on the choice of instrumental variables. It turns out that this dependence can be expressed in the form of a mild SPR condition on some transfer function. Furthermore, this condition gives insight for the choice of instruments.

Another goal of this chapter is to provide an analytic expression for the asymptotic covariance of the controller parameter estimates. It is shown that this covariance depends on the covariance of the estimates of the cross-correlation function. The expression for the asymptotic accuracy of the controller parameter estimates is useful since it allows one to construct the optimal instrumental variables.

The second part of this chapter explores situations when a large number of data is available. In this case, the influence of noise is within an acceptable level with respect to the required accuracy of the solution. Therefore, it is possible to use the deterministic Newton-Raphson algorithm to find the roots of the cross-correlation function. This algorithm converges faster than the Robbins-Monro scheme, which makes it more adapted to industrial applications. Due to the presence of noise, the obtained estimated controller parameters converge toward a region around the decorrelating controller instead of to one single point. An asymptotic expression for this region is derived and, based on it, a stopping condition for the iterative procedure is introduced.

Chapter outline: Section 3.2 presents the numerical stochastic approximation method used to compute the controller parameters. Conditions for the convergence of this algorithm are discussed and appropriate choices of instrumental variables are proposed. The study of the accuracy of the controller parameters as the number of iterations goes to infinity finishes this section. Section 3.3 treats the case when the number of data is sufficiently large to use the Newton-Raphson algorithm to update the controller parameters. An application to an experimental setup is detailed in Section 3.4. Finally, Section 3.5 gives some concluding remarks.

3.1 The control design criterion

The cross-correlation function that reflects the idea expressed in the previous section is as follows:

$$f(\rho) \triangleq E\{\bar{f}(\rho)\} \tag{3.1}$$

where $E\{\cdot\}$ denotes the mathematical expectation and $\bar{f}(\rho)$ is defined as follows

$$\bar{f}(\rho) = \frac{1}{N}\sum_{t=1}^{N} \zeta(t)\varepsilon_{oe}(\rho, t) \tag{3.2}$$

where N is the number of data and $\zeta(t)$ an n_ζ-dimensional column vector of instrumental variables that are correlated with the reference signal $r(t)$ and independent of the disturbance $v(t)$. The instrumental variable vector $\zeta(t)$ may be a function of the controller parameter vector ρ and will be denoted by $\zeta(\rho, t)$.

Note that, if the transfer function of the true plant were known, the controller K° that perfectly decorrelates the output error and the reference signal could be computed analytically as follows

$$K^\circ = K_d \frac{G_d}{G} \tag{3.3}$$

This controller may be improper or of very high order. Furthermore, it may destabilize the system if the unstable zeros and poles of G are not contained in G_d. On account of this fact, two different situations can be distinguished:

1. The decorrelating controller K° exists, stabilizes the closed-loop system and belongs to the parameterized set of controllers. Though, this assumption seems to be too restrictive, it allows the parametric convergence and the accuracy of the estimates to be studied. These analyses give important guidelines for the choice of instrumental variables and the improvement of the convergence rate of the iterative algorithm.

   The parameter vector of this controller, ρ°, is evidently a solution of the correlation equation

   $$f(\rho) = 0 \tag{3.4}$$

2. The decorrelating controller K° does not exist or does not belong to the controller set. In this case, the controller parameters can be computed

as the minimizing argument of some norm of the correlation function (3.1). This case will be studied in detail in Chapter 4.

3.2 Iterative solution using the Robbins-Monro procedure

In this chapter, assuming that a decorrelating controller exists, the parameters of the tuned controller are computed as a solution of the correlation equation (3.4). In fact, if $n_\zeta = n_\rho$, (3.4) represents a system of n_ρ nonlinear equations in n_ρ unknowns. Since this system of equations can be expressed in vector form and its solution can be expressed as a vector, in the following (3.4) will be called simply "equation".

Following the discussion from Section 2.3, it is easy to see that the equation (3.4) is of the exact type for which the Robbins-Monro stochastic approximation algorithm is intended. In other words, a solution of this correlation equation can be found using the following iterative stochastic approximation algorithm

$$\rho_{i+1} = \rho_i - \gamma_i \bar{f}(\rho_i) \tag{3.5}$$

where γ_i is a positive scalar step size and $\bar{f}(\rho_i)$ can be easily computed from (3.2) using data collected during the closed-loop experiment with the controller $K(\rho_i)$.

Before proceeding to analyze the properties of this procedure in the context of correlation-based tuning, let us introduce some general assumptions.

3.2.1 Assumptions

(A1) The system to be controlled is SISO, linear time-invariant, finite order and strictly causal.

(A2) The noise $v(t)$ is a zero-mean stationary stochastic process with bounded fourth moments and a rational, nonsingular spectral density matrix. Realizations of the noise in different experiments are mutually independent.

(A3) The reference signal $r(t)$ is persistently exciting of sufficiently high order (with respect to the number of controller parameters) and is uncorrelated with the disturbance $v(t)$.

(A4) The signals in the loop are bounded, i.e. the computed controllers stabilize the closed-loop system at each iteration.

(A5) The correlation function $f(\rho)$ possesses continuous partial derivatives of first and second order with respect to ρ.

(A6) Given the orders of the decorrelating controller K° (n_r° and n_s°), the orders n_r and n_s of the tuned controller satisfy the following inequality

$$\min(n_r - n_r^\circ, n_s - n_s^\circ) \geq 0 \tag{3.6}$$

(A7) The solution ρ° of the correlation equation is unique.

Assumption A1 defines the class of systems to be considered. Assumption A2 ensures that a solution of the correlation equation (3.4) exists. Observe from (3.1), (3.2) and (3.4) that this solution exists if $\zeta(\rho^\circ, t)$ or $\varepsilon_{oe}(\rho^\circ, t)$ are zero-mean signals. If $v(t)$ is zero mean, then $\varepsilon_{oe}(\rho^\circ, t)$ is a zero-mean signal. If A2 is not satisfied, $\varepsilon_{oe}(\rho^\circ, t)$ can be made zero mean by introducing an integrator term into the controller. Indeed, the integrator forces $\varepsilon_{oe}(\rho^\circ, t) = \mathcal{S}(K(\rho^\circ), G)v(t)$ to zero at low frequencies. If the integrator is not desirable, $\zeta(\rho^\circ, t)$ can be chosen so as to be zero mean. Assumption A3 is a classical assumption for the excitation signal in parameter estimation algorithms based on the correlation approach. Assumption A4 may be rather restrictive for some systems, but it is absolutely required for implementing the controllers on the real system in each iteration. In practice, a stability test based on the designed model of the plant G_d or the model identified in the previous iteration can be performed before implementing a controller. Assumption A5 is verified for rational controllers (under assumption A1). Assumption A6 implies that there is at least one solution to the correlation equation and this solution is attainable by the estimates.

3.2.2 Convergence

In this section, the conditions for which the controller parameters updated with (3.5) converge toward the solution ρ° of the equation (3.4) are stated.

Theorem 3.1 *Under Assumptions A1-A7, the iterative parameter update algorithm defined by (3.2) and (3.5) converges to a solution of the correlation equation (3.4) when $i \to \infty$ almost surely, provided that:*

(C1) *The sequence γ_i of positive step sizes satisfies*

$$\sum_{i=1}^{\infty} \gamma_i = \infty \quad \text{and} \quad \sum_{i=1}^{\infty} \gamma_i^2 < \infty.$$

(C2) *$f(\rho)$ is monotonically increasing in the vicinity of the solution ρ°, i.e. the following condition holds:*

$$Q(\rho) = E\left\{ \left. \frac{\partial \bar{f}(\rho)}{\partial \rho} \right|_{\rho} \right\} > 0, \quad \exists \delta_\rho > 0 \text{ such that } |\rho - \rho^\circ| < \delta_\rho \tag{3.7}$$

Proof. The proof of the theorem follows by applying Theorem 2.1 stated in Section 2.3 to the iterative algorithm defined by (3.2) and (3.5). If one sets $h(\rho) = f^T(\rho) f(\rho)$, then condition (i) of Theorem 2.1 follows naturally. Conditions (ii) and (iii) follow from C2, while condition (iv) is satisfied due to A2 and A5. □

Observe that the principal requirement for convergence is the positive definiteness of $Q(\rho)$ in the vicinity of the solution. The fulfillment of this requirement depends on the choice of the instrumental variables $\zeta(t)$, which is studied below.

3.2.3 Choice of instrumental variables

Let the gradient of the closed-loop output error with respect to ρ be denoted by $\psi(\rho, t)$ and the instrumental variables be a function of ρ, then the matrix $Q(\rho)$ can be represented as

$$Q(\rho) = E\left\{ \frac{1}{N} \sum_{t=1}^{N} \frac{\partial \zeta(\rho, t)}{\partial \rho} \varepsilon_{oe}(\rho, t) + \frac{1}{N} \sum_{t=1}^{N} \zeta(\rho, t) \psi^T(\rho, t) \right\} \tag{3.8}$$

Near the solution, the first term in equation 3.8 is close to zero (because the derivatives of the instrumental variables are not correlated with the closed-loop output error) and can be neglected. Now, it is clear that an ideal choice of the instrumental variables is a noise-free estimate of the gradient $\psi(\rho,t)$, which makes $Q(\rho)$ as close as possible to a positive definite matrix. On the other hand, the gradient of the closed-loop output error can be expressed in terms of the regressor vector $\phi(\rho,t)$ as was demonstrated in Section 2.2

$$\psi^T(\rho,t)=\frac{\partial \varepsilon_{oe}(\rho,t)}{\partial \rho}=\frac{\partial y(\rho,t)}{\partial \rho}=\frac{B(q^{-1})}{A_c(K(\rho),G)}\phi^T(\rho,t) \tag{3.9}$$

Therefore, a noise-free estimate of the gradient can be obtained in the following ways:

1) IV based on designed closed loop: A noise-free estimate of the gradient is based on the model G_d, the controller K_d, and the signals in the designed closed-loop system.

$$\begin{aligned}\zeta(t)=\psi_d(t) \;&=\; \frac{B_d(q^{-1})}{A_c(q^{-1},K_d,G_d)}[-u_d(t-1),\cdots,-u_d(t-n_r),\\ &\quad e_d(t),\cdots,e_d(t-n_s)]^T\end{aligned} \tag{3.10}$$

where $A_c(q^{-1},K_d,G_d)$ is the characteristic polynomial of the designed closed-loop system. This IV variant is very simple and needs no extra computational effort at each iteration. In addition, the instrumental variables are not functions of ρ, and the first term in (3.8) is identically zero. However, if the modeling error $G-G_d$ is large, the estimation error will be large and the positive definiteness of Q may not be guaranteed.

2) IV based on controller parameters: The instrumental variables are based on the controller $K(\rho)$ and the available model of the plant G_d.

$$\zeta(\rho,t)=\tilde{\psi}(\rho,t)=\frac{B_d(q^{-1})}{A_c(q^{-1},K(\rho),G_d)}\tilde{\phi}(\rho,t) \tag{3.11}$$

where $\tilde{\phi}(\rho,t)$ is defined as

$$\begin{aligned}\tilde{\phi}(\rho,t) &= [-\tilde{u}(\rho,t-1),\cdots,-\tilde{u}(\rho,t-n_r),\\ &\quad \tilde{e}(\rho,t),\cdots,\tilde{e}(\rho,t-n_s)]^T\end{aligned} \tag{3.12}$$

with $\tilde{u}(\rho,t) = \mathcal{U}(K(\rho),G_d)r(t)$ and $\tilde{e}(\rho,t) = \mathcal{S}(K(\rho),G_d)r(t)$. With this choice of IV, the positive definiteness of $Q(\rho)$ in neighborhood of ρ° can be shown and so the convergence of the algorithm can be ensured under some weak conditions.

3) IV based on the identified model: The instrumental variables are based on the controller $K(\rho)$ and the identified model of the plant $\hat{G} = \hat{B}/\hat{A}$.

$$\zeta(\rho,t) = \psi_{im}(\rho,t) = \frac{\hat{B}(q^{-1})}{A_c(q^{-1},K(\rho),\hat{G})}\phi_{im}(\rho,t) \tag{3.13}$$

where $\phi_{im}(\rho,t)$ is defined as

$$\begin{aligned}\phi_{im}(\rho,t) &= [-\hat{u}(\rho,t-1),\cdots,-\hat{u}(\rho,t-n_r),\\ &\quad \hat{e}(\rho,t),\cdots,\hat{e}(\rho,t-n_s)]^T\end{aligned} \tag{3.14}$$

with $\hat{u}(\rho,t) = \mathcal{U}(K(\rho),\hat{G})r(t)$ and $\hat{e}(\rho,t) = \mathcal{S}(K(\rho),\hat{G})r(t)$. For this choice of IV, one might identify a model in the initial iteration and use it subsequently through the iterative procedure. Another possibility is to identify models in the first few iterations (since better control-oriented models are obtained as the computed controllers are closer to the decorrelating controller) and then to "freeze" the identification. It is also possible to make the convergence condition milder using this choice of IV.

3.2.4 Fixed terms in the controller

In order to preserve certain properties of the initial controller (e.g. integral action), fixed terms can be considered in the R and S polynomials (i.e., $R = R'R_{fix}$ and $S = S'S_{fix}$). In this case, the input $u(t)$ and the output $y(t)$ of the system are replaced in $\psi(\rho,t)$ by $u'(t) = R_{fix}u(t)$ and $y'(t) = S_{fix}y(t)$, respectively. Then, R' and S' are computed using the iterative algorithm

and later multiplied by the fixed terms to obtain the controller polynomials R and S.

3.2.5 Algorithm

Having elucidated the choice of instrumental variables, let us summarize the CbT algorithm.

Algorithm 3.1 *Starting with the initial controller* $K(q^{-1}, \rho_i) = K_d(q^{-1})$, $i = 0$, *computed using the model* $G_d(q^{-1})$, *perform the following steps:*

(1) Collect N samples of the signals $u(\rho_i)$ *and* $y(\rho_i)$ *from the closed-loop experiment with the controller* $K(q^{-1}, \rho_i)$ *operating on the actual system. If needed, filter* $u(\rho_i)$ *and* $y(\rho_i)$ *with* R_{fix} *and* S_{fix}, *respectively.*

(2) Construct the vector of instrumental variables $\zeta(\rho_i)$ *as one of the choices presented in Section 3.2.3. Compute* $\bar{f}(\rho_i)$ *from (3.2) using the acquired data and constructed* $\zeta(\rho_i)$.

(3) Calculate the new controller parameter vector ρ_{i+1} *according to the recursion (3.5). Add the fixed terms* R_{fix} *and* S_{fix} *if applicable.*

(4) Using G_d *or an identified model, test the stability of the closed-loop system formed by this model and the controller* $K(q^{-1}, \rho_{i+1})$. *If the test fails, reduce* γ_i *in (3.5) as follows* $\gamma_i = \alpha\gamma_i$, $0 < \alpha < 1$, *and go to step (3).*

(5) Replace i *with* $i+1$ *and repeat steps (1)-(4) until* $\|\rho_{i+1} - \rho_i\| < \epsilon$, *where* ϵ *is appropriately chosen.*

Let us recall that no gradient estimates are needed for this algorithm to converge. Note that all quantities required for this algorithm are either known to the user or measurable on the closed-loop system. The sequence of step sizes γ_i should satisfy the condition $C1$, but it is a user choice. A possible choice for γ_i is to take $\gamma_i = 1/i$. Finally, observe that only one experiment per iteration is required, which is advantageous compared to the related IFT method.

3.2.6 2DOF controllers

The CbT scheme can be applied in a straightforward manner for the tuning of two-degree-of-freedom controllers. Let us consider an RST controller with the following control law:

$$R(q^{-1})u(t) = -S(q^{-1})y(t) + T(q^{-1})r(t) \tag{3.15}$$

where $R(q^{-1})$ and $S(q^{-1})$ are defined in Section 2.1 and

$$T(q^{-1}) = t_0 + t_1 q^{-1} + \cdots + t_{n_t} q^{-n_t} \tag{3.16}$$

Hence, the controller output can be presented in regression form:

$$u(t) = \phi_e^T(\rho_e, t)\rho_e \tag{3.17}$$

where the regressor vector $\phi_e(\rho_e, t)$ and the vector of controller parameters ρ_e are defined as follows:

$$\begin{aligned} {\phi_e}^T(\rho_e, t) &= [-u(t-1), \cdots, -u(t-n_r), \\ &\quad -y(t), \cdots, -y(t-n_s), r(t), \cdots, r(t-n_t)] \qquad (3.18) \\ \rho_e^T &= [r^{(1)}, \cdots, r^{(n_r)}, s^{(0)}, \cdots, s^{(n_s)}, t^{(0)}, \cdots, t^{(n_t)}] \qquad (3.19) \end{aligned}$$

Now, it suffices in Algorithm 3.1 to replace ρ_i with ρ_{ei}, $\phi(\rho, t)$ with $\phi_e(\rho_e, t)$ and, if necessary, to introduce the fixed term T_{fix} in steps (1) and (3). Observe that the introduction of an additional degree of freedom does not increase the required number of experiments per iteration.

3.2.7 Sufficient condition for positive-definiteness of $Q(\rho)$

It should be noted that the crucial condition for the convergence of the iterative algorithm (3.5) is the positive definiteness of $Q(\rho)$. Now, let $Q(\rho)$ be evaluated at ρ° for the IV choice based on controller parameters

$$Q(\rho^\circ) = E\left\{\frac{1}{N}\sum_{t=1}^{N} \tilde{\psi}(\rho^\circ, t)\psi^T(\rho^\circ, t)\right\} \tag{3.20}$$

It is clear that the positive definiteness of $Q(\rho^\circ)$ guarantees the positive definiteness of $Q(\rho)$ in the vicinity of the solution because of the assumption on the continuity of the derivative of $Q(\rho)$. Furthermore, the gradient vector $\psi(\rho,t)$ can be expressed as

$$\begin{aligned}\psi^T(\rho,t) =& \frac{B}{A_c(K(\rho),G)}\left[\frac{-AS}{A_c(K(\rho),G)}r(t-1),\cdots,\frac{-AS}{A_c(K(\rho),G)}r(t-n_r),\right.\\ &\left.\frac{AR}{A_c(K(\rho),G)}r(t),\cdots,\frac{AR}{A_c(K(\rho),G)}r(t-n_s)\right]+\psi_v^T(\rho,t)\\ =& \frac{AB}{A_c^2(K(\rho),G)}[r(t),\cdots,r(t-n_\rho+1)]\,M^T(\rho)+\psi_v^T(\rho,t) \qquad (3.21)\end{aligned}$$

where $\psi_v(\rho,t)$ is the noisy part of the gradient vector (uncorrelated with the reference signal) and $M^T(\rho)$ an $n_\rho \times n_\rho$ dimensional Sylvester matrix associated with the polynomials $S(q^{-1})$ and $R(q^{-1})$ defined as

$$M(\rho)=\begin{bmatrix} 0 & -s^{(0)} & \cdots & -s^{(n_s)} & & \\ & & \ddots & & \ddots & 0 \\ 0 & & & -s^{(0)} & \cdots & -s^{(n_s)} \\ 1 & r^{(1)} & \cdots & r^{(n_r)} & & \\ & \ddots & \ddots & & \ddots & 0 \\ 0 & & 1 & r^{(1)} & \cdots & r^{(n_r)} \end{bmatrix} \qquad (3.22)$$

In the same way, the noise-free estimate of the gradient can be expressed by

$$\tilde{\psi}^T(\rho,t)=\frac{A_dB_d}{A_c^2(K(\rho),G_d)}[r(t),\cdots,r(t-n_\rho+1)]\,M^T(\rho) \qquad (3.23)$$

Then, substituting (3.23) and (3.21) into (3.20) and considering the fact that $\tilde{\psi}(\rho,t)$ is not correlated with $\psi_v(\rho,t)$, gives

$$\begin{aligned}Q(\rho^\circ) \;=\; & M(\rho^\circ)E\left\{\frac{1}{N}\sum_{t=1}^{N}\mathcal{H}(\rho^\circ)[r_f(t),\cdots,r_f(t-n_\rho+1)]^T\right.\\ & \left.\times\,[r_f(t),\cdots,r_f(t-n_\rho+1)]\right\}M^T(\rho^\circ) \qquad (3.24)\end{aligned}$$

where

$$r_f(t)=\frac{AB}{A_c^2(K(\rho^\circ),G)}r(t) \qquad (3.25)$$

and

$$\mathcal{H}(\rho^\circ) = \frac{\mathcal{S}(K(\rho^\circ), G_d)\mathcal{T}(K(\rho^\circ), G_d)}{\mathcal{S}(K(\rho^\circ), G)\mathcal{T}(K(\rho^\circ), G)} = \frac{\mathcal{S}(K(\rho^\circ), G_d)\mathcal{T}(K(\rho^\circ), G_d)}{\mathcal{S}_d\,\mathcal{T}_d} \quad (3.26)$$

Note that at the decorrelating solution ρ°, the sensitivity and complementary sensitivity functions of the achieved closed-loop system are equal to those of the designed one.

Theorem 3.2 *Suppose that Assumptions A1-A7 hold and $\zeta(\rho, t) = \tilde{\psi}(\rho, t)$ (defined in equation 3.11). Then, $Q(\rho^\circ)$ defined in (3.20) is positive definite if:*

(i) *$r_f(t)$ is a stationary stochastic process or a deterministic periodic signal persistently exciting of order equal to or greater than n_ρ.*

(ii) *The transfer function $\mathcal{H}(\rho^\circ)$ is strictly positive real.*

Proof: It is well known that the Sylvester matrix $M(\rho^\circ)$ is not singular if and only if the polynomials R^* and S^* are coprime [83] (this condition is satisfied under Assumptions A6-A7). Therefore, $Q(\rho^\circ)$ is positive definite if and only if

$$\begin{aligned} Z(\rho^\circ) \;=\; E\Bigg\{ & \frac{1}{N}\sum_{t=1}^{N} \mathcal{H}(\rho^\circ)[r_f(t), \cdots, r_f(t-n_\rho+1)]^T \\ & [r_f(t), \cdots, r_f(t-n_\rho+1)]\Bigg\} > 0 \end{aligned} \quad (3.27)$$

Let $x = [x_1 \dots x_{n_\rho}]^T$ be an arbitrary nonzero vector and define $X(q^{-1}) = x_1 + x_2 q^{-1} + \cdots + x_{n_\rho} q^{-n_\rho+1}$. Then, by definition $Z(\rho^\circ) > 0$ iff $x^T Z(\rho^\circ) x > 0$. One has

$$\begin{aligned} x^T Z(\rho^\circ) x &= E\left\{ \frac{1}{N}\sum_{t=1}^{N} [\mathcal{H}(\rho^\circ) X(q^{-1}) r_f(t)][X(q^{-1}) r_f(t)] \right\} \\ &= \frac{1}{2\pi}\int_{-\pi}^{\pi} \mathcal{H}(\rho^\circ, e^{j\omega}) |X(e^{j\omega})|^2 \Phi_{r_f}(\omega) d\omega \\ &= \frac{1}{2\pi}\int_{-\pi}^{\pi} Re[\mathcal{H}(\rho^\circ, e^{j\omega})] |X(e^{j\omega})|^2 \Phi_{r_f}(\omega) d\omega \end{aligned} \quad (3.28)$$

where $\Phi_{r_f}(\omega)$ is the spectral density of r_f which according to (i) is nonzero at least in n_ρ frequencies. Therefore, if $\mathcal{H}(\rho^\circ)$ is SPR, then $Z(\rho^\circ)$ and consequently $Q(\rho^\circ)$ are positive definite. □

Remarks:

1. The SPR condition is a sufficient condition. In fact, if $Re\{\mathcal{H}(\rho^\circ, e^{j\omega})\} > 0$ in the frequency region where the spectrum of the excitation signal is large, $Q(\rho_i)$ is positive definite. For example, for a sum of sinusoidal signals, it suffices that the real part of the sensitivity function estimates $\mathcal{S}$ and $\mathcal{T}$ based on the plant model in the frequency domain have the same sign as those of the real sensitivity functions in the excited frequencies. This condition is likely to be satisfied if a closed-loop identified model is used to construct the instrumental variables. Note that the model used for constructing the instrumental variables should only satisfy equation (3.28) and it is not necessarily a good model for controller design.

2. The results can be extended to deterministic nonperiodic signals if the number of data N goes to infinity.

For the IV choice based on controller parameters, the results of Theorems 3.1 and 3.2 allow the sufficient condition for the convergence of the Algorithm 3.1 to be precisely stated.

Proposition 3.1 *Consider the choice of instrumental variables based on controller parameters (3.11). Let the Assumptions A1-A7 hold. Then, the Algorithm 3.1 converges to a solution of the correlation equation (3.4) when $i \to \infty$ almost surely, provided that:*

(C1) *The sequence γ_i of positive step sizes satisfies*

$$\sum_{i=1}^{\infty} \gamma_i = \infty \quad \text{and} \quad \sum_{i=1}^{\infty} \gamma_i^2 < \infty.$$

(C2′) *$r_f(t)$ defined in (3.25) is a stationary stochastic process or a deterministic periodic signal, persistently exciting of order equal to or greater than n_ρ.*

(C2″) *The transfer function $\frac{\mathcal{S}(K(\rho^\circ),G_d)\mathcal{T}(K(\rho^\circ),G_d)}{\mathcal{S}_d\,\mathcal{T}_d}$ is strictly positive real.*

Remark: The results of Proposition 3.1 apply mutatis mutandis to the choice of instrumental variables based on the identified model. This is not surprising considering that in some implementations G_d and $\hat{G}$ may coincide, i.e. G_d might be obtained as a result of closed-loop identification.

Next, when conditions for the convergence to a solution of the cross-correlation function are established, the behavior of the controller parameter estimates around the solution will be analyzed.

3.2.8 Asymptotic accuracy when i tends to infinity

In this section, the asymptotic distribution of the controller parameter estimates will be analyzed through the following theorem.

Theorem 3.3 *Assume that*

(i) The Algorithm 3.1 converges to ρ° almost surely as $i \to \infty$.

(ii) The sequence of step sizes is chosen as $\gamma_i = \frac{\alpha}{i}$ where α is a positive constant.

(iii) The matrix $D = I/2 - \alpha Q(\rho^\circ)$ has all eigenvalues with negative real parts.

Then, the sequence $\sqrt{i}(\rho_i - \rho^\circ)$ converges asymptotically in distribution to a normally distributed zero-mean random variable with covariance matrix

$$V = \alpha^2 \int_0^\infty e^{Dx} P_f \, e^{D^T x} dx \tag{3.29}$$

where the covariance matrix P_f of $\bar{f}(\rho^\circ)$ is defined as follows:

$$P_f = E\left\{\bar{f}(\rho^\circ)\bar{f}^T(\rho^\circ)\right\} \tag{3.30}$$

Proof. The proof follows directly by applying Theorem 2.2 stated in Section 2.3. □

This analysis can help one to obtain a measure of the accuracy of the estimates. However, the covariance matrix V depends on the unknown vector of controller parameters ρ° and cannot be computed. Here, a natural

estimate of V using the available information at the i-th iteration is given. Let us assume that the disturbance $v(t)$ can be described as

$$v(t) = H(q^{-1})\eta(t) \tag{3.31}$$

where $H(q^{-1})$ is a linear, asymptotically stable noise model, and $\eta(t)$ is the zero-mean white noise with variance σ^2. Then, after straightforward calculations (see Section 3.3.3), the asymptotic expression for the covariance of $\bar{f}(\rho^\circ)$ when $N \to \infty$ is given as

$$\lim_{N\to\infty} P_f = \lim_{N\to\infty} E\left\{\bar{f}(\rho^\circ)\bar{f}^T(\rho^\circ)\right\} = \sigma^2 E\{\zeta_f(\rho^\circ, t)\zeta_f^T(\rho^\circ, t)\} \tag{3.32}$$

where

$$\zeta_f(\rho^\circ, t) = H(q^{-1})\mathcal{S}(K(\rho^\circ), G)\zeta(\rho^\circ, t) = H(q^{-1})\,\mathcal{S}_d\,\zeta(\rho^\circ, t) \tag{3.33}$$

Note that the designed closed-loop transfer function $\mathcal{S}_d$ is equal to the decorrelating one, $\mathcal{S}(K(\rho^\circ), G)$, and is used instead. By replacing H in (3.33) with an estimate $\hat{H}$, a reasonable estimate $\hat{\zeta}_f(\rho_i, t)$ of $\zeta_f(\rho_i, t)$ can be obtained. Then, an estimate of the covariance matrix P_f, when the number of data N is large, can be obtained with the current estimates of the controller parameters as follows

$$\hat{P}_f = \frac{\sigma^2}{N}\sum_{t=1}^{N} \hat{\zeta}_f(\rho_i, t)\hat{\zeta}_f^T(\rho_i, t) \tag{3.34}$$

Then, an estimate of the covariance matrix V can be given by

$$\hat{V} = \alpha^2 \int_0^\infty e^{\hat{D}x}\,\hat{P}_f\,e^{\hat{D}^T x}dx \tag{3.35}$$

where $\hat{D} = I/2 - \alpha\hat{Q}(\rho_i)$ and

$$\hat{Q}(\rho_i) = \frac{1}{N}\sum_{t=1}^{N} \zeta(\rho_i, t)\hat{\psi}^T(\rho_i, t) \tag{3.36}$$

The matrix $\hat{Q}(\rho_i)$ is an estimate of the Jacobian of the correlation function based on the estimate of the gradient $\hat{\psi}^T(\rho_i, t)$ that can be computed using

the model of the plant and the controller $K(\rho_i)$ as follows

$$\hat{\psi}^T(\rho_i, t) = \frac{B_d}{A_c(K(\rho_i), G_d)}\phi(\rho_i, t) \tag{3.37}$$

Note that the instrumental variable $\zeta(\rho_i, t)$ is not necessarily dependent on ρ_i, for example $\zeta(\rho_i, t) = \psi_d(t)$.

3.3 Iterative solution using the Newton-Raphson algorithm

In the previous section, an iterative stochastic approximation procedure for solving equation (3.4) is proposed. Although the proposed procedure converges under weak conditions to the solution ρ°, the convergence rate is slow and therefore not suitable for industrial applications. However, if the number of data can be chosen to be sufficiently large so that, for a fixed controller, the variation of $\bar{f}(\rho)$ in different experiments with different noise realizations is within an acceptable range, the Newton-Raphson algorithm can be used to search for ρ°. This is the topic of this section.

3.3.1 Newton-Raphson algorithm

Within this algorithm, the controller parameters are updated in the following way

$$\rho_{i+1} = \rho_i - \gamma_i \hat{Q}^{-1}(\rho_i)\bar{f}(\rho_i) \tag{3.38}$$

where the Jacobian estimate $\hat{Q}(\rho_i)$ is given in (3.36). The step-size γ_i is typically chosen to be equal to 1 in all iterations. In practice, however, γ_i can be reduced in iterations where the resulting controller destabilizes the system.

Although the Jacobian estimate is sensitive to modeling errors, an inaccuracy in this estimate does not hinder the convergence. In fact, as mentioned in Section 1.5, this inaccuracy reduces the convergence rate [48]. The following example, taken from [42], investigates the influence of modeling errors on the convergence speed in the absence of noise. It will be shown that, with reduced-order identified models, the proposed algorithm converges to

the solution of the cross-correlation equation.

Example 3.1 The output of the plant is generated as follows:

$$y(t) = \frac{q^{-1} + 0.5q^{-2}}{1 - 1.5q^{-1} + 0.7q^{-2}} u(t) \tag{3.39}$$

The designed closed-loop system is given in the form of the following reference model:

$$\mathcal{T}_d = \frac{-0.0781q^{-1} - 0.0625q^{-2} - 0.0117q^{-3}}{1 - 1.5781q^{-1} + 0.6375q^{-2} - 0.0117q^{-3}}$$

which has two poles at 0.7794 and one pole at 0.019. Using the pole-placement technique, the decorrelating controller can be easily computed as: $R^\circ(q^{-1}) = 1$ and $S^\circ(q^{-1}) = -0.0781 - 0.0234q^{-1}$ which gives $\rho^\circ = [-0.0781 \quad -0.0234]^T$. The same structure is considered for the initial controller with the initial parameter vector $\rho_0 = [0.075 \quad 0]^T$ which represents a proportional controller that stabilizes the closed-loop system.

Table 3.1: Influence of the modeling error

$n_{\hat{A}} = deg(\hat{A})$	0	1	1	2	2
$n_{\hat{B}} = deg(\hat{B})$	1	1	2	1	2
No. iter.	55	11	9	6	5

Consider the CbT variant where the instrumental variables are computed using the current controller and the plant model $\hat{G} = \hat{B}/\hat{A}$ identified in closed loop. The reference signal $r(t)$ is a PRBS generated by an 11-bit shift register (data length $N = 2047$). Table 3.1 gives the number of iterations needed to achieve a parametric distance of 1e-9, defined as $PD = (\rho_i - \rho^\circ)^T(\rho_i - \rho^\circ)$, for different orders of the polynomials $\hat{A}$ and $\hat{B}$.

It is clearly seen that the speed of convergence depends on the order of the identified plant model. Furthermore, note that Algorithm 3.2 gives consistent estimates even when the plant is modeled only by a gain ($n_{\hat{A}} = 0$ and $n_{\hat{B}} = 1$). ⊡

3.3.2 Relation to standard IFT

To facilitate comparison, the standard IFT method will be presented in regression form. By substituting (2.42) and (2.44) in (2.43), one has

$$\rho_{i+1} = \rho_i - \gamma_i \left\{ \sum_{t=1}^{N} \psi_{IFT}(\rho_i, t) \psi_{IFT}^T(\rho_i, t) \right\}^{-1} \sum_{t=1}^{N} \psi_{IFT}^T(\rho_i, t) \varepsilon_{cl}(\rho_i, t) \quad (3.40)$$

where

$$\psi_{IFT}^T(\rho_i, t) = \left[\frac{\partial K(\rho)}{\partial \rho} y_{e2}(\rho_i, t) \right] \quad (3.41)$$

It is interesting to compare the expression (3.40) with that of the correlation approach with, for example, the instrumental variables $\zeta(\rho, t) = \tilde{\psi}(\rho, t)$:

$$\rho_{i+1} = \rho_i - \gamma_i \left\{ \sum_{t=1}^{N} \tilde{\psi}(\rho, t) \hat{\psi}^T(\rho_i, t) \right\}^{-1} \sum_{t=1}^{N} \tilde{\psi}(\rho, t) \varepsilon_{cl}(\rho_i, t) \quad (3.42)$$

It is clear that these two equations are very similar. However, in the presence of noise, the methods are clearly different. The matrix in braces in (3.40) is a biased Gauss-Newton approximation of the Hessian due to the disturbance in the second experiment [34]. This generally decreases the convergence rate of IFT in the neighborhood of the solution. Note that, with two additional special experiments at each iteration of the IFT algorithm, one can construct an unbiased estimate of the Hessian directly from data collected on the closed loop system [76]. On the other hand, the estimate of the Jacobian matrix in (3.42) is not affected by noise in the vicinity of the solution (since $\tilde{\psi}$ is not correlated with the noisy part of the gradient estimate $\hat{\psi}$). Thus, even for the same number of iterations (three times more experiments for the IFT for the tuning of two-degree-of-freedom controllers), it is expected that the correlation method gives better results.

Although CbT and IFT are closely related methods, one should keep in mind that they differ in two very important aspects: (i) underlying control objective; (ii) way of obtaining the gradient estimates.

The two methods are compared in the following example. Observe that two-degree-of-freedom controllers are tuned, which imposes a different construction of the regressor vector for CbT, see Section 3.2.6.

Example 3.2 Extensive Monte Carlo simulations have been performed in order to compare the proposed correlation approach to standard IFT. The simulated test system is given by the following transfer function:

$$G = \frac{q^{-1} + 0.5q^{-2}}{(1 - 1.5q^{-1} + 0.7q^{-2})(1 - 0.5q^{-1})} \tag{3.43}$$

The dominant dynamics is characterized by one very oscillatory mode. The initial controller is calculated by pole placement using the following reduced-order model:

$$G_d = \frac{8q^{-1} + 2.6q^{-2}}{1 - 1.2q^{-1} + 0.6q^{-2}} \tag{3.44}$$

This model was purposely chosen as a poor approximation to the true plant G. The first design specification is to obtain a closed-loop system that preserves the natural frequency of the dominant mode of the open-loop system, but with a damping factor of 0.95. As a second requirement, the polynomial $R(q^{-1}, \rho_0)$ should contain the fixed factor $R_{fix}(q^{-1}) = 1 - q^{-1}$ in order to provide integral action. The precompensator $T(q^{-1}, \rho_0)$ is chosen to obtain unity closed-loop gain. The initial controller reads:

$$R(q^{-1}, \rho_0) = 1 - 0.7238q^{-1} - 0.2762q^{-2} \tag{3.45}$$

$$S(q^{-1}, \rho_0) = 0.1189 - 0.1565q^{-1} + 0.0637q^{-2} \tag{3.46}$$

$$T(q^{-1}, \rho_0) = 0.0261 \tag{3.47}$$

The instrumental variables based on identified closed-loop models (3.13) are chosen. The plant model $\hat{G}$ is identified in closed loop using a second-order ARMAX structure. Model-order mismatch is introduced to show that an approximate model can be used in the calculations without significant loss in performance.

In order to compare the standard IFT algorithm and CbT, the averaged control criterion, ACC, is introduced:

$$ACC(i) = \frac{1}{n_{mc}} \sum_{k=1}^{n_{mc}} J^{(k)}(\rho_i) \tag{3.48}$$

where n_{mc} denotes the number of simulations and i denotes the iteration number. $J^{(k)}$ is the IFT control criterion defined in (2.39) for the k-th

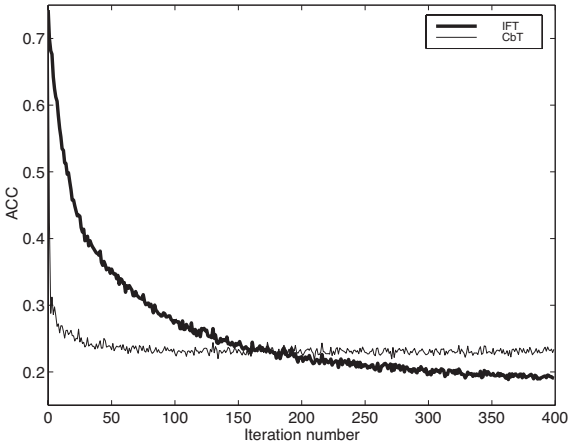

Figure 3.1: Criterion J averaged over 100 noise realizations for IFT (thick line) and CbT (thin line) over 400 iterations

Monte Carlo simulation. Although the criterion (2.39) is not minimized by the CbT method, it is reduced because this method tries to suppress the correlated part of the closed-loop output error.

In the first part, in order to compare the asymptotic behavior of two algorithms, 100 Monte Carlo simulations are performed. For each simulation run, the optimization is carried out over 400 iterations. Each experiment is performed with a different realization of the measurement noise, which is generated as a zero-mean, stationary, white Gaussian sequence with a standard deviation $\sigma = \pm 0.025$. The reference signal is a unit step.

A Gauss-Newton update direction with step size $\gamma_i = 1$ is used in the IFT procedure. Penalty on the control effort is not incorporated in the criterion. The step size $\gamma_i = 1$ is also chosen for CbT. The two approaches are compared in terms of ACC in Fig. 3.1. It is clear from the figure that IFT, as expected, converges to a lower value of the criterion ACC than CbT. However, in the first iterations CbT reduces the criterion much faster.

Since, in practice, only the first few iterations are of interest, in the second part, 500 simulations are performed, each with 9 iterations, i.e. 27 experiments in the case of IFT and 9 experiments for CbT. The simulation conditions (measurement noise, reference signal and designed output) are

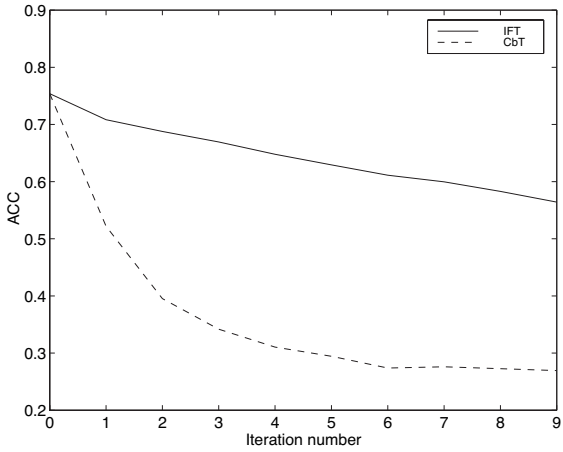

Figure 3.2: Criterion J averaged over 500 noise realizations for IFT (solid) and CbT (dashed) over 9 iterations

the same as those in the first part. Fig. 3.2 shows that CbT reaches the final value after 6 iterations, while the cost with IFT decreases at a much slower rate. Notice the remarkable speed of convergence and the low ACC value for CbT. ⊡

3.3.3 Asymptotic accuracy when N tends to infinity

In practice, the solution of the correlation equation may necessitate a large number of iterations for convergence. Furthermore, the limited amount of data points in each experiment affects the stochastic properties of the controller parameter estimates. Finally, process disturbances and measurement noise introduce errors in the solution. It is therefore of interest to study the convergence rate of the algorithm. Other important questions that arise in this context are when to stop the iterations and how close the resulting controller is to the decorrelating one.

In this section, a confidence interval based on the covariance of the correlation function is introduced. This confidence interval helps determine to what extent the current controller decorrelates the closed-loop output error from the reference signal. An expression, asymptotic in data length N, for

the accuracy of the controller parameters around the solution of the correlation equation is derived. This allows one to construct a region around the resulting controller that contains the decorrelating controller with a given probability. An asymptotic expression for the accuracy of the controller transfer function estimate that characterizes this region is also derived. Another reason for studying these properties is that the covariance matrix of the controller parameter estimates helps choose optimal instruments in the sense that they provide maximal accuracy.

When the number of data points N tends to infinity, the iterative procedure (3.38) converges to the unique solution ρ° of the correlation equation (3.4) provided that it exists. However, for a finite N, a different solution to (3.4) results for each realization of the noise, i.e. instead of a unique solution one has a set of solutions. This set is centered around ρ° and its "size" depends strongly on the stochastic properties of the noise. The size of this set is characterized by the covariance of the correlation equation. Expressions that are asymptotic in N for this covariance are derived next.

The asymptotic expressions for the accuracy of the controller transfer function estimate derived in this section are dual to the variance formulas for the estimated plant model of an LTI system in the field of system identification [53, 54, 20]. To show this, the following assumptions are introduced in this section: (i) the disturbance $v(t)$ acting at the plant output (see upper part of Fig. 2.1) can be expressed in the form:

$$v(t) = G(q^{-1})w(t) \tag{3.49}$$

where $w(t)$ is a zero-mean stationary random process, and (ii) G is inversely stable. In addition, for mathematical convenience, the controller parameter vector and the regressor vector are constructed differently compared to the remainder of this thesis. That is, assuming $n_s = n_r - 1 = n$, the controller parameter vector $\tilde{\rho}$ is written as follows:

$$\tilde{\rho}^T = [\tilde{\rho}_1^T, \tilde{\rho}_2^T, \ldots, \tilde{\rho}_n^T] \tag{3.50}$$

where $\tilde{\rho}_l^T = [r^{(l)}, s^{(l-1)}]$, $l = 1, \ldots n$; $\dim(\tilde{\rho}) = n_{\tilde{\rho}} = 2n$. With (3.49) and Assumption (ii), it can be considered as if $w(t)$ acts at the plant input (see

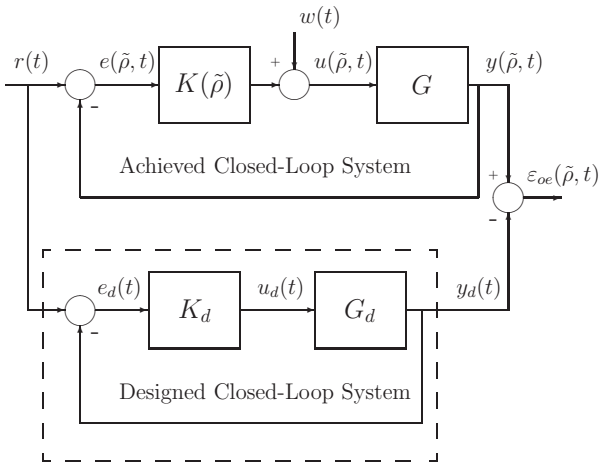

Figure 3.3: Closed-loop output error resulting from a comparison of the achieved and designed closed-loop systems

upper part of Fig. 3.3):

$$u(\tilde{\rho}, t) = K(q^{-1}, \tilde{\rho})e(\tilde{\rho}, t) + w(t) \tag{3.51}$$

It is assumed that the measurements of $r(t)$ and $y(\tilde{\rho}, t)$ are available. The excitation signal $r(t)$ is assumed to be uncorrelated with the disturbance signal $w(t)$. It is furthermore assumed that $w(t)$ is described by:

$$w(t) = H_n(q^{-1})\eta(t) \tag{3.52}$$

where $H_n(q^{-1})$ is a linear, asymptotically stable and inversely stable noise model, and $\eta(t)$ the zero-mean white noise with variance σ^2.

We denote

$$\vartheta^T(\tilde{\rho}, t-1) = [-u(\tilde{\rho}, t-1), e(\tilde{\rho}, t)] \tag{3.53}$$

and form the $2n$-dimensional regressor vector

$$\phi_\vartheta^T(\tilde{\rho}, t) = [\vartheta^T(\tilde{\rho}, t-1), \cdots, \vartheta^T(\tilde{\rho}, t-n)]. \tag{3.54}$$

Now, the derivative of $\varepsilon_{cl}(\tilde{\rho}, t)$ with respect to $\tilde{\rho}$ can formally be expressed

as:

$$\psi_{\vartheta}^{T}(\tilde{\rho},t)=\frac{\partial\varepsilon_{cl}(\tilde{\rho},t)}{\partial\tilde{\rho}}=\frac{B(q^{-1})}{A_c(K(\tilde{\rho}),G)}\phi_{\vartheta}^{T}(\tilde{\rho},t) \tag{3.55}$$

Stopping condition

There is no use continuing the iterations if each element of the vector $f(\tilde{\rho}_i)$ is within a confidence interval defined by the corresponding element on the main diagonal of the covariance matrix of $\bar{f}(\tilde{\rho}^{\circ})$. Let us assume that, based on this idea, the iterative procedure stops after m iterations and the controller $\tilde{\rho}_m$ is obtained. Then, from the expression for the covariance of $\bar{f}(\tilde{\rho}^{\circ})$, it is possible to calculate the asymptotic variance of the controller parameter estimates, as will be shown below. This variance, in turn, allows one to construct the confidence ellipsoid around the optimal controller $\tilde{\rho}^{\circ}$ that contains the controller $\tilde{\rho}_m$ with the probability P_m. Now, using the explicit expression for the variance of the controller parameter estimates at the optimal solution, it is possible to construct around $\tilde{\rho}_m$ a region containing the optimal controller $\tilde{\rho}^{\circ}$ with the same probability P_m. This region could be interpreted as a controller uncertainty set. Expressions for this region that are asymptotic in N are derived below for both the controller parameters and the controller transfer function.

Using the Central Limit Theorem [54], the distribution of the random variable $\sqrt{N}\bar{f}(\tilde{\rho}^{\circ})$ can be characterized. The following result can be established.

Theorem 3.4 *Consider expression (3.2). Suppose that the assumptions A1-A4 and A7 hold. Then, as the data length N tends to infinity, $\sqrt{N}\bar{f}(\tilde{\rho}^{\circ})$ tends in distribution to a normal distribution with zero mean and covariance P_{fn} defined as:*

$$P_{fn}=\sigma^2 E\left\{\zeta_{fn}(\tilde{\rho}^{\circ},t)\zeta_{fn}^{T}(\tilde{\rho}^{\circ},t)\right\} \tag{3.56}$$

where $\zeta_{fn}(\tilde{\rho}^{\circ},t)=H_{cl}(\tilde{\rho}^{\circ})\zeta(\tilde{\rho}^{\circ},t)$ with

$$H_{cl}(\tilde{\rho}^{\circ})=\frac{BR(\tilde{\rho}^{\circ})}{A_c(K(\tilde{\rho}^{\circ}),G)}H_n=G\mathcal{S}(K(\tilde{\rho}^{\circ}),G)H_n=\sum_{i=0}^{\infty}h_i q^{-i} \tag{3.57}$$

Proof. The proof follows the ideas of Theorem 5.1 and its corollary in [74], p. 75, where the asymptotic distribution of parameter estimates for

the extended IV open-loop estimator is investigated. Here, since the data are collected in closed loop, the transfer function between the white-noise input $\eta(t)$ and the output $y(t)$ is $H_{cl}(\tilde{\rho}^\circ)$ defined in (3.57). Considering that the number of parameters is equal to the number of instrumental variables, the proof follows easily. □

Using this result as a stopping condition, one can test whether the k-th element of the correlation equation $f(k, \tilde{\rho}_i)$ falls inside the confidence interval (see Fig. 3.4):

$$|f(k, \tilde{\rho}_i)| \leq \sqrt{\frac{\hat{P}_{fn}(k,k)}{N}} \mathcal{N}_\alpha \quad \forall k = 1, \ldots, n_{\tilde{\rho}} \tag{3.58}$$

where

$$\hat{P}_{fn} = \frac{\sigma^2}{N} \sum_{t=1}^{N} \hat{\zeta}_{fn}(\tilde{\rho}_i, t) \hat{\zeta}_{fn}^T(\tilde{\rho}_i, t) \tag{3.59}$$

and $\mathcal{N}_\alpha$ is the α-level of the normal distribution $\mathcal{N}(0,1)$. In $\hat{\zeta}_{fn}(\tilde{\rho}_i, t)$, it is necessary to replace G, H_{cl} and $\mathcal{S}$ by their estimates $\hat{G}$, $\hat{H}_{cl}$ and $\hat{\mathcal{S}}$.

In practice, this test shows whether the selected controller order is appropriate. If $f(k, \tilde{\rho}_i),\ \forall k = 1, \ldots, n_{\tilde{\rho}}$ does not enter the confidence interval after a large number of iterations, the controller order should be increased.

Asymptotic variance of controller parameter estimates

The variance of the controller parameter estimates in the neighborhood of the optimal controller is calculated as follows. Assume that the optimal controller is used and one step of the iterative procedure is taken to produce the neighboring estimate $\tilde{\rho}_{nb}$:

$$\tilde{\rho}_{nb} = \tilde{\rho}^\circ - \gamma_i \hat{Q}_\vartheta^{-1}(\tilde{\rho}^\circ) \bar{f}(\tilde{\rho}^\circ) \tag{3.60}$$

where

$$\hat{Q}_\vartheta(\tilde{\rho}^\circ) = \frac{1}{N} \sum_{t=1}^{N} \zeta(\tilde{\rho}^\circ, t) \hat{\psi}_\vartheta{}^T(\tilde{\rho}^\circ, t) \tag{3.61}$$

The random variable $\tilde{\rho}_{nb} - \tilde{\rho}^\circ$ provides information regarding the accuracy of the method around the solution, and its asymptotic covariance matrix

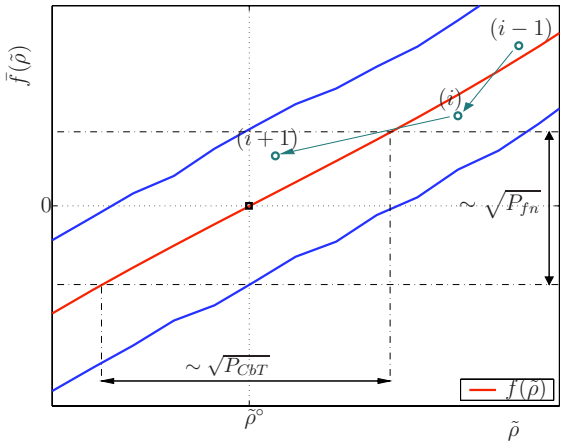

Figure 3.4: Confidence interval around $\tilde{\rho}^\circ$ for $n_{\tilde{\rho}} = 1$

characterizes the region containing $\tilde{\rho}_m$. The following result can be obtained.

Theorem 3.5 *Consider the parameter update law (3.60). Suppose that the Assumptions A1-A4 and A7 hold. Furthermore, assume that the step size γ_i is constant and equal to 1 throughout the iterations. Then, as the data length N tends to infinity, the distribution of the random variable $\sqrt{N}(\tilde{\rho}_{nb} - \tilde{\rho}^\circ)$ is asymptotically Gaussian:*

$$\sqrt{N}(\tilde{\rho}_{nb} - \tilde{\rho}^\circ) \in As\ \mathcal{N}(0, P_{CbT}) \tag{3.62}$$

with the covariance matrix P_{CbT} given as follows:

$$P_{CbT} = Q_\vartheta(\tilde{\rho}^\circ)^{-1} P_{fn} Q_\vartheta(\tilde{\rho}^\circ)^{-T} \tag{3.63}$$

where

$$Q_\vartheta(\tilde{\rho}^\circ) = \lim_{N\to\infty} \hat{Q}_\vartheta(\tilde{\rho}^\circ) = E\left\{\zeta(\tilde{\rho}^\circ, t)\psi_\vartheta^T(\tilde{\rho}^\circ, t)\right\} \tag{3.64}$$

Proof. This assertion follows immediately from Theorem 3.4 and the lemma A4.2 and its corollary in [74], p. 214. □

In practice, (3.63) can be evaluated by replacing the optimal controller parameter vector $\tilde{\rho}^\circ$ by the current value $\tilde{\rho}_i$. In the same way, since the exact value of $Q_\vartheta(\tilde{\rho}^\circ)$ is unknown, its estimate $\hat{Q}_\vartheta(\tilde{\rho}_i)$ is calculated using

expression (3.36).

Equations (3.56), (3.57) and (3.63) show that the covariance matrix P_{CbT} depends on the choice of the instrumental variable ζ in a rather complex way. In addition, P_{CbT} depends on the noise model $H_n(q^{-1})$ and the true plant. Since both are unknown, it is difficult to optimize the accuracy of the controller parameters. Fortunately, a solution to this problem has already been proposed in the field of system identification [74], and it will be detailed below.

Optimal choice of instrumental variables

In this section, a lower bound for P_{CbT} is first established, and then the choice of instrumental variables that makes this bound achievable is presented.

Let us denote by $\tilde{\phi}_\vartheta(\tilde{\rho}^\circ, t)$ the noise-free part of the regressor vector $\phi_\vartheta(\tilde{\rho}^\circ, t)$:

$$\tilde{\phi}_\vartheta(\tilde{\rho}^\circ, t) = [\tilde{\vartheta}^T(\tilde{\rho}^\circ, t-1), \cdots, \tilde{\vartheta}^T(\tilde{\rho}^\circ, t-n)]^T \tag{3.65}$$

with

$$\tilde{\vartheta}(\tilde{\rho}^\circ, t-1) = \left(-\frac{AS(\tilde{\rho}^\circ)}{A_c(K(\tilde{\rho}^\circ), G)} r(t-1), \frac{AR(\tilde{\rho}^\circ)}{A_c(K(\tilde{\rho}^\circ), G)} r(t) \right)^T \tag{3.66}$$

Theorem 3.6 *P_{CbT} given in (3.63) is bounded from below by:*

$$\underline{P} = \sigma^2 E \left\{ \frac{1}{R(\tilde{\rho}^\circ) H_n} \tilde{\phi}_\vartheta(\tilde{\rho}^\circ, t) \frac{1}{R(\tilde{\rho}^\circ) H_n} \tilde{\phi}_\vartheta{}^T(\tilde{\rho}^\circ, t) \right\}^{-1} \tag{3.67}$$

Moreover, $P_{CbT} = \underline{P}$ when the following relationship holds:

$$\sum_{i=0}^{\infty} \zeta(\tilde{\rho}^\circ, t+i) h_i = \frac{1}{R(\tilde{\rho}^\circ) H_n} \tilde{\phi}_\vartheta(\tilde{\rho}^\circ, t) \tag{3.68}$$

Proof. This is similar to the proof of Theorem 6.1 in [74], p. 96. Taking into account that $\zeta(\tilde{\rho}^\circ, t)$ is uncorrelated with $w(t)$, it follows from (3.64) with (3.55) and (3.57):

$$\begin{aligned} Q_\vartheta(\tilde{\rho}^\circ) &= E\left\{\zeta(\tilde{\rho}^\circ,t)\frac{B}{A_c(K(\tilde{\rho}^\circ),G)}\tilde{\phi}_\vartheta^T(\tilde{\rho}^\circ,t)\right\} \\ &= E\left\{\zeta(\tilde{\rho}^\circ,t)\sum_{i=0}^{\infty}h_i q^{-i}\frac{B}{A_c(K(\tilde{\rho}^\circ))H_{cl}(\tilde{\rho}^\circ)}\tilde{\phi}_\vartheta^T(\tilde{\rho}^\circ,t)\right\} \\ &= E\left\{\sum_{i=0}^{\infty}\zeta(\tilde{\rho}^\circ,t)h_i\frac{1}{R(\tilde{\rho}^\circ)H_n}\tilde{\phi}_\vartheta^T(\tilde{\rho}^\circ,t-i)\right\} \\ &= E\left\{\left[\sum_{i=0}^{\infty}\zeta(\tilde{\rho}^\circ,t+i)h_i\right]\frac{1}{R(\tilde{\rho}^\circ)H_n}\tilde{\phi}_\vartheta^T(\tilde{\rho}^\circ,t)\right\} \end{aligned} \tag{3.69}$$

Furthermore, the assumption of stationarity gives:

$$\frac{P_{fn}}{\sigma^2} = E\left\{\sum_{i=0}^{\infty}\zeta(\tilde{\rho}^\circ,t+i)h_i \times \sum_{l=0}^{\infty}\zeta(\tilde{\rho}^\circ,t+l)^T h_l\right\} \tag{3.70}$$

The matrix inequality

$$\begin{aligned} E\left\{\left[\frac{1}{R(\tilde{\rho}^\circ)H_n}\tilde{\phi}_\vartheta^T(\tilde{\rho}^\circ,t) \quad \sum_{i=0}^{\infty}\zeta^T(\tilde{\rho}^\circ,t+i)h_i\right]^T\right. \\ \left.\times\left[\frac{1}{R(\tilde{\rho}^\circ)H_n}\tilde{\phi}_\vartheta^T(\tilde{\rho}^\circ,t) \quad \sum_{i=0}^{\infty}\zeta^T(\tilde{\rho}^\circ,t+i)h_i\right]\right\} \geq 0 \end{aligned} \tag{3.71}$$

can equivalently be expressed as:

$$\begin{aligned} &E\left\{\frac{1}{R(\tilde{\rho}^\circ)H_n}\tilde{\phi}_\vartheta(\tilde{\rho}^\circ,t)\frac{1}{R(\tilde{\rho}^\circ)H_n}\tilde{\phi}_\vartheta^T(\tilde{\rho}^\circ,t)\right\} \\ &-\left[E\left\{\frac{1}{R(\tilde{\rho}^\circ)H_n}\tilde{\phi}_\vartheta(\tilde{\rho}^\circ,t)\sum_{i=0}^{\infty}\zeta^T(\tilde{\rho}^\circ,t+i)h_i\right\}\right. \\ &\times E\left\{\sum_{i=0}^{\infty}\zeta(\tilde{\rho}^\circ,t+i)h_i\sum_{i=0}^{\infty}\zeta^T(\tilde{\rho}^\circ,t+i)h_i\right\}^{-1} \\ &\left.\times E\left\{\sum_{i=0}^{\infty}\zeta(\tilde{\rho}^\circ,t+i)h_i\frac{1}{R(\tilde{\rho}^\circ)H_n}\tilde{\phi}_\vartheta^T(\tilde{\rho}^\circ,t)\right\}\right] \geq 0 \end{aligned} \tag{3.72}$$

Now, from (3.63), (3.67), (3.69), (3.70), and (3.72), it follows that $P_{CbT}^{-1} \leq \underline{P}^{-1}$. Finally, it is easy to verify that $P_{CbT} = \underline{P}$ when (3.68) holds. □

From (3.68), it is obvious that the choice of instruments

$$\zeta_{opt}(\tilde{\rho}^\circ, t) = \frac{1}{R(\tilde{\rho}^\circ)H_n H_{cl}(\tilde{\rho}^\circ)} \tilde{\phi}_\vartheta(\tilde{\rho}^\circ, t) \tag{3.73}$$

provides best accuracy. However, in order to implement ζ_{opt} throughout the iterations, one has to estimate the models of the noise H_n and the plant G, which imposes additional computational effort on the algorithm. In addition, in the filter in expression (3.73), the optimal parameters $\tilde{\rho}^\circ$ need to be replaced by the current values $\tilde{\rho}_i$. This seems to be a reasonable approximation considering the assumption that the current controller is in the neighborhood of the optimal controller.

Note that the data collected in closed loop can be filtered by a linear filter. This way, additional design variables are available to improve accuracy. However, this issue will not be addressed in this thesis.

Asymptotic variance of transfer function estimate

This section derives the variance expression for the transfer function estimate. This expression is asymptotic in both the number of data points and the model order.

Since $\tilde{\rho}_{nb}$ is in the vicinity of $\tilde{\rho}^\circ$, it follows from (3.63) and the Gauss approximation formula [54] that

$$\sqrt{N}(K(\tilde{\rho}_{nb}) - K(\tilde{\rho}^\circ)) \in As\ \mathcal{N}(0, \mathcal{P}_n(\omega)) \tag{3.74}$$

with

$$\mathcal{P}_n(\omega) = T(\omega, \tilde{\rho}^\circ) P_{CbT} T^T(-\omega, \tilde{\rho}^\circ) \tag{3.75}$$

where $T(\omega, \tilde{\rho}^\circ)$ is a $2n$-dimensional row vector representing the derivatives of $K(\tilde{\rho}^\circ)$ with respect to $\tilde{\rho}$.

The expression (3.75) is asymptotic in N, but exact in n. A simpler expression can be obtained for $n \to \infty$. To establish the result, the following lemma from [88] will be used.

Lemma 3.1 *Let $R_n^{(l)}$ be a $2n \times 2n$ block-Toeplitz matrix where the $(i-j)$*

2×2 *block is* $r_l(i-j)$. *Let*

$$\Phi_l(\omega) = \sum_{\tau=-\infty}^{\infty} r_l(\tau) e^{-j\omega\tau} \quad l = 1, 2$$

Then

$$\lim_{n\to\infty} \frac{1}{n} W_n(\omega)[R_n^{(1)}]^{-1} R_n^{(2)} W_n^T(-\omega) = [\Phi_1(\omega)]^{-1}\Phi_2(\omega)$$

where

$$W_n(\omega) = \begin{bmatrix} e^{-j\omega}I & e^{-2j\omega}I & \cdots & e^{-nj\omega}I \end{bmatrix} \tag{3.76}$$

I *being the* 2×2 *identity matrix.*

Proof. See the proof of Lemma 4.3 in [88]. □

Now, the result is given in the following theorem.

Theorem 3.7 *As* n *and* N *tend to infinity, the variance of the controller transfer function becomes:*

$$\operatorname{Var} K(\tilde{\rho}^\circ) \simeq \frac{n}{N} \frac{\Phi_w(\omega)}{\Phi_e^r(\omega)} \tag{3.77}$$

where Φ_e^r *is the contribution of the reference signal* $r(t)$ *to the spectrum of the control error:*

$$\Phi_e^r(\omega) = |\mathcal{S}(\omega)|^2 \Phi_r(\omega)$$

with $\Phi_r(\omega)$ *being the spectrum of the reference signal* $r(t)$.

Proof. Let us introduce the vector of instrumental variables

$$\zeta^T(t) = \begin{bmatrix} z^T(t-1), z^T(t-2), \cdots, z^T(t-n) \end{bmatrix} \tag{3.78}$$

where

$$z^T(t) = \begin{bmatrix} Z_1(q^{-1})r(t), Z_2(q^{-1})r(t) \end{bmatrix} = Z(q^{-1})r(t). \tag{3.79}$$

The derivative of $K(\tilde{\rho}^\circ)$ with respect to $\tilde{\rho}$ can be expressed as:

$$T(\omega, \tilde{\rho}^\circ) = D_\vartheta(\omega, \tilde{\rho}^\circ) W_n(\omega) \tag{3.80}$$

where

$$\begin{aligned} D_\vartheta(q^{-1},\tilde{\rho}^\circ) &= \left[-\frac{S(q^{-1},\tilde{\rho}^\circ)}{R^2(q^{-1},\tilde{\rho}^\circ)}, \frac{q}{R(q^{-1},\tilde{\rho}^\circ)}\right] \\ &= \frac{1}{R(q^{-1},\tilde{\rho}^\circ)}\Gamma^T(\tilde{\rho}^\circ) \end{aligned} \tag{3.81}$$

with $\Gamma^T(\tilde{\rho}^\circ) = \begin{bmatrix} -K(q^{-1},\tilde{\rho}^\circ) & q \end{bmatrix}$.

Assume that a regularizing term λI is added to the right-hand side of (3.64) and the resulting $Q_\vartheta(\tilde{\rho}^\circ) = E\left\{\zeta(\tilde{\rho}^\circ,t)\psi_\vartheta^T(\tilde{\rho}^\circ,t)\right\} + \lambda I$ is used to calculate P_{CbT} in (3.63). The elements $\vartheta(\tilde{\rho}^\circ,t)$ of the regression vector $\phi_\vartheta(\tilde{\rho}^\circ,t)$ can be expressed as:

$$\vartheta(\tilde{\rho}^\circ,t) = \frac{AR(\tilde{\rho}^\circ)}{A_c(K(\tilde{\rho}^\circ),G)}\Gamma(\tilde{\rho}^\circ)r(t) = \mathcal{S}(K(\tilde{\rho}^\circ),G)\Gamma(\tilde{\rho}^\circ)r(t) \tag{3.82}$$

with $\mathcal{S}(K(\tilde{\rho}^\circ),G)$ being the output sensitivity function. For the sake of simplicity of notation, the arguments $\tilde{\rho}^\circ$ and G are omitted in the following whenever appropriate. The cross-spectrum between $\zeta(t)$ and $\psi_\vartheta(t)$ reads:

$$\Phi_{\zeta\psi_\vartheta}(\omega) = Z(e^{-i\omega})\mathcal{S}(e^{i\omega})\frac{B(e^{i\omega})}{A_c(e^{i\omega})}\Gamma^T(e^{i\omega})\Phi_r(\omega) \tag{3.83}$$

Similarly, the Fourier transform of the Toeplitz matrix P_{fn} in (3.56) reads:

$$\Phi_{\zeta_{fn}}(\omega) = \sigma^2\left|H_{cl}(e^{-i\omega})\right|^2 Z(e^{-i\omega})Z^T(e^{i\omega})\Phi_r(\omega) \tag{3.84}$$

Finally, applying lemma 2.1 twice to the inner product of (3.75) and (3.80) gives:

$$\begin{aligned} \mathcal{M}_\lambda(\omega) &= \lim_{n\to\infty}\frac{1}{n}W_n(\omega)P_{CbT}W_n^T(-\omega) \\ &= \left(Z\mathcal{S}^*\frac{B^*}{A_c^*}\Gamma^{*T}\Phi_r + \lambda I\right)^{-1} \times \Phi_{\zeta_{fn}} \\ &\times \left(\mathcal{S}\frac{B}{A_c}\Gamma Z^{*T}\Phi_r + \lambda I\right)^{-1} \end{aligned} \tag{3.85}$$

where the arguments are omitted for the sake of simplicity and an asterisk is used to denote the complex conjugate. After straightforward but tedious

calculation, the expression from (3.85) can be reformulated as

$$\mathcal{M}_\lambda(\omega) = \frac{\sigma^2|H_{cl}|^2}{|\mathcal{S}|^2|\frac{B}{A_c}|^2\Phi_r}\frac{ZZ^{*T}}{|\Gamma Z^{*T} + \lambda I/(\mathcal{S}\frac{B}{A_c}\Phi_r)|^2} \tag{3.86}$$

Now, from (3.57), (3.75), (3.80), (3.81) and (3.86), one has

$$\begin{aligned}
\mathcal{P}(\omega) &= \lim_{\lambda\to 0}\lim_{n\to\infty}\frac{1}{n}\mathcal{P}_n(\omega,\lambda) \\
&= \lim_{\lambda\to 0} D_\vartheta(w,\tilde{\rho}^\circ)\mathcal{M}_\lambda(\omega)D_\vartheta^T(-w,\tilde{\rho}^\circ) \\
&= \lim_{\lambda\to 0}\frac{\Gamma^T}{R}\frac{\sigma^2|RH_n|^2}{|\mathcal{S}|^2\Phi_r}\times\frac{ZZ^{*T}}{|\Gamma Z^{*T} + \lambda I/(\mathcal{S}\frac{B}{A_c}\Phi_r)|^2}\frac{\Gamma^*}{R^*} \\
&= \frac{\sigma^2|H_n|^2}{|\mathcal{S}|^2\Phi_r}
\end{aligned} \tag{3.87}$$

Combining this expression with (3.31), one finally obtains:

$$\mathcal{P}(\omega) = \frac{\Phi_w(\omega)}{\Phi_e^r(\omega)} \tag{3.88}$$

where Φ_w denotes the spectrum of the random noise $w(t)$ and Φ_e^r the contribution of the reference signal $r(t)$ to the spectrum of the control error. The expression for the asymptotic variance of $K(\tilde{\rho}^\circ)$ follows readily from (3.88). □

The result (3.77) is interesting and not at all surprising. In fact, the variance is proportional to the ratio of the noise spectrum to the contribution of the reference signal $r(t)$ to the control error spectrum (Φ_w/Φ_e^r), with the factor of proportionality being the ratio of the number of parameters to the number of data points (n/N). This result is exactly dual to that in system identification [53, 54, 20], where the covariance of the plant model is proportional to the spectral ratio of the plant output noise and the plant input signal, with the same factor of proportionality. Note also that the estimate $K(\tilde{\rho}^\circ)$ is asymptotically based on only input-output properties at the frequency ω, i.e. independent of the choice of the instrumental variables.

3.3.4 Algorithm

Now, having introduced the stopping condition, the controller parameters are updated according to the following algorithm.

Algorithm 3.2 *Starting with the initial controller* $K(q^{-1}, \rho_i) = K_d(q^{-1})$, $i = 0$ *computed using the model* $Gd(q^{-1})$, *perform the following steps:*

(1) Collect N samples of the signals $u(\rho_i)$ *and* $y(\rho_i)$ *from the closed-loop experiment with the controller* $K(q^{-1}, \rho_i)$ *operating on the actual system. If needed, filter* $u(\rho_i)$ *and* $y(\rho_i)$ *with* R_{fix} *and* S_{fix}, *respectively.*

(2) Construct the vector of instrumental variables $\zeta(\rho_i)$ *as one of the choices presented in Section 3.2.3. Compute* $\bar{f}(\rho_i)$ *from (3.2) using the acquired data and constructed* $\zeta(\rho_i)$.

(3) Estimate the Jacobian using (3.36).

(4) Calculate the new controller parameter vector ρ_{i+1} *according to (3.38). Add the fixed terms* R_{fix} *and* S_{fix} *if applicable.*

(5) Using G_d *or an identified model, test the stability of the closed-loop system formed by this model and the controller* $K(q^{-1}, \rho_{i+1})$. *If the test fails, reduce* γ_i *in (3.38) as follows* $\gamma_i = \alpha\gamma_i$, $0 < \alpha < 1$, *and go to step (4).*

(6) Replace i *with* $i+1$ *and repeat steps (1)-(5) until the stopping condition (3.58)-(3.59) is met.*

3.3.5 Simulation example

In this section, a simulation example is provided in order to illustrate the basic features of Algorithm 3.2.

Example 3.3 Consider that the plant output is generated by the discrete-time model

$$y(t) = \frac{(q^{-1} + 0.5q^{-2})(1 - 0.4q^{-1})}{1 - 1.5q^{-1} + 0.7q^{-2}}u(t) + \frac{1 + 0.5q^{-1} + 0.5q^{-2}}{1 - 1.5q^{-1} + 0.7q^{-2}}\eta(t) \quad (3.89)$$

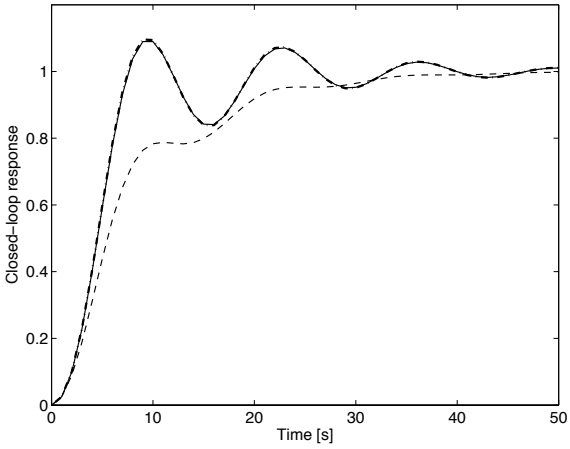

Figure 3.5: Closed-loop step responses: designed (solid), initial (dashed), obtained with the decorrelation procedure after 8 iterations (dash-dot)

where $\eta(t)$ is zero-mean, stationary, white Gaussian noise with standard deviation $\sigma = \pm\,0.025$. Assume that the designed model of the plant is

$$G_d(q^{-1}) = \frac{q^{-1} + 0.5q^{-2}}{1 - 1.5q^{-1} + 0.7q^{-2}} \tag{3.90}$$

and the controller satisfying certain control specifications for this model reads

$$K_d(q^{-1}) = \frac{0.025}{1 - q^{-1}} \tag{3.91}$$

The step response of the designed closed-loop system (K_d, G_d) is presented in Fig. 3.5 (solid line). However, the noise-free step response of the achieved closed-loop system with the full-order model G and the designed controller K_d (Fig. 3.5, dashed line) is far from the designed closed-loop response.

In this simulation study, a different realization of the noise $\eta(t)$ is used in each iteration. The level of the noise acting on the output of the closed-loop system strongly depends on the controller used. The noise-to-signal ratio varies considerably throughout the iterations. In the initial iteration, the noise-to-signal ratio is over 20% in terms of variance. The reference signal is a PRBS generated by a 10-bit shift register with data length $N = 1023$.

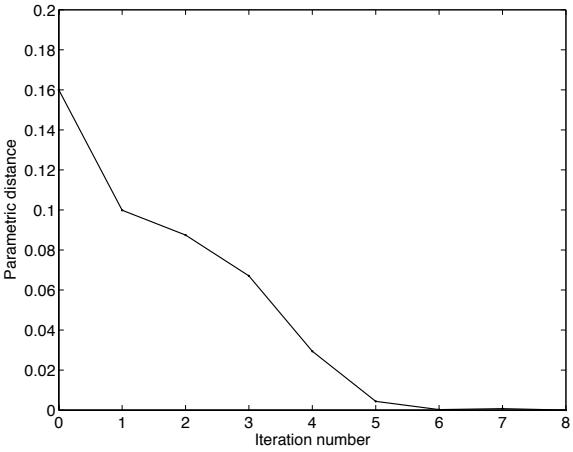

Figure 3.6: Parametric distance versus iteration number

The fixed factor $R_{fix} = (1 - q^{-1})$ is included in the polynomial R to provide integral action. Since the data length is sufficiently large, the correlation function is assumed to be nearly deterministic and Algorithm 3.2 with $\gamma_i = 1$ is used. The plant model used in (3.37) for the estimation of the gradient $\hat{\psi}$ is identified in the first iteration using a second-order Output Error (OE) structure. The decorrelating controller can be easily computed using (3.3)

$$K^{\circ}(q^{-1}) = \frac{0.025}{(1 - q^{-1})(1 - 0.4q^{-1})} \tag{3.92}$$

Hence, a controller with the same structure is chosen

$$K(q^{-1}) = \frac{s_0}{(1 - q^{-1})(1 + r_1 q^{-1})} \tag{3.93}$$

The vector of the controller parameters to be updated is $\rho = [r_1, s_0]^T$ and that of the decorrelating controller $\rho^{\circ} = [-0.4, 0.025]^T$. The initial (designed) controller parameter vector is $\rho_d = [0, 0.025]^T$. Instrumental variables based on controller parameters are used, where an identified model of the plant is used instead of G_d (the same model is used for the estimation of the gradient, as mentioned above). The stopping condition (3.58) with an α-level of 95% is met after 8 iterations. In spite of the presence

of a significant amount of noise, the resulting closed-loop step response (dash-dot) is very close to the desired one (Fig. 3.5). Fig. 3.6 gives the evolution of the parametric distance, defined as $PD_i = (\rho_i - \rho^\circ)^T(\rho_i - \rho^\circ)$, as a function of the iteration number. The final controller with the parameter vector $\rho_8 = [-0.3994, 0.0253]^T$ provides the parametric distance $PD_8 = 7.4463 \times 10^{-7}$. ⊡

3.4 Application to a magnetic suspension system

In this section, the effectiveness of the decorrelation procedure is demonstrated experimentally on a nonlinear and unstable magnetic suspension system. First, the experimental set up is described. Then, the design of the initial controller is explained, and the results of iterative tuning using the proposed method and standard IFT are shown.

3.4.1 The magnetic suspension system

The magnetic suspension system is illustrated in Fig. 3.7. A ferromagnetic sphere is suspended in the air using a magnetic force to compensate for the gravitational force. The actuator in the system is a solenoid which produces a magnetic force when current flows through the coil. The manipulated input u is the voltage to a U/I (voltage-to-current) converter that supplies current to the coil. The position of the sphere is measured by an optical sensor: variations in the position of the sphere change the intensity of the measured light, which in turn changes the voltage in the measurement circuit. The output y is the measured voltage corresponding to the position of the sphere. The system is controlled by a Sun workstation via an I/O board. A model of the system is needed to design the initial controller. A momentum balance gives:

$$m\ddot{x} = F_g - F_m \tag{3.94}$$

where m and x denote the mass of the sphere and its position, respectively, $F_g = mg$ denotes the gravitational force, while F_m denotes the magnetic

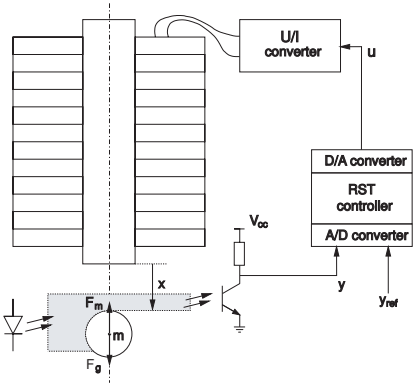

Figure 3.7: Magnetic suspension system

force. The latter can be expressed as $F_m = -\frac{1}{2}\frac{dL}{dx}i^2$, where L is the inductance that decreases with x. The dynamics of the current i can be approximated well by a first-order system. The current loop is controlled by an analog high-gain controller and, therefore, its dynamics can be neglected. Since $\frac{dL}{dx}$ depends nonlinearly on x, it is necessary to linearize the system dynamics around a stationary point. The resulting transfer function is given by:

$$G_d(s) = \frac{K_{ui}}{\tau_{ui}s + 1}\frac{b}{s^2 - a} \tag{3.95}$$

where K_{ui} and τ_{ui} denote the gain and the time constant of the U/I converter, respectively. Note that the parameters a and b vary with the linearization point. The linearization of equation (3.95) around the stationary point $x = 0.0525\,m$ gives the values of the parameters that are shown in Table 3.2.

K_{ui}	τ_{ui}	b	a
0.1033	0.0173	15749.4	1238

Table 3.2: Model parameters obtained after linearization around the stationary point

The magnetic suspension system is unstable and requires a controller for stabilization. The reference input, y_{ref}, is the voltage corresponding to the

desired sphere position. The system is sampled at the frequency $f_s = 100$ Hz.

It should be emphasized that this model will not be used in the iterative scheme, and is computed only for determining a reasonable reference model and the initial controller.

3.4.2 Experimental results

For implementation purposes, u and y correspond to deviations from a stationary operating point (u_0, y_0). The value u_0 is manually adjusted to make y_0 approach r_0, the stationary value of the reference signal, without static offset. A square wave signal is chosen as the reference r with an amplitude of 0.3 V and a period of 1 s. The data length used in each experiment is 4 s.

Discretization of equation (3.95) with the sampling rate 100 Hz gives the following discrete-time model:

$$G_d(q^{-1}) = \frac{0.0137q^{-1} + 0.0481q^{-2} + 0.0103q^{-3}}{1.0 - 2.6861q^{-1} + 2.1922q^{-2} - 0.5610q^{-3}} \tag{3.96}$$

The initial controller is in the form of a two-degree-of-freedom RST controller. Pole placement is used to compute the coefficients of the polynomials $R(q^{-1}, \rho_0)$ and $S(q^{-1}, \rho_0)$, while the precompensator $T(q^{-1}, \rho_0)$ is chosen to obtain unity closed-loop gain. The initial RST polynomials are:

$$R(q^{-1}, \rho_0) = 1 + 0.6859q^{-1} + 0.1631q^{-2} \tag{3.97}$$

$$S(q^{-1}, \rho_0) = 21.8601 - 26.7734q^{-1} + 8.1504q^{-2} \tag{3.98}$$

$$T(q^{-1}, \rho_0) = 1.8297 \tag{3.99}$$

Since G_d is only a rough approximation of the real system in the vicinity of the operating point, the designed and achieved closed-loop responses differ considerably as seen in Fig. 3.8. In order to improve the closed-loop performance, and to make the responses of the achieved and designed closed-loop systems as close as possible, two iterative tuning procedures are used and compared.

The standard IFT scheme with the following design choices is applied first: Gauss-Newton direction, step size $\gamma_i = 1$, control weight $\lambda = 0$.

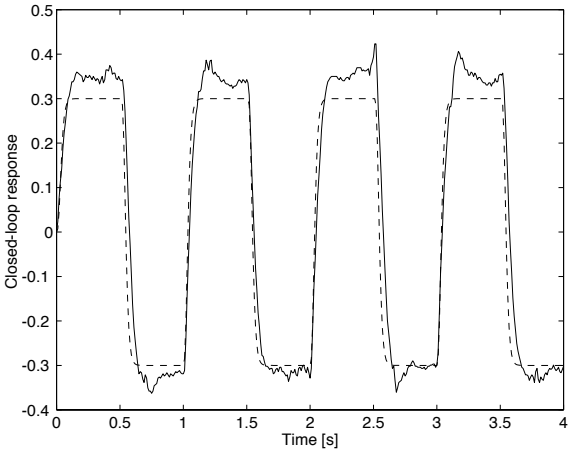

Figure 3.8: Closed-loop response achieved with the initial RST controller (solid) and designed response (dashed)

At each step of the iterative design, a second experiment is performed by feeding back, at the reference input, the error between the reference signal and the output of the first experiment. The third experiment is performed in the same way as the first experiment. The closed-loop response obtained after 8 iterations (24 experiments) is shown in Fig. 3.9 (solid line), with the designed response shown as a dashed line. The resulting closed-loop system has dynamics and static gain very close to the desired ones. The cost J in (2.39) is reduced by 93%.

Then, starting with the same initial controller and using the input-output data of the first experiment in the first iteration of the IFT procedure, a new controller is calculated using the correlation approach. In this way, it is ensured that both iterative tuning techniques have the same initial conditions. The step size is also fixed at $\gamma_i = 1$. An ARMAX structure ($n_a = 3, n_b = 3, n_c = 3, n_k = 1$) is considered for the plant model and no special effort is carried out for order estimation or model validation in order to show that the algorithm is not very sensitive to modeling error. After 6 iterations, this procedure leads to the closed-loop response shown in Fig. 3.10 (solid line). A comparison with the initial response (Fig. 3.8) shows that CbT improves the performance significantly.

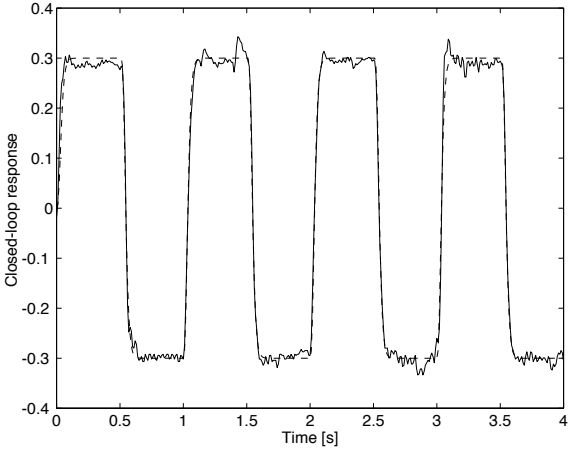

Figure 3.9: Closed-loop response achieved with the IFT after 8 iterations (solid), and designed response (dashed)

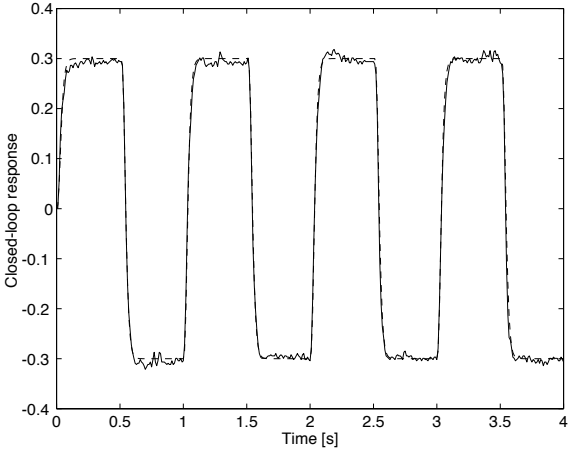

Figure 3.10: Closed-loop response achieved with the CbT after 6 iterations (solid), and designed response (dashed)

Iteration	0	1	2	3	4	5	6	7	8
IFT	1.9454	0.6722	0.3246	0.1919	0.1455	0.1671	0.2507	0.1483	0.1217
CbT	1.9454	0.4680	0.1589	0.1126	0.1303	0.0830	0.0590	0.1156	0.0920

Table 3.3: Observed sum of squared output errors of 9 successive controllers for both IFT and CbT

Although the correlation approach calculates the parameters of the controller by solving the correlation equation (3.4), it can also reduce the sum of squared output errors with a specific choice of the instrumental variables. Table 3.3 compares the observed sum of squared output errors of 9 successive controllers for both IFT and CbT. It is evident that the correlation approach converges faster than standard IFT. Note that the value obtained with CbT after 3 iterations (i.e. 3 experiments) is less than that of IFT after 8 iterations (and 24 experiments). This may be explained intuitively by the fact that the estimation of the Hessian is affected by noise, whereas the estimation of the Jacobian is not.

3.5 Conclusions

In this chapter, decorrelation of the closed-loop output error and the reference signal is considered for tuning the controller parameters using closed-loop data. From a theoretical point of view, solving the correlation equation using the stochastic approximation method has many advantages. The approach is very simple and converges to a unique solution of the correlation equation. The results are not asymptotic in the number of data N but in the number of iterations. The gradient of the closed-loop output error is not directly involved in the solution and is used only to construct the instrumental variables. This way, an approximate gradient leads to the correct solution under some weak conditions. However, the convergence rate may be too slow for practical implementation on real plants.

In practice, if the number of data N is sufficiently large, the fast convergent Newton-Raphson algorithm can be used to solve the equation. With this method, a gradient estimate of the performance criterion is required. Nevertheless, an unbiased gradient estimate is not a must, i.e. the algorithm converges toward the solution even when this estimate is not accurate. The

decorrelation procedure is applied to a nonlinear magnetic suspension system and excellent results are obtained already after a few iterations.

Observe that, when the number of controller parameters is small, the cross-correlation function represents the correlation between the closed-loop output error and the reference signal computed for only few delays. In other words, the computed $K(\rho^\circ)$ does not necessarily decorrelate these two signals for other delays. One solution to overcome this problem would be to increase the number of controller parameters. However, if the controller order is too high, this will induce pole-zero cancellations in the tuned controller transfer functions, which, in turn, will lead to numerical problems in the algorithm. A more elegant solution would be to adopt a FIR controller structure. This way, there are no numerical problems even when the controller order is overestimated. However, since the plant can be of high order in many practical situations, perfect decorrelation would require the use of rarely acceptable high-complexity controllers.

Note that the size of the instrumental variable vector represents the number of lags in which the correlation between $\varepsilon(\rho, t)$ and $r(t)$ is computed. If one computes the controller parameters by minimizing a norm of the cross-correlation function, then the size of the instrumental variable vector is independent of the controller order. Hence, the cross-correlation function can be computed for a large number of delays regardless the controller order. This is the topic of the next chapter.

Chapter 4

Correlation Reduction

4.1 Introduction

If one considers that the order of the true plant G is infinite, perfect decorrelation of the closed-loop output error and the reference signal would require an infinite-order controller. In other words, in the context of restricted-complexity controllers, the solution of the correlation equation (3.4) does not exist. This means, in turn, that Algorithms 3.1 and 3.2 cannot be used to update the parameters of a restricted-complexity controller. A natural way to circumvent this problem is to reformulate the control design criterion as the minimization of the two-norm of the cross-correlation function (3.1). The scheme relying on this new criterion is labeled the correlation-reduction method.

Ideally, to claim that two signals are not correlated, one should verify the correlation between these two signals for all delays. In practice, however, one can verify this cross-correlation only for a finite number of delays. Within the decorrelation procedure, the controller parameters are updated so as to ensure that the closed-loop output error and the reference signal are not correlated in n_ζ delays. Since the number of instrumental variables n_ζ is equal to the number of controller parameters n_ρ for this CbT variant, when n_ρ is small there is a possibility that there exist delays for which these two signals are correlated. In contrast, within the correlation-reduction method, n_ζ does not depend on n_ρ. Therefore, n_ζ can be chosen freely so as to better reflect the correlation between the closed-loop output error and the reference signal.

The two-norm of the cross-correlation function can be minimized itera-

tively using the extended instrumental variables method. It can be shown that the iterative algorithm converges to a local minimum provided that an unbiased gradient of the criterion with respect to the controller parameters is available. The frequency behavior of the resulting closed-loop system is compared with that of the designed one using the asymptotic frequency interpretation of the criterion. The analysis shows that the achieved closed-loop system approaches the designed one in terms of the output and complementary sensitivity functions. In addition, it is shown that under certain conditions the achieved controller automatically compensates for additive uncertainties. In other words, in the frequency regions where the additive uncertainties are not large, the achieved controller is close to the designed one, whilst in the frequency regions where the additive uncertainties are large, the gain of the achieved controller is reduced to improve the robustness of the system.

The design specifications for tracking and output disturbance rejection can be handled using the aforementioned criterion. However, one could also make demands on the input sensitivity function. In order to handle mixed sensitivity specifications, this criterion can be generalized by adding the two-norm of the cross-correlation function between the closed-loop input error and the reference signal. This way, the desired closed-loop output can be attained while taking into account some penalty on the control action, i.e. it is possible to make a trade-off between the specifications given in terms of the output sensitivity and those given in terms of the input sensitivity function. Analysis of the proposed generalized criterion in the frequency domain reveals the benefit of incorporating the new term.

The CbT approach was originally proposed for the model-following problem. Nevertheless, this approach can be adapted for tuning restricted-order controllers that need to reject disturbances in certain frequency regions. Assuming the disturbance signal can be measured, the idea is to tune the controller parameters such that the closed-loop output be uncorrelated with the measured disturbance. This concept can be used even in the case where the disturbances cannot be measured but there is the possibility of injecting a known test signal.

Similarly to the decorrelation procedure, when a large number of data is available, it is possible to use some of the fast converging determinis-

tic schemes such as the Gauss-Newton algorithm. Within this context, a stopping condition based on the statistical properties of the criterion is proposed.

The correlation-reduction method is applied to solve the benchmark problem of the special issue of the European Journal of Control on "Design and optimization of restricted-complexity controllers" [79, 51]. The benchmark problem involves the design of the simplest controller capable of ensuring good disturbance rejection for an active suspension system. The control specifications are stated in terms of constraints on the sensitivity functions. Although the CbT procedure does not consider specifications in the frequency domain explicitly, these can be met thanks to a frequency analysis of the criterion.

Chapter outline: The control design criterion is introduced in Section 4.2, and the iterative procedures for its minimization are given in Section 4.3. A frequency-domain analysis of the tuning criterion is presented in Section 4.4. A generalization of the tuning criterion is developed in Section 4.5. Section 4.6 introduces a stopping condition for the iterative algorithm. The algorithm is summarized in Section 4.7. Section 4.8 briefly presents the correlation approach for the regulation problem. The penultimate section describes the application of this approach to the benchmark problem. Finally, some concluding remarks are given in Section 4.10.

4.2 The control design criterion

Let the vector of instrumental variables be chosen as

$$\zeta(t) = [r(t+n_z)\cdots r(t)\cdots r(t-n_z)]^T \tag{4.1}$$

where n_z is large enough with respect to the order of the closed-loop system. In this case, since the number of equations is greater than the number of controller parameters, there is no solution to the correlation equation. Therefore, a correlation criterion can be reformulated as follows

$$J(\rho) = \bar{f}^T(\rho)\bar{f}(\rho) = E\{\bar{f}^T(\rho)\}E\{\bar{f}(\rho)\} = \sum_{\tau=-n_z}^{\tau=n_z} R_{oe}^2(\tau) \tag{4.2}$$

where

$$R_{oe}(\tau) = E\{\varepsilon_{oe}(\rho, t) r(t-\tau)\} \tag{4.3}$$

is the cross-correlation function between $\varepsilon_{oe}(\rho, t)$ and $r(t)$. This criterion represents a better indicator of the correlation between signals than the correlation equation (3.4) since it does not depend on the controller order. Moreover, the global minimum of the criterion corresponds to the solution of the correlation equation, if one exists. However, with a finite number of data, the criterion (4.2) cannot be directly minimized using the Robbins-Monro procedure because $J(\rho)$ cannot be represented as the mathematical expectation of a stochastic function. Therefore, let us define the following criterion

$$J_u(\rho) = E\{\bar{f}^T(\rho)\bar{f}(\rho)\} \tag{4.4}$$

This criterion can be minimized using the stochastic approximation method. Moreover, by developing the following expression,

$$\begin{aligned} \left(\bar{f}(\rho) - f(\rho)\right)^T \left(\bar{f}(\rho) - f(\rho)\right) &\geq 0 \\ \bar{f}^T(\rho)\bar{f}(\rho) - \bar{f}^T(\rho)f(\rho) - f^T(\rho)\bar{f}(\rho) + f^T(\rho)f(\rho) &\geq 0 \end{aligned}$$

applying mathematical expectation to it, and taking into account (3.1), one has

$$\begin{aligned} E\left\{\bar{f}^T(\rho)\bar{f}(\rho)\right\} - f^T(\rho)f(\rho) &\geq 0 \\ J_u(\rho) &\geq J(\rho). \end{aligned} \tag{4.5}$$

In fact, $J_u(\rho)$ is an upper bound of $J(\rho)$. In addition, with an ergodicity assumption on the signals, $J_u(\rho)$ tends to $J(\rho)$ when N tends to infinity.

4.3 Iterative solution

4.3.1 Robbins-Monro procedure

The criterion (4.4) can be minimized using the following iterative algorithm

$$\rho_{i+1} = \rho_i - \gamma_i J'_u(\rho_i) \tag{4.6}$$

where

$$J'_u(\rho_i) = \bar{Q}^T(\rho_i)\bar{f}(\rho_i) \tag{4.7}$$

and

$$\bar{Q}(\rho_i) = \left.\frac{\partial \bar{f}}{\partial \rho}\right|_{\rho_i} = \frac{1}{N}\sum_{t=1}^{N} \zeta(t)\hat{\psi}^T(\rho_i, t). \tag{4.8}$$

This algorithm converges to a local minimum of the criterion under Assumptions A1-A5 and Condition C1 of Theorem 3.1 provided that $\hat{\psi}(\rho_i, t)$ is an unbiased estimate of the gradient of the closed-loop output. Note that Condition C2 of Theorem 3.1 is inherently satisfied when the equation to be solved is the gradient of a quadratic criterion. The estimate of the closed-loop output gradient can be obtained without any model of the plant by an extra special experiment on the system at each iteration as is proposed in the IFT approach [31]. Another approach uses the designed model for computing the gradient (from Eq. 3.37) which does not need a new experiment. However, in this case, the local convergence of the criterion cannot be guaranteed. Another possibility for computing the gradient is to use the identified full-order model. If this model is unbiased the algorithm converges.

4.3.2 Gauss-Newton algorithm

When the number of data N is large enough, the correlation function (3.2) may be considered as a deterministic function and its two-norm can be minimized using the Gauss-Newton iterative algorithm giving faster convergence. Thus

$$\rho_{i+1} = \rho_i - \gamma_i \bar{Q}^+(\rho_i)\bar{f}(\rho_i) \tag{4.9}$$

where $\bar{Q}^+(\rho_i)$ is the pseudo-inverse of $\bar{Q}(\rho_i)$:

$$\bar{Q}^+(\rho_i) = \left[\bar{Q}(\rho_i)\bar{Q}(\rho_i)^T\right]^{-1}\bar{Q}(\rho_i) \tag{4.10}$$

Upon comparing (4.6), (4.7) and (4.9), (4.10) one notices that the term in brackets in (4.10) corresponds to an approximation of the Hessian matrix.

4.4 Frequency-domain analysis of the control design criterion

In this section the frequency characteristics of the achieved closed-loop system are compared with those of the designed closed-loop system. The relation between cross-correlation functions and spectral density functions helps one to obtain an asymptotic equivalent of the criterion in the frequency domain.

When n_z in (4.2) tends to infinity, and using Parseval's formula, the criterion in the frequency domain reads as

$$\lim_{n_z\to\infty} J(\rho) = \lim_{n_z\to\infty} \sum_{\tau=-n_z}^{\tau=n_z} R_{oe}^2(\tau) = \frac{1}{2\pi}\int_{-\pi}^{\pi} |\Phi_{oe}(\omega)|^2 d\omega \tag{4.11}$$

where $\Phi_{oe}(\omega)$ is the cross-spectral density of $\varepsilon_{oe}(\rho,t)$ and $r(t)$. It should be mentioned that to obtain a good approximation in the frequency domain, the number of data N and the number of delays in the cross-correlation function n_z should be sufficiently large. However, the number of lags n_z should be less than $N/2$ to have a good estimation of the cross-correlation function. On the other hand, as $R_{oe}(\tau)$ is negligible for large values of τ, a reasonable value of n_z ensures perfect decorrelation between the reference signal and the output error[1].

Also, the closed-loop output error can be expressed as

$$\varepsilon_{oe}(\rho,t) = \left(\mathcal{T}(K(\rho),G) - \mathcal{T}_d\right) r(t) + \mathcal{S}(K(\rho),G)v(t) \tag{4.12}$$

Now, using the fact that $r(t)$ and $v(t)$ are not correlated, $\Phi_{oe}(\omega)$ is given by

$$\Phi_{oe}(\omega) = \left(\mathcal{T}(e^{j\omega},K(\rho),G) - \mathcal{T}_d(e^{j\omega})\right)\Phi_r(\omega) \tag{4.13}$$

where $\Phi_r(\omega)$ is the spectral density of the reference signal $r(t)$. Thus, the criterion can be presented asymptotically in the frequency domain as

$$\lim_{n_z\to\infty} J(\rho) = \frac{1}{2\pi}\int_{-\pi}^{\pi} |\mathcal{T}(e^{j\omega},K(\rho),G) - \mathcal{T}_d(e^{j\omega})|^2 \Phi_r^2(\omega) d\omega \tag{4.14}$$

[1]Normally, one should choose n_z to cover the non-zero part of the impulse response of the closed-loop system; however, since this quantity is not known, one can approximate it with a value larger than the closed-loop system order

It is interesting to compare this criterion with that of the closed-loop output error minimization (2.39) in the frequency domain. Using the expression of $\varepsilon_{oe}(\rho, t)$ in (4.12), straightforward calculations give:

$$\begin{aligned} J_{\varepsilon}(\rho) &= \frac{1}{2\pi}\int_{-\pi}^{\pi} \big\{ |\mathcal{T}(e^{j\omega}, K(\rho), G) - \mathcal{T}_d(e^{j\omega})|^2 \Phi_r(\omega) \\ &\quad + |\mathcal{S}(e^{j\omega}, K(\rho), G)|^2 \Phi_v(\omega) \big\}\, d\omega \end{aligned} \tag{4.15}$$

This criterion shows that there is a trade-off between noise attenuation (through the sensitivity function $\mathcal{S}(e^{j\omega}, K(\rho), G)$) and model following (from $|\mathcal{T}(e^{j\omega}, K(\rho), G) - \mathcal{T}_d(e^{j\omega})|$). One can see clearly that the criterion based on the correlation approach (4.14) is not influenced by the noise signal $v(t)$ and that the spectral density of the reference signal is emphasized with a power of two in the criterion.

If the reference signal is white noise and n_z tends to infinity, one has:

$$\begin{aligned} \rho^{\min} &\triangleq \arg\min_{\rho} \int_{-\pi}^{\pi} |\mathcal{T}(e^{j\omega}, K(\rho), G) - \mathcal{T}_d(e^{j\omega})|^2 d\omega \\ &= \arg\min_{\rho} \int_{-\pi}^{\pi} |\mathcal{S}(e^{j\omega}, K(\rho), G) - \mathcal{S}_d(e^{j\omega})|^2 d\omega \\ &= \arg\min_{\rho} \int_{-\pi}^{\pi} |\mathcal{S}(e^{j\omega}, K(\rho), G)|^2 |KG - K_d G_d|^2 |\mathcal{S}_d(e^{j\omega})|^2 d\omega \end{aligned} \tag{4.16}$$

These relations show that the achieved complementary sensitivity function $\mathcal{T}(e^{j\omega}, K(\rho), G)$ and, consequently, the achieved sensitivity function $\mathcal{S}(e^{j\omega}, K(\rho), G)$ tend to their respective designed functions. Thus, the tuned controller ensures the designed performance in tracking and disturbance rejection for the real closed-loop system (robust performance). It can also be seen that the open-loop gain of the real system KG will be close to the designed one $K_d G_d$ in the frequencies where the magnitude of the sensitivity function is high.

Now, consider the effect of the tuned controller on the input sensitivity function $\mathcal{U}(K(\rho), G)$. For this purpose expression (4.16) is rearranged as follows (the arguments are omitted):

$$\rho^{\min} = \arg\min_{\rho} \int_{-\pi}^{\pi} |\mathcal{S}|^2 \{|G_d(K-K_d) + K(G-G_d)|^2\} |\mathcal{S}_d|^2 d\omega \quad (4.17)$$

Consider the frequency regions where G_d is small but the additive uncertainty $(G-G_d)$ is large (the middle and high frequencies). In these regions, the algorithm tries to minimize $|\mathcal{U}(K(\rho),G)|^2|G-G_d|^2|\mathcal{S}_d|^2$. Since $\mathcal{S}_d$ is approximately 1 at high frequencies, the amplitude of the input sensitivity function $\mathcal{U}(\rho)$ is reduced where the additive uncertainties are large (robust stability).

The robustness properties of the proposed tuning method are illustrated through the simulation example that follows.

Example 4.1 The plant $G(s) = B(s)/A(s)$, taken from [72], with

$$\begin{aligned} B(s) &= 6.599\cdot 10^{-5}s^9 - 2.552\cdot 10^{-3}s^8 - 0.1264s^7 \\ &\quad -0.2836s^6 - 4.195s^5 + 6.983s^4 - 13.74s^3 \\ &\quad +215.2s^2 + 144.0s + 1057 \\ A(s) &= s^9 + 2.401s^8 + 32.68s^7 + 54.78s^6 \\ &\quad +347.2s^5 + 351.2s^4 + 1256s^3 \\ &\quad +488.8s^2 + 635.3s + 105.9 \end{aligned}$$

is considered. The plant model is discretized using the sampling period $T_s = \pi/8$. The initial controller is calculated by pole placement using the following identified 4th-order model $G_d(q^{-1}) = B_d(q^{-1})/A_d(q^{-1})$ with

$$\begin{aligned} B_d(q^{-1}) &= -4.51\cdot 10^{-4}q^{-1} + 0.0218q^{-2} \\ &\quad +0.0378q^{-3} + 0.0152q^{-4} \\ A_d(q^{-1}) &= 1 - 2.721q^{-1} + 2.516q^{-2} \\ &\quad -0.751q^{-3} - 0.0366q^{-4} \end{aligned}$$

The log-magnitude Bode plots of the plant G and the model G_d are shown in Fig. 4.1. The curves corresponding to G and G_d show quite a good match around the first resonant mode at 0.765 rad/s, whereas there is a

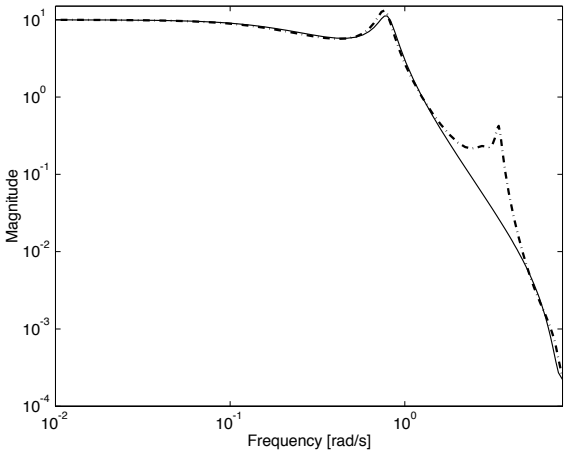

Figure 4.1: Bode plots of $G(e^{j\omega T_s})$ (dash-dot) and $G_d(e^{j\omega T_s})$ (solid)

large discrepancy around the second resonant mode at 3.45 rad/s.

The design objective is to damp the dominant oscillatory modes of the open-loop system, while still preserving their natural frequencies. The controller contains two fixed terms. Firstly, to enforce no static error and to suppress low frequency disturbances, the integrator $R_{fix} = 1 - q^{-1}$ is included in the polynomial R. Secondly, to avoid noise amplification and control signal saturation a factor $S_{fix} = 1 + 0.975q^{-1}$ is included in the polynomial S, which reduces the controller gain close to the Nyquist frequency. The resulting 5th-order initial controller $K_d = K(q^{-1}, \rho_0) = S_d(q^{-1})/R_d(q^{-1})$ is given as follows:

$$\begin{aligned} S_d(q^{-1}) &= (1 + 0.975q^{-1}) \cdot \big(0.4177 - 1.4736q^{-1} \\ &\quad +1.6283q^{-2} - 0.5154q^{-3} - 0.0560q^{-4}\big) \\ R_d(q^{-1}) &= (1 - q^{-1}) \cdot \big(1 - 0.2841q^{-1} + 0.2301q^{-2} \\ &\quad +0.0521q^{-3} + 0.0138q^{-4}\big) \end{aligned}$$

A 7th-order controller K is to be tuned on the real system. Note that the order of the optimal controller K° that would perfectly decorrelate the output error ε_{oe} with the instrumental variables ζ is 18 (there is no zero-

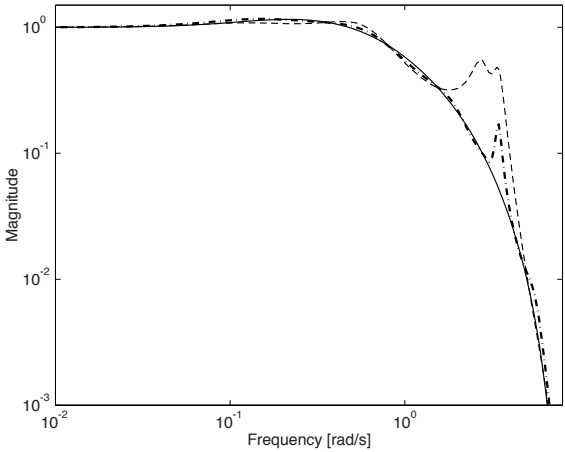

Figure 4.2: Magnitude plots of the complementary sensitivity functions: designed $\mathcal{T}_d(e^{j\omega T_s})$ (solid), initial $\mathcal{T}(e^{j\omega T_s}, K_d, G)$ (dashed) and final $\mathcal{T}(e^{j\omega T_s}, K(\rho), G)$ (dash-dot)

pole cancellation between the transfer functions G and $K_d G_d$ in (3.3)). The instrumental variable vector is chosen as in (4.1) with $n_z = 19$.

The tuning procedure is carried out in 8 iterations, with each one being performed using a different realization of the noise $v(t)$ with a noise-to-signal ratio of about 7.5% in terms of variance. The reference signal is a PRBS generated by a 7-bit shift register with data length $N = 2048$. In all iterations, the constant step size $\gamma_i = 0.5$ is used.

Fig. 4.2 shows the complementary sensitivity functions $\mathcal{T}_d$, $\mathcal{T}(K_d, G)$ and $\mathcal{T}(K(\rho), G)$ for the designed, initial and final closed-loop systems, respectively. It can be seen that, though the obtained controller K reduces the peak of the complementary sensitivity function around 3.45 rad/s, it does not suppress it completely. This can be explained by the fact that the order of the controller is not sufficient for perfect decorrelation.

Fig. 4.3 depicts the corresponding sensitivity functions $\mathcal{S}_d$, $\mathcal{S}(K_d, G)$ and $\mathcal{S}(K(\rho), G)$. A comparison of the curves shows the great similarity of the designed and resulting sensitivity functions. This leads to the conclusion that the resulting closed-loop system exhibits robust performance.

The input sensitivity functions $\mathcal{U}(K_d, G)$ and $\mathcal{U}(K(\rho), G)$ are given in Fig.

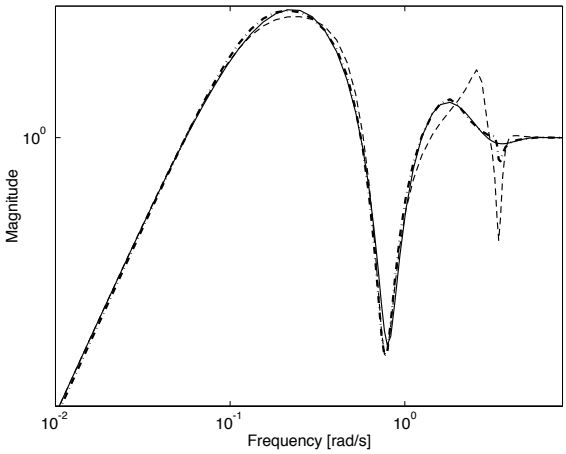

Figure 4.3: Magnitude plots of the output sensitivity functions: designed $\mathcal{S}_d(e^{j\omega T_s})$ (solid), initial $\mathcal{S}(e^{j\omega T_s}, K_d, G)$ (dashed) and final $\mathcal{S}(e^{j\omega T_s}, K(\rho), G)$ (dash-dot)

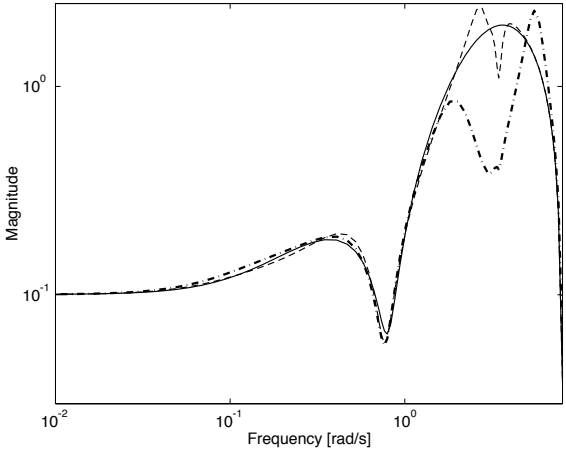

Figure 4.4: Magnitude plots of the input sensitivity functions: designed $\mathcal{U}_d(e^{j\omega T_s})$ (solid), initial $\mathcal{U}(e^{j\omega T_s}, K_d, G)$ (dashed) and final $\mathcal{U}(e^{j\omega T_s}, K(\rho), G)$ (dash-dot)

4.4 together with that of the designed model $\mathcal{U}_d$. These curves clearly show that the resulting controller K reduces the sensitivity function $\mathcal{U}(K(\rho), G)$ at the frequencies where the model uncertainty is large (around 3.45 rad/s), thus trying to improve robustness. ⊡

4.5 Generalized correlation criterion

The frequency domain analysis of the correlation criterion (4.2) showed that the difference between the desired and achieved complementary sensitivity functions is minimized. However, when minimizing this criterion, the achieved input sensitivity function $\mathcal{U}(e^{j\omega}, K(\rho), G)$ does not necessarily approach the designed one $\mathcal{U}_d$. At some frequencies $\mathcal{U}(e^{j\omega}, K(\rho), G)$ obtained by controller tuning may grow large, i.e. at some frequencies the controlled input $u(t)$ may exert a substantial effort on the actuators. In order to handle mixed sensitivity specifications, a generalized correlation criterion can be defined as follows

$$J_g(\rho) = k_{oe} E\{\bar{f}^T(\rho)\bar{f}(\rho)\} + k_{ie} E\{\bar{g}^T(\rho)\bar{g}(\rho)\} \tag{4.18}$$

where k_{oe} and k_{ie} are positive weighting factors and

$$\bar{g}(\rho) = \frac{1}{N}\sum_{t=1}^{N} \zeta(t)\varepsilon_{ie}(\rho, t) \tag{4.19}$$

with $\varepsilon_{ie}(\rho, t)$ being the closed-loop input error defined in (2.11). This way, both the input and the output of the achieved closed-loop system will follow the corresponding desired signals independently of the noise dynamics.

From Fig. 4.5, $\varepsilon_{ie}(\rho, t)$ can be written as:

$$\varepsilon_{ie}(\rho, t) = [\mathcal{U}(K(\rho), G) - \mathcal{U}_d]\, r(t) - \mathcal{U}(K(\rho), G)v(t) \tag{4.20}$$

Considering the vector of instrumental variables given in (4.1), and letting n_z tend to infinity, gives asymptotically (after straightforward calculations

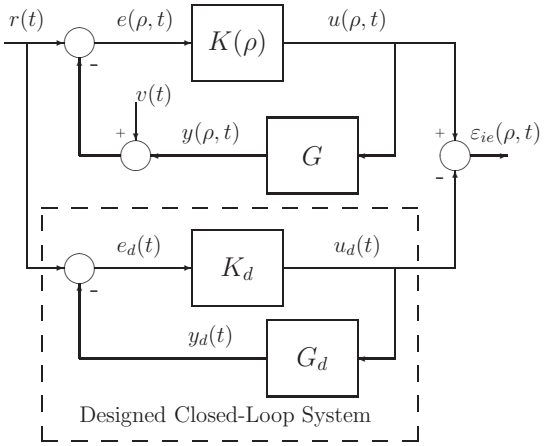

Figure 4.5: Closed-loop input error resulting from a comparison of the achieved and designed closed-loop systems

similar to those in Section 4.4):

$$\lim_{n_z\to\infty} J_g(\rho) = \frac{1}{2\pi}\int_{-\pi}^{\pi} \left[k_{oe}|\mathcal{T}(e^{j\omega},K(\rho),G)-\mathcal{T}_d(e^{j\omega})|^2 + k_{ie}|\mathcal{U}(e^{j\omega},K(\rho),G)-\mathcal{U}_d(e^{j\omega})|^2\right]\Phi_r^2(\omega)d\omega \quad (4.21)$$

If $r(t)$ is white noise, one has:

$$\begin{aligned}\rho^{\min} &= \arg\min_{\rho}\int_{-\pi}^{\pi}\left\{k_{oe}|\mathcal{T}(e^{j\omega},K(\rho),G)-\mathcal{T}_d(e^{j\omega})|^2 + k_{ie}|\mathcal{U}(e^{j\omega},K(\rho),G)-\mathcal{U}_d(e^{j\omega})|^2\right\}d\omega \\ &= \arg\min_{\rho}\int_{-\pi}^{\pi}\left\{k_{oe}|\mathcal{S}(e^{j\omega},K(\rho),G)-\mathcal{S}_d(e^{j\omega})|^2 + k_{ie}|\mathcal{U}(e^{j\omega},K(\rho),G)-\mathcal{U}_d(e^{j\omega})|^2\right\}d\omega \quad (4.22)\end{aligned}$$

This relation shows that there is a trade-off between the minimization of $||\mathcal{S}(K(\rho),G)-\mathcal{S}_d||_2$ and that of $||\mathcal{U}(K(\rho))-\mathcal{U}_d||_2$. By minimizing this criterion, the mixed sensitivity specifications are satisfied, and the achieved closed-loop system tries to preserve the robustness properties of the designed one. Furthermore, it is easy to see that the criterion (4.18) is not influenced by the disturbance signal $v(t)$. With regard to this criterion, two extreme

cases can be considered: (i) when $(k_{oe}, k_{ie}) = (1, 0)$, (4.22) reduces to (4.14) and $\mathcal{S}(K(\rho), G)$ is forced toward $\mathcal{S}_d$; (ii) when $(k_{oe}, k_{ie}) = (0, 1)$, $\mathcal{U}(K(\rho), G)$ is pushed toward its designed function $\mathcal{U}_d$.

The criterion can be minimized using the stochastic approximation or the Gauss-Newton method when the number of data is sufficiently large (the variation of the criterion for a fixed controller can be ignored in experiments with different noise realizations).

The properties of the proposed generalized correlation criterion are illustrated by an example.

Example 4.2 Consider the following 4th-order true plant:

$$G = \frac{0.385q^{-2} + 0.525q^{-3}}{1 - 1.353q^{-1} + 1.55q^{-2} - 1.282q^{-3} + 0.915q^{-4}}$$

The system has two very lightly damped resonant modes and one unstable zero. The following second-order model G_d has been identified:

$$G_d = \frac{0.6043q^{-2} - 0.1562q^{-3} - 0.0306q^{-4}}{1 - 1.5822q^{-1} + 0.9629q^{-2}}$$

Let the initial 3rd-order controller K_d be:

$$K_d = \frac{-0.1530q^{-1} - 0.038q^{-2}}{1 - 0.8093q^{-1} + 0.2141q^{-2} - 0.012q^{-3}}$$

When K_d is applied to the true plant G, there is significant discrepancy between the designed $\mathcal{S}_d$ and the initial $\mathcal{S}(K_d, G)$ output sensitivity functions due to model mismatch (see solid and dashed lines in Figs. 4.6 and 4.7). To improve the behavior of the closed-loop system, a 4th-order controller K is tuned on the true plant for three different choices of the weighting factors k_{oe} and k_{ie}. The tuning procedure is carried out in 8 iterations with each iteration being performed using a different realization of the disturbance signal $v(t)$ with a noise-to-signal ratio of 7% in terms of variance. The vector of instrumental variables is chosen as in (4.1) with $n_z = 72$, and the reference signal $r(t)$ is a PRBS generated by a 7-bit shift register with data length $N = 2048$. In all iterations, the initial step size $\gamma_i = 0.5$ is used. If the algorithm provides a controller that destabilizes the closed-loop system, the step-size is then divided by 2.

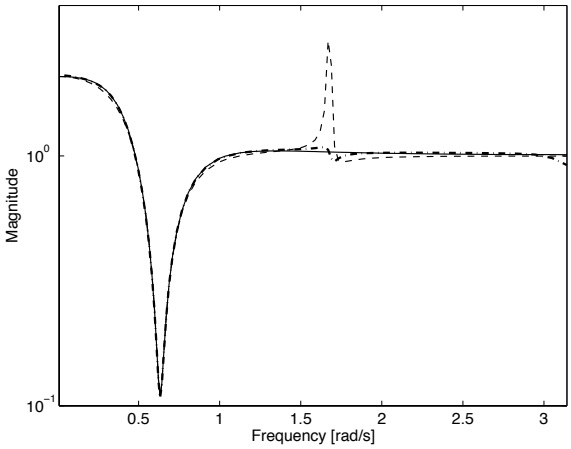

Figure 4.6: Output sensitivity functions: designed $\mathcal{S}_d(e^{j\omega})$ (solid), initial $\mathcal{S}(e^{j\omega}, K_d, G)$ (dashed) and final $\mathcal{S}(e^{j\omega}, K(\rho), G)$ (dash-dot) for $(k_{oe}, k_{ie}) = (1, 0)$

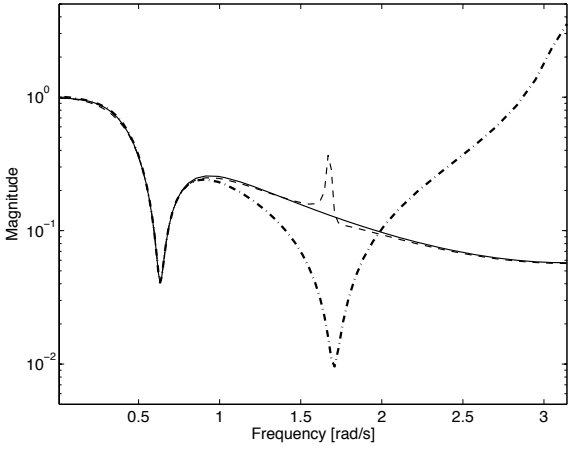

Figure 4.7: Input sensitivity functions: designed $\mathcal{U}_d(e^{j\omega})$ (solid), initial $\mathcal{U}(e^{j\omega}, K_d, G)$ (dashed) and final $\mathcal{U}(e^{j\omega}, K(\rho), G)$ (dash-dot) for $(k_{oe}, k_{ie}) = (1, 0)$

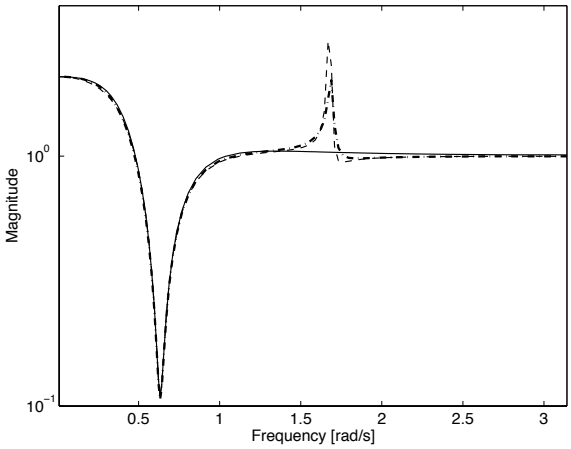

Figure 4.8: Output sensitivity functions: designed $\mathcal{S}_d(e^{j\omega})$ (solid), initial $\mathcal{S}(e^{j\omega}, K_d, G)$ (dashed) and final $\mathcal{S}(e^{j\omega}, K(\rho), G)$ (dash-dot) for $(k_{oe}, k_{ie}) = (0, 1)$

The first choice of weighting factors $(k_{oe}, k_{ie}) = (1, 0)$ corresponds to the minimization of $||\mathcal{S}(K(\rho), G) - \mathcal{S}_d||_2$. Fig. 4.6 shows the output sensitivity functions $\mathcal{S}_d$, $\mathcal{S}(K_d, G)$ and $\mathcal{S}(K(\rho), G)$ for the designed, initial and final closed-loop systems, respectively. It can be seen that $\mathcal{S}(K_d, G)$ and $\mathcal{S}(K(\rho), G)$ are almost superposed, i.e. the tuning algorithm has succeeded in minimizing $||\mathcal{S}(K(\rho), G) - \mathcal{S}_d||_2$ to a large extent. However, comparing the corresponding input sensitivity functions $\mathcal{U}_d$, $\mathcal{U}(K_d, G)$ and $\mathcal{U}(K(\rho), G)$ shown in Fig. 4.7, it is easy to see that $\mathcal{U}(K(\rho), G)$ becomes large at high frequencies.

For $(k_{oe}, k_{ie}) = (0, 1)$, $||\mathcal{U}(K(\rho), G) - \mathcal{U}_d||_2$ is minimized. Figs. 4.8 and 4.9 depict the corresponding output sensitivities $\mathcal{S}_d$, $\mathcal{S}(K_d, G)$ and $\mathcal{S}(K(\rho), G)$, and input sensitivities $\mathcal{U}_d$, $\mathcal{U}(K_d, G)$ and $\mathcal{U}(K(\rho), G)$. A comparison of the curves shows that, though the resulting controller K has not succeeded in reducing the peak of the output sensitivity function $\mathcal{S}(K(\rho), G)$, the final input sensitivity function $\mathcal{U}(K(\rho), G)$ is very similar to $\mathcal{U}_d$.

Finally, for the case $(k_{oe}, k_{ie}) = (0.5, 0.5)$, there is a trade-off in minimizing $||\mathcal{S}(K(\rho), G) - \mathcal{S}_d||_2$ and $||\mathcal{U}(K(\rho), G) - \mathcal{U}_d||_2$. Figs. 4.10 and 4.11 show that the resulting controller K has reduced the peak of the output sensitivity function $\mathcal{S}(K(\rho), G)$ and, at the same time, the discrepancy between $\mathcal{U}_d$

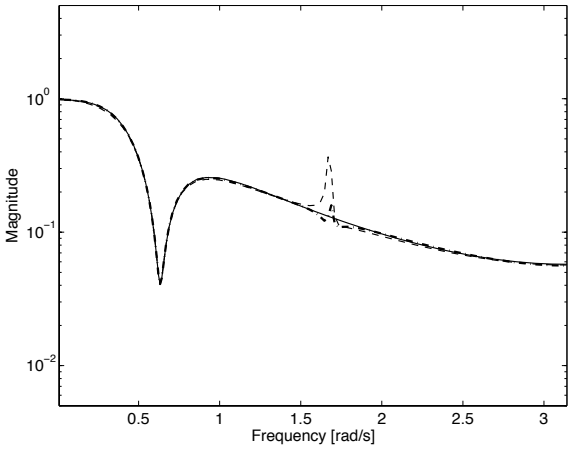

Figure 4.9: Input sensitivity functions: designed $\mathcal{U}_d(e^{j\omega})$ (solid), initial $\mathcal{U}(e^{j\omega}, K_d, G)$ (dashed) and final $\mathcal{U}(e^{j\omega}, K(\rho), G)$ (dash-dot) for $(k_{oe}, k_{ie}) = (0, 1)$

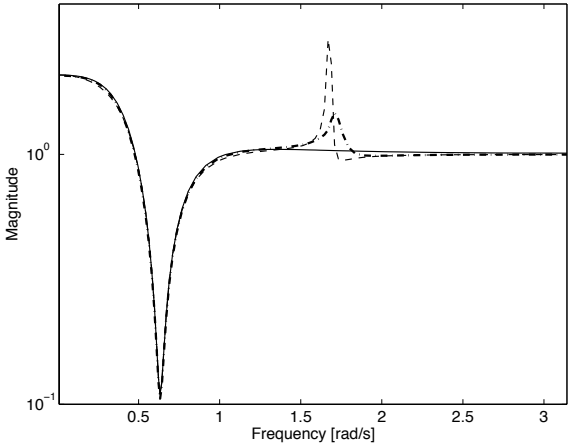

Figure 4.10: Output sensitivity functions: designed $\mathcal{S}_d(e^{j\omega})$ (solid), initial $\mathcal{S}(e^{j\omega}, K_d, G)$ (dashed) and final $\mathcal{S}(e^{j\omega}, K(\rho), G)$ (dash-dot) for $(k_{oe}, k_{ie}) = (0.5, 0.5)$

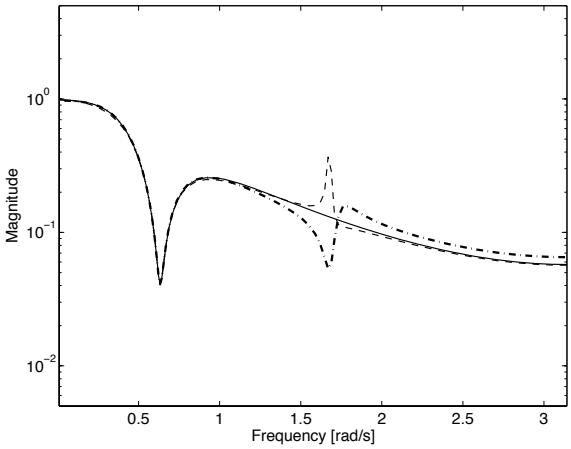

Figure 4.11: Input sensitivity functions: designed $\mathcal{U}_d(e^{j\omega})$ (solid), initial $\mathcal{U}(e^{j\omega}, K_d, G)$ (dashed) and final $\mathcal{U}(e^{j\omega}, K(\rho), G)$ (dash-dot) for $(k_{oe}, k_{ie}) = (0.5, 0.5)$

Table 4.1: Results of tuning

	Iteration	$\|\|\mathcal{S}(K(\rho), G) - \mathcal{S}_d\|\|_2$	$\|\|\mathcal{U}(K(\rho), G) - \mathcal{U}_d\|\|_2$
	1^{st}	0.3002	0.0388
$k_{oe} = 1, k_{ie} = 0$	8^{th}	0.0284	0.4209
$k_{oe} = 0, k_{ie} = 1$	8^{th}	0.1493	0.0091
$k_{oe} = k_{ie} = 0.5$	8^{th}	0.1018	0.0284

and $\mathcal{U}(K(\rho), G)$ remains small.

Table 4.1 gives the performance of the tuning procedure as a function of the weighting factors k_{oe} and k_{ie}. These numerical results confirm the qualitative shapes seen in Figs. 4.6-4.11. The minima of $||\mathcal{S}(K(\rho), G) - \mathcal{S}_d||_2$ and $||\mathcal{U}(K(\rho), G) - \mathcal{U}_d||_2$ are achieved for $(k_{oe}, k_{ie}) = (1, 0)$ and $(k_{oe}, k_{ie}) = (0, 1)$, respectively. However, when minimizing only $||\mathcal{S}(K(\rho), G) - \mathcal{S}_d||_2$ or $||\mathcal{U}(K(\rho), G) - \mathcal{U}_d||_2$, the deviation of the other sensitivity does increase. In contrast, the controller obtained with $(k_{oe}, k_{ie}) = (0.5, 0.5)$ reduces both $||\mathcal{S}(K(\rho), G) - \mathcal{S}_d||_2$ and $||\mathcal{U}(K(\rho), G) - \mathcal{U}_d||_2$.

$\boxdot$

4.6 Stopping condition

Inspired by the cross-correlation test for model validation available in the field of identification [75, 54], a stopping condition for the iterative algorithms (4.6) and (4.9) is provided in this section.

In general, the variance of the criterion cannot be computed at its minimum for a finite number of data. So it is assumed that ρ° exists and belongs to the set of parameterized controllers. Then, the variance of the criterion $J_u(\rho)$ at ρ° is computed and used to obtain the confidence interval with a given probability.

Let us denote the estimate of the cross-correlation between $\varepsilon_{oe}(\rho^\circ, t)$ and $r(t)$ based on N data points by:

$$\hat{R}_{oe}(\tau) = \frac{1}{N}\sum_{t=1}^{N} \varepsilon_{oe}(\rho^\circ, t) r(t-\tau) \tag{4.23}$$

It is shown in [54] that, for $N \to \infty$, the sequence of random variables $\sqrt{N}\hat{R}_{oe}(\tau)$ converges in distribution to the normal distribution with zero mean and covariance matrix P_r, i.e.

$$\sqrt{N}\hat{R}_{oe}(\tau) \in As\mathcal{N}(0, P_r) \Rightarrow \sqrt{\frac{N}{P_r}}\hat{R}_{oe}(\tau) \in As\mathcal{N}(0, 1) \tag{4.24}$$

where

$$P_r = \sum_{\tau=-\infty}^{\infty} R_\varepsilon(\tau) R_r(\tau) \tag{4.25}$$

with $R_\varepsilon(\tau)$ and $R_r(\tau)$ being the autocorrelation functions of $\varepsilon_{oe}(\rho^\circ, t)$ and $r(t)$, respectively.

Consider the following lemma taken from [75]:

Lemma 4.1 *Let $x \in As\mathcal{N}(m, P)$ be of dimension n. Then $(x-m)^T P^{-1}(x-m) \in As\chi^2(n)$.*

With this lemma (4.24) gives:

$$\frac{N}{P_r}\sum_{\tau=-n_z}^{n_z} \hat{R}^2_{oe}(\tau) \in As\chi^2(2n_z+1) \tag{4.26}$$

Thus, if $\chi^2_\alpha(2n_z+1)$ denotes the α-level of the $\chi^2(2n_z+1)$ distribution, the iteration should be stopped when the criterion (4.4) is statistically not different from zero with the confidence level α:

$$J_u(\rho_i) = \sum_{\tau=-n_z}^{n_z} \hat{R}^2_{oe}(\tau) \leq \frac{\hat{P}_r}{N}\chi^2_\alpha(2n_z+1) \tag{4.27}$$

where

$$\hat{P}_r = \sum_{\tau=-n_z}^{n_z} \hat{R}_\varepsilon(\tau)\hat{R}_r(\tau)$$

is the estimate of P_r based on the current parameter vector ρ_i.

Therefore, as long as the computed value of J_u falls outside the confidence region, the iteration should be continued. The stopping condition (4.27) can also show whether the selected controller order is appropriate. If the iterative procedure does not succeed in meeting the stopping condition after a large number of iterations, one should consider increasing the order of the controller. On the other hand, reaching the test threshold "too quickly" indicates that the order of the controller might have to be reduced.

The effectiveness of the stopping condition is illustrated in the following example.

Example 4.3 The experimental conditions and the plant are given in Example 3.3. In this example one is looking for the controller $K(q^{-1}) = s^{(0)}/R_{fix}$ that minimizes (4.4). The vector of instrumental variables is chosen as in (4.1) with $n_z = 4$.

Table 4.2: Results of tuning

Iteration	J_u	$\frac{\hat{P}_r}{N}\chi^2_\alpha(2n_z+1)$	$\|\|\mathcal{T}-\mathcal{T}_d\|\|_2$
initial	2.54×10^{-3}	8.1×10^{-4}	0.1953
1st	1.13×10^{-3}	8.69×10^{-4}	0.1426
2nd	7.64×10^{-4}	7.89×10^{-4}	0.1362

The stopping condition (4.27) with $\alpha = 0.05$ is met after only 2 iterations. The results are shown in Table 4.2. It can be seen that the two-norm of the discrepancy between $\mathcal{T}$ and $\mathcal{T}_d$ is reduced by 30% and the criterion

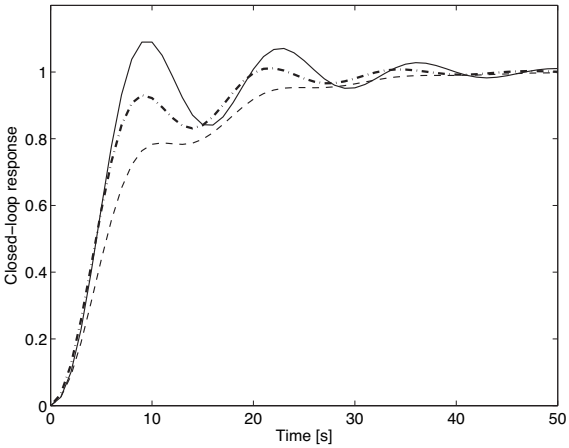

Figure 4.12: Closed-loop step responses: designed (solid), initial (dashed), obtained with the correlation-reduction method after 3 iterations (dash-dot)

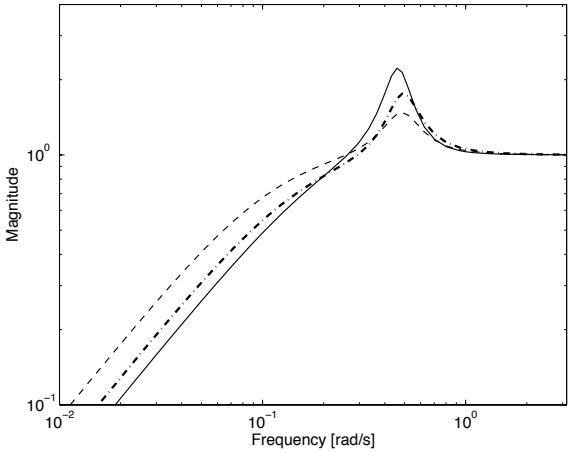

Figure 4.13: Output sensitivity functions: designed $\mathcal{S}_d(e^{j\omega})$ (solid), initial $\mathcal{S}(e^{j\omega}, K_d, G)$ (dashed) and final $\mathcal{S}(e^{j\omega}, K(\rho), G)$ (dash-dot)

J_u is reduced by 70%. The resulting closed-loop step response is shown in Fig. 4.12 (dash-dot). Fig. 4.13 shows the output sensitivity functions $\mathcal{S}_d$, $\mathcal{S}(K_d, G)$ and $\mathcal{S}(\rho, G)$ for the designed, initial and final closed-loop systems, respectively. From these figures, one can conclude that the iterative procedure makes the resulting closed-loop system approach the desired one. However, due to the chosen controller structure, perfect decorrelation is not possible and, therefore, some discrepancy between the designed and achieved systems is inevitable. ⊡

4.7 Algorithm

Let us summarize the correlation-reduction algorithm.

Algorithm 4.1 *Construct the vector of instrumental variables $\zeta(t)$ as given in (4.1), where n_z should be chosen as discussed in Section 4.4. Starting with the initial controller $K(q^{-1}, \rho_i) = K_d(q^{-1})$, $i = 0$, computed using the model $G_d(q^{-1})$, perform the following steps:*

(1) Collect N samples of the signals $u(\rho_i)$ and $y(\rho_i)$ from the closed-loop experiment with the controller $K(q^{-1}, \rho_i)$ operating on the actual system. If needed, filter $u(\rho_i)$ and $y(\rho_i)$ with R_{fix} and S_{fix}, respectively.

(2) Compute $\bar{f}(\rho_i)$ from (3.2) using the acquired data and constructed $\zeta(t)$.

(3) If N is large, compute $\bar{Q}^+(\rho_i)$ from (4.10). Update the controller parameter vector ρ_{i+1} according to the recursion (4.9). Otherwise, update the controller parameter vector ρ_{i+1} according to (4.6). Add the fixed terms R_{fix} and S_{fix} if applicable.

(4) Using G_d or an identified model, test the stability of the closed-loop system formed by this model and the controller $K(q^{-1}, \rho_{i+1})$. If the test fails, reduce γ_i in (4.6) or (4.9) as follows $\gamma_i = \alpha\gamma_i$, $0 < \alpha < 1$, and go to step (3).

(5) Replace i with $i+1$ and repeat steps (1)-(4) until the stopping condition (4.27) is met.

Observe that this algorithm is easy to extend to the generalized correlation criterion. It is sufficient to add the terms corresponding to $\bar{g}(\rho_i)$ from (4.19) in steps (2) and (3) of Algorithm 4.1.

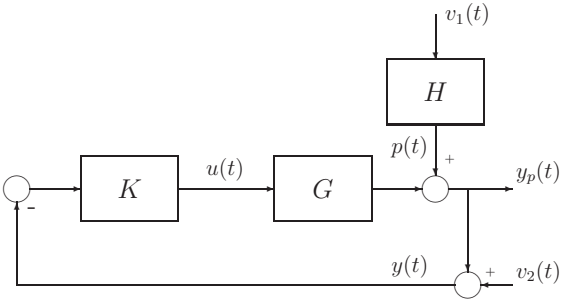

Figure 4.14: Controlled plant with the measured disturbance v_1 and the measurement noise v_2

4.8 Correlation-reduction method for the disturbance rejection problem

In this section, the correlation-reduction method is adapted for the regulation problem depicted in Fig. 4.14. Note that this problem can be considered as a model-following problem with the reference model equal to zero. Let the measured output of the plant be described as:

$$y(t) = G(q^{-1})u(t) + H(q^{-1})v_1(t) + v_2(t) \tag{4.28}$$

where $v_1(t)$ is the measured disturbance, $v_2(t)$ a zero-mean measurement noise independent of $v_1(t)$, $G(q^{-1})$ and $H(q^{-1})$ LTI SISO discrete-time transfer operators. The signals $y_p(t)$ and $p(t)$ denote the plant output and the output of the disturbance model H, respectively. The plant is controlled by the controller $K(q^{-1})$ defined in (2.3).

The objective is to tune the controller parameters such that the feedback controller exactly compensates the effect of the measured disturbance at the plant output. In other words, the measured output should ideally contain only the effect of measurement noise that is uncorrelated with $v_1(t)$. Evidently, with a low-order causal controller, perfect decorrelation of $y(t)$ and $v_1(t)$ is not possible. Therefore, it is natural to formulate the design objective as the minimization of some norm of the cross-correlation function of these two signals.

Let the correlation function $f_r(\rho)$ be defined as follows:

$$f_r(\rho) = E\left\{\frac{1}{N}\sum_{t=1}^{N}\zeta_r(t)y(\rho,t)\right\} \tag{4.29}$$

where the instrumental variables are defined as:

$$\zeta_r^T(t) = [v(t+n_z), v(t+n_z-1), \ldots, v(t), v(t-1), \ldots, v(t-n_z)] \tag{4.30}$$

and

$$v(t) = W_r(q^{-1})v_1(t) \tag{4.31}$$

with $W_r(q^{-1})$ being a linear generic filter and n_z a sufficiently large integer number. Then, the tuning objective can be defined as the minimization of the following criterion:

$$J_r(\rho) = f_r^T(\rho)f_r(\rho) = \sum_{\tau=-n_z}^{n_z} R_{yv}^2(\tau) \tag{4.32}$$

where $R_{yv}(\tau)$ is the cross-correlation function between the filtered disturbance $v(t)$ and the closed-loop output $y(\rho,t)$:

$$R_{yv}(\tau) = E\{y(\rho,t)v(t-\tau)\} \tag{4.33}$$

Hence, the control parameter vector $\rho^{\min}$ is given by:

$$\rho^{\min} = \arg\min_{\rho} J_r(\rho) \tag{4.34}$$

When n_z tends to infinity, applying Parseval's formula to (4.32) leads to:

$$\lim_{n_z\to\infty} J_r(\rho) = \frac{1}{2\pi}\int_{-\pi}^{\pi}|\Phi_{yv}(\omega)|^2 d\omega \tag{4.35}$$

where $\Phi_{yv}(\omega)$ is the cross-spectral density between $y(\rho,t)$ and $v(t)$.

Moreover, the closed-loop output can be expressed as:

$$y(\rho,t) = \mathcal{S}(q^{-1}, K(\rho), G)(H(q^{-1})v_1(t) + v_2(t)) \tag{4.36}$$

Thus, from expressions (4.31) and (4.36), and using the fact that $v(t)$ and

$v_2(t)$ are independent, the cross-spectral density $\Phi_{yv}(\omega)$ reads:

$$\Phi_{yv}(\omega) = \mathcal{S}(e^{j\omega}, K(\rho), G)H(e^{j\omega})W_r^{-1}(e^{j\omega})\Phi_v(\omega) \tag{4.37}$$

where $\Phi_v(\omega)$ is the spectrum of the filtered disturbance signal $v(t)$. Finally, using $\Phi_{yv}(\omega)$ of (4.37) in (4.35) gives:

$$\lim_{n_z\to\infty} J_r(\rho) = \frac{1}{2\pi}\int_{-\pi}^{\pi} |\mathcal{S}(e^{j\omega}, K(\rho), G)|^2 |H(e^{j\omega})|^2 |W_r(e^{j\omega})|^2 \Phi_{v_1}^2(\omega) d\omega \tag{4.38}$$

with $\Phi_{v_1}(\omega) = |W_r^{-1}(e^{-j\omega})|^2\Phi_v(\omega)$ being the spectrum of $v_1(t)$. This equation indicates that the criterion based on the correlation approach is not affected by the noise signal $v_2(t)$. Furthermore, when $W_r(q^{-1}) = 1$ and $v_1(t)$ is white noise, the tuning algorithm tries to minimize the magnitude of the sensitivity function $\mathcal{S}$ in the frequency regions where $|H(e^{-j\omega})|$ is large.

4.9 Application to an active suspension system

The methodology developed in the previous section is applied to a benchmark problem. The objective of the benchmark is to design a reduced-complexity controller for the active suspension system of Laboratoire d'Automatique de Grenoble (LAG) [79].

4.9.1 System description

The active suspension system setup in this benchmark is used to test the disturbance attenuation in a large frequency band. Fig. 4.15 shows the scheme of the active hydro-suspension system used to reduce the machine vibrations. The principal parts of the active suspension system are:

- an elastomer cone that encloses the main chamber filled with silicon oil (1);
- an inertia chamber enclosed with a flexible membrane (2);

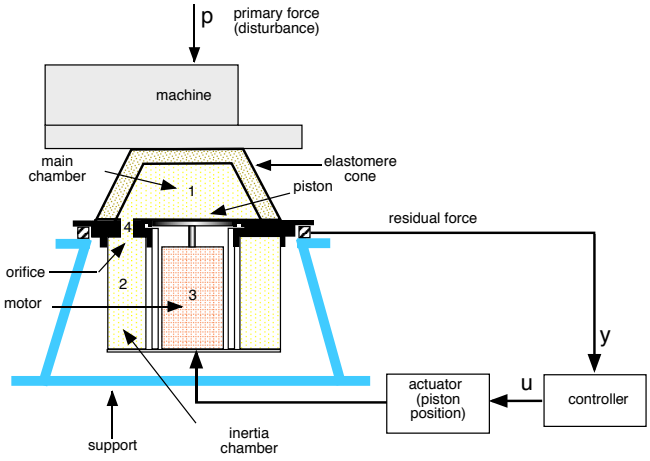

Figure 4.15: The schematic diagram of the active suspension system

- a piston (3) that is fixed on a DC motor. When the position of the piston is fixed, the suspension system is passive;
- an orifice (4) that allows oil flow between the two chambers.

The principal idea of the active suspension is to change the elasticity of the system in order to absorb the vibrations generated by the machine that is to be isolated. For experimental purposes the machine is replaced by a shaker which is driven by a computer generated control signal. The output of the system is the measured voltage corresponding to the residual force. The control input drives the position of the piston using an actuator. The system is controlled by a PC through a data acquisition system. The sampling frequency is a design parameter (upper limit: 1 kHz).

4.9.2 Experimental results

The block diagram of the active suspension system is presented in Fig. 4.16.

The system is excited by the primary force $v_1(t)$ generated by a computer-controlled shaker. The transfer function C_r/D_r between the primary and the residual forces is called the primary path. The disturbance signal $p(t)$ is the output of the primary path. The output $y(t)$ is the measured voltage

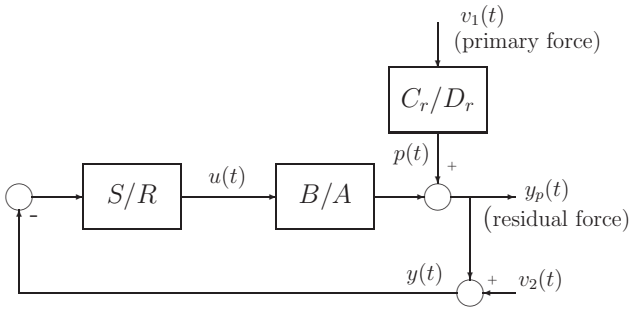

Figure 4.16: Block diagram of the active suspension system

corresponding to the residual force $y_p(t)$. The nonparametric model of the primary path shows that there are several vibrational modes, with the first mode at 31.47 Hz and the second mode around 160 Hz being the most important ones (dashed line in Fig. 4.17).

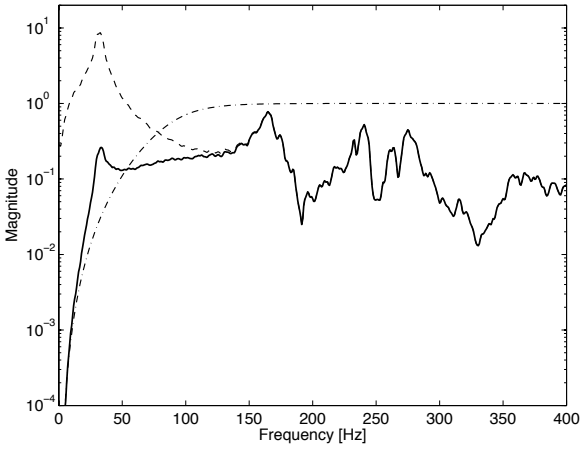

Figure 4.17: Magnitudes of $C_r(e^{-j\omega})/D_r(e^{-j\omega})$ (dashed), $W_r(e^{-j\omega})$ (dash-dot), and aggregate weighting $W_r(e^{-j\omega})C_r(e^{-j\omega})/D_r(e^{-j\omega})$ (solid) used in (4.38)

The control input $u(t)$ drives the piston that can modify the residual force. The secondary path is defined as the transfer function B/A between the control input and the residual force.

The design objective is to compute a low-order linear discrete-time con-

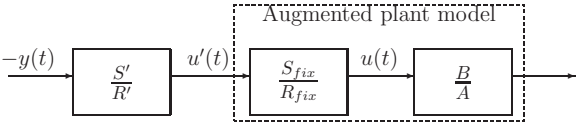

Figure 4.18: Incorporating fixed terms in the secondary path

troller $S(q^{-1})/R(q^{-1})$ that minimizes the residual force around the first and second vibrational modes of the primary path while trying to distribute the amplification over higher frequencies. The control specifications are expressed as constraints on the output sensitivity function $\mathcal{S}$ and input sensitivity function $\mathcal{U}$. In addition, since the controller gain should be zero at the Nyquist frequency, the term $S_{fix}(q^{-1}) = 1 + q^{-1}$ is incorporated in the controller.

The tuning procedure is modified as follows in order to include the fixed terms R_{fix} and S_{fix} in R and S, i.e. $R = R'R_{fix}$ and $S = S'S_{fix}$: The secondary path model B/A is augmented with the fixed terms R_{fix} and S_{fix} (Fig. 4.18). Then $u(t)$ in the regressor vector (2.8) is replaced by the input of the augmented plant $u'(t) = \frac{R_{fix}}{S_{fix}}u(t)$. The estimate of the gradient (3.9) is calculated by replacing $\hat{B}$, $\hat{A}$, R and S with $\hat{B}S_{fix}$, $\hat{A}R_{fix}$, R' and S', respectively. Finally, R' and S' are computed using the iterative algorithm and later multiplied by the fixed terms to obtain the controller polynomials R and S.

Experiments performed on the real suspension system showed that the plant varies slightly with time, thereby reducing the convergence rate of the algorithm. Because of this and the fact that the number of real-time experiments available in this benchmark study is limited, a high-order model of the secondary path (available from the benchmark web site [79]) is used to simulate the secondary path B/A and generate the data needed in this "data-driven" controller tuning procedure. The same model is also used to compute the estimates of gradient and Hessian of the criterion (4.32). Moreover, open-loop experimental data are available from the benchmark web site, where $v_1(t)$ is a PRBS generated by a 10-bit shift register with data length $N = 20000$ and the measured signal $y(t)$ corresponds to $p(t) + v_2(t)$. Thus, the model C_r/D_r of the primary path is not involved in the controller tuning procedure.

The following controller structure is used:

$$K(q^{-1}) = \frac{(s^{(0)} + s^{(1)}q^{-1})(1 + q^{-1})}{1 + r^{(1)}q^{-1} + r^{(2)}q^{-2}} \tag{4.39}$$

A 2nd-order controller is chosen since it corresponds to the lowest order still capable of meeting the benchmark specifications. All the parameters of the controller are initialized to zero except for $s^{(0)} = 0.0025$. It is also verified that the initial controller $K(\rho_0) = s^{(0)}(1 + q^{-1})$ stabilizes the closed-loop system.

Considering the spectrum of the primary path (dashed line in Fig. 4.17) and choosing $W_r(q^{-1}) = 1$ in (4.38), it is evident that the algorithm will reduce the sensitivity function $\mathcal{S}$ mainly around the first resonant mode. However, in order to accentuate the higher frequencies, the vector of instrumental variables is filtered by a 3rd-order high-pass Butterworth filter with the cut-off frequency of 100 Hz:

$$W_r(q^{-1}) = \frac{0.4459 - 1.3377q^{-1} + 1.3377q^{-2} - 0.4459q^{-3}}{1 - 1.459q^{-1} + 0.9104q^{-2} - 0.1978q^{-3}}$$

The magnitude plot of this filter is presented as the dash-dot line in Fig. 4.17, while the aggregate weighting $|C_r(e^{-j\omega})/D_r(e^{-j\omega})||W_r(e^{-j\omega})|$ of $\mathcal{S}$ in (4.38) is shown as the solid line. The length of the instrumental variables vector should be larger than the number of controller parameters to be tuned but much smaller than the data length. Here $n_z = 28$ is chosen.

A local optimum is reached after 8 iterations. In all iterations the initial step size $\gamma_i = 1$ is used. When the tuning procedure provides a controller that destabilizes the closed-loop system (which is readily verified with the available plant model), the step size is simply divided by 2. Note that destabilizing controllers were frequently found due to the fact that the underlying open-loop plant has several oscillatory modes.

Fig. 4.19 shows the output and input sensitivity functions $\mathcal{S}$ and $\mathcal{U}$ before tuning (dash-dot), after 3 iterations (dashed), and after 8 iterations (thick solid line) along with the constraints (thin solid line) provided in the benchmark problem. The resulting controller reduces $\mathcal{S}$ considerably around the first and second resonant modes without violating the constraints on the input sensitivity function $\mathcal{U}$.

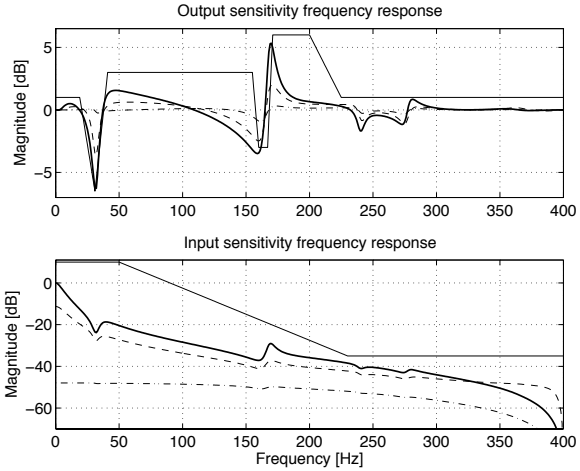

Figure 4.19: Output and input sensitivity functions of the closed-loop system: before tuning (dash-dot), after 3 iterations (dashed), after 8 iterations (thick solid line), and constraints (thin solid line)

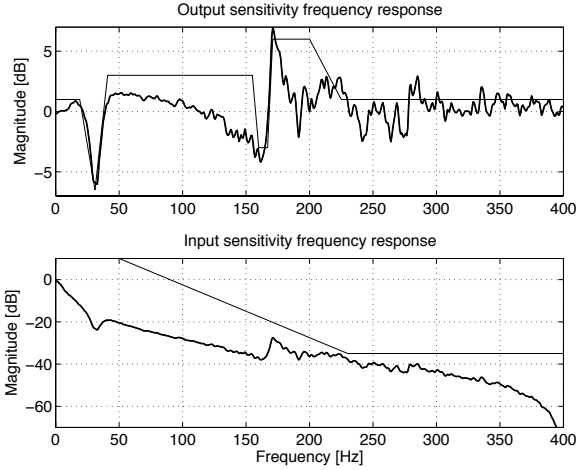

Figure 4.20: Closed-loop output and input sensitivity functions estimated from data collected on the experimental setup with the final controller (thick line) and constraints (thin line)

The controller obtained in simulation is implemented on the experimental setup and Fig. 4.20 shows the corresponding sensitivity functions. The output sensitivity function estimated by spectral analysis slightly violates the constraints at some frequencies. This can be explained by the fact that the model used to generate the data needed for controller design does not describe the experimental system very well around these frequencies. Nevertheless, satisfactory experimental results are obtained using the 2nd-order controller.

4.10 Conclusions

In this chapter, the controller parameters are updated by minimizing the correlation criterion that represents the cross-correlation between the closed-loop output error and the reference signal. The correlation criterion, for sufficiently large n_z, expresses the amount of correlation (or decorrelation) between two signals. Here, "sufficiently large n_z" means that n_z should be at least as large as the length of the non-zero part of the impulse response of the closed-loop system.

The frequency interpretation of the criterion shows that the decorrelating controller, if it exists and belongs to the selected controller class, is the unique global minimum of the criterion. Since in practice such a controller does not exist or does not belong to the selected controller class, the algorithm minimizes the two-norm of the difference between the achieved and desired closed-loop systems provided that the excitation signal is white noise. This is performed independently of the noise characteristics, which is the main objective of controller tuning. In addition, the input sensitivity function is decreased in the frequency regions where the additive uncertainty is large. The convergence and frequency analysis results are asymptotic both in the number of data and number of iterations. An unbiased estimate of the gradient of the output error is necessary to guarantee the convergence of the algorithm to a local minimum of the criterion. This gradient can be estimated using a full-order identified model of the plant or the closed-loop data from a specific experiment as is proposed in the IFT approach. It should be noted that, in practice, an approximate gradient based on the designed model can be used to minimize the criterion, although the convergence is

not guaranteed. Observe that in the case of the decorrelation procedure, an inaccurate estimate of the Jacobian will not prevent the controller parameter vector to converge to ρ° but will affect the convergence speed. On the contrary, in the case of correlation reduction, the iteration will stagnate once the residual $||\rho_i - \rho^{\min}||$ is roughly of the same size as the error in the gradient. For more details on these two iterative methods, the reader is referred to Chapter 5.4 in [48] and Chapter 2.3.1 in [49], respectively.

Within the correlation-reduction method, the choice of the instrumental variables vector is very simple, and no additional effort is necessary for its construction it as was the case with the decorrelation procedure.

A generalization of the correlation criterion has also been proposed. The new criterion is defined as the weighted sum of the two-norms of the cross-correlation functions between a reference signal and the output and input closed-loop errors. If the assumption of independence between the reference signal and the disturbance holds, the criterion remains asymptotically unaffected by the disturbance characteristics. A frequency-domain analysis of the proposed criterion has shown that, depending on the values of the weighting factors k_{oe} and k_{ie}, there is a trade-off in meeting the designed output and input sensitivities. The features and the applicability of the correlation-reduction approach based on the generalized criterion are illustrated by means of a simulation example.

Furthermore, the correlation-reduction method has been modified to address the disturbance rejection problem in the cases where it is possible to measure the disturbance signal. This approach can also be used with systems where the disturbance cannot be measured but there is the possibility of injecting a known test signal. Though the proposed controller-tuning algorithm uses data collected in the time domain, a frequency analysis indicates how to handle the control specifications expressed in terms of constraints on the sensitivity functions.

This algorithm has been applied very successfully to an international benchmark on the design and optimization of restricted-order controllers for an active suspension system [51].

Chapter 5

Correlation-based tuning of linear decoupling multivariable controllers

5.1 Introduction

A common approach to multivariable control is the two-step procedure, whereby one first designs a "decoupler" to deal with process interactions and then a set of controllers is designed for the "diagonalized" plant obtained in the first step [73]. The design of decouplers and controllers using standard model-based methods may be very sensitive to modelling errors and uncertainties. A suitable control-oriented model is often difficult to obtain. On the other hand, data-driven methods use the data collected in closed-loop operation. Since these data reflect accurately the local behavior of the plant in the vicinity of the current operating conditions, it is clear that the use of this "implicit model" for the computation of decouplers and controllers is advantageous in the sense that the performance is likely to be improved.

However, the application of data-driven methods to the control of LTI multivariable systems has a few drawbacks. First, for a data-driven method that minimizes a norm of some error signal, it is not possible to incorporate the decoupler design into the criterion if all references are excited simultaneously. Instead, for eliminating the influence of a reference on a particular output, it is necessary to excite that reference while keeping the other references constant and minimize an error signal norm related to that output, as this is done with IFT in [24]. For MIMO systems with several plant inputs, n_u, and outputs, n_y, this requires a large number of experiments. Another

difficulty is the calculation of the gradient of the criterion. Typically, the number of experiments needed to estimate the gradient increases with n_u and n_y. For example, the IFT approach requires $n_y n_u + 1$ experiments per iteration [30]. However, some efforts have been made recently to reduce the number of experiments with this approach (for more details see [15, 16, 38]).

In this chapter, the tuning of LTI multivariable controllers using the correlation approach is proposed. For simplicity of presentation it is assumed an equal number of inputs and outputs. The off-diagonal elements of the controller transfer function matrix are tuned to eliminate interaction between the controlled outputs (in the sequel this will be called "diagonalization of the closed-loop system"), while the elements on the main diagonal are tuned to provide the desired closed-loop performance. The fact that the decoupling is done in a natural way by decorrelating a given reference from the non-corresponding outputs without the need for additional experiments makes CbT particularly appealing for tuning MIMO controllers. The controllers on the main diagonal feature the same characteristics as those for SISO systems. The parameters of the resulting decouplers and controllers are asymptotically not affected by noise. A single experiment per iteration is sufficient for the tuning of all controllers and decouplers regardless of the number of inputs and outputs since all reference inputs can be excited simultaneously.

Unfortunately, there is a drawback resulting from the simultaneous excitation of all references. Due to the decoupling specifications, the simultaneous excitation of all references increases the variance of the estimated controller parameters. To obtain more accurate estimates, one can perform n_y experiments per iteration. However, even in this case, CbT has a considerable advantage in terms of decoupling compared to other data-driven control design methods, where the controller parameters are calculated by minimizing the norm of some error signal, such as in IFT. Using the latter methods, perfect decoupling cannot be achieved due to the nature of the underlying criterion, since the minimization of an error signal norm induces a trade-off between satisfying the decoupling specifications and noise rejection. In contrast, the CbT criterion is asymptotically independent of noise so that the resulting controller, provided that it is of appropriate structure, perfectly satisfies the decoupling specifications.

Similarly to the SISO case, two methods for computing the controller parameters can be distinguished: the decorrelation procedure and correlation-reduction method. The features of these two variants are discussed and compared in terms of applicability to practical control situations where one can collect a large number of data.

Chapter outline: Some notations are introduced in Section 5.2. Section 5.3 presents the basic idea of multivariable CbT approach and deals with the tuning of LTI multivariable controllers by both the decorrelation procedure and correlation reduction. Simulation results are presented in Section 5.4, and concluding remarks are given in Section 5.5.

5.2 Notations and system description

In Section 2.1, the basic notations for SISO systems are given. Although the same notational convention is used in this chapter, the notations for MIMO systems will be presented in this section to avoid possible confusion.

For the sake of simplicity, and without loss of generality, it is assumed that the plant has two inputs and two outputs. Consider the block diagram of the model-following problem presented in Fig. 5.1. The upper part shows the achieved closed-loop system with the unknown true plant whose outputs can be described by the following LTI multivariable discrete-time model:

$$y(t) = G(q^{-1})u(t) + v(t) \tag{5.1}$$

where $y(t) \in \mathcal{R}^2$ denotes the outputs of the true plant at time t, $u(t) \in \mathcal{R}^2$ the control signals, $v(t) \in \mathcal{R}^2$ the disturbances on the outputs, and $G(q^{-1})$ is a 2×2 transfer function matrix with q^{-1} being the backward-shift operator. It is assumed that $v(t)$ is a zero-mean stationary stochastic process.

The 2×2 controller transfer function matrix $K(q^{-1}, \rho)$ is parameterized by the parameter vector $\rho \in \mathcal{R}^{n_\rho}$, and $r(t) \in \mathcal{R}^2$ represents external reference signals.

The (j, k) element of the controller transfer function matrix is:

$$K_{jk}(q^{-1}, \rho) = \frac{S_{jk}(q^{-1}, \rho)}{R_{jk}(q^{-1}, \rho)} \quad j, k = 1, 2 \tag{5.2}$$

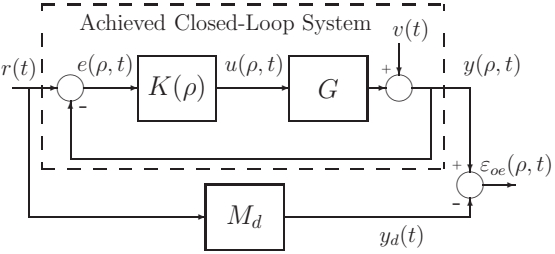

Figure 5.1: Achieved multivariable closed-loop system and its reference model M_d

where

$$\begin{aligned} R_{jk}(q^{-1},\rho) &= 1 + r_{jk}^{(1)}q^{-1} + \cdots + r_{jk}^{(n_r)}q^{-n_r} \\ S_{jk}(q^{-1},\rho) &= s_{jk}^{(0)} + s_{jk}^{(1)}q^{-1} + \cdots + s_{jk}^{(n_s)}q^{-n_s} \end{aligned}$$

It is assumed, for simplicity of notation, that all controllers $K_{jk}(q^{-1},\rho)$, $j = 1,2$, $k = 1,2$ have the same number of poles and the same number of zeros. Moreover, it is assumed that the controllers have no common parameters. The controller parameter vector ρ can be written as follows:

$$\rho^T = [\rho_{K_{11}}^T, \rho_{K_{12}}^T, \rho_{K_{21}}^T, \rho_{K_{22}}^T] \tag{5.3}$$

where

$$\rho_{K_{jk}}^T = [r_{jk}^{(1)}, r_{jk}^{(2)}, \ldots, r_{jk}^{(n_r)}, s_{jk}^{(0)}, s_{jk}^{(1)}, \ldots, s_{jk}^{(n_s)}]$$

Thus, $n_\rho = 4(n_r + n_s + 1)$.

The lower part of Fig. 5.1 shows the reference model M_d defining the desired behavior of the closed-loop outputs $y_d(t)$ in response to the reference signals $r(t)$. The reference model can be constructed, for example, as the closed-loop system containing a model G_d of the plant and the controller K_d:

$$M_d \triangleq \begin{pmatrix} M_{d11} & M_{d12} \\ M_{d21} & M_{d22} \end{pmatrix} = (I + G_d K_d)^{-1} G_d K_d \tag{5.4}$$

with $I \in \mathcal{R}^{2\times 2}$ being the identity matrix. It is assumed that G_d and G are diagonalizable by output feedback, and that the reference model M_d has a diagonal structure with $M_{d12} = M_{d21} = 0$. Regarding the necessary and

sufficient conditions for a linear multivariable system to be diagonalizable, the reader is referred to [12, 10, 11] and references therein.

The closed-loop response can be written as:

$$y(\rho, t) = \mathcal{T} r(t) + \mathcal{S} v(t), \tag{5.5}$$

and the control error is:

$$e(\rho, t) = r(t) - y(\rho, t) = \mathcal{S}\left(r(t) - v(t)\right), \tag{5.6}$$

where $\mathcal{S}$ denotes the output sensitivity function:

$$\mathcal{S} = (I + GK)^{-1} \tag{5.7}$$

and $\mathcal{T}$ the complementary sensitivity function:

$$\mathcal{T} = (I + GK)^{-1} GK \tag{5.8}$$

The closed-loop output error is defined as:

$$\varepsilon_{oe}(\rho, t) = y(\rho, t) - y_d(t). \tag{5.9}$$

Notational remarks: The signals collected under closed-loop operation using the controller $K(\rho)$ will carry the argument ρ. The elements of signal vectors and transfer function matrices will carry the position as a subscript. For example, $y_k(\rho, t)$ will denote the k^{th} component of the output vector $y(\rho, t)$. In contrast, the coefficients in numerator and denominator polynomials of the controllers $K_{jk}(q^{-1}, \rho)$ will carry the position as a superscript. Furthermore, the backward-shift operator q^{-1} will be omitted whenever appropriate.

5.3 CbT for MIMO systems

5.3.1 Idea of multivariable correlation-based tuning

Consider the controller structure presented in Fig. 5.2, with the following design specifications:

- The diagonal elements $K_{11}(\rho)$ and $K_{22}(\rho)$ of the controller transfer

matrix $K(\rho)$ are tuned to provide satisfactory tracking of $y_{d1}(t)$ by $y_1(\rho,t)$ and $y_{d2}(t)$ by $y_2(\rho,t)$, respectively.

- The off-diagonal elements $K_{12}(\rho)$ and $K_{21}(\rho)$ are tuned to be decouplers. That is, the controller $K_{12}(\rho)$ is tuned to eliminate the influence of the reference signal $r_2(t)$ on the output $y_1(\rho,t)$. Hence, if the decoupler $K_{21}(\rho)$ is tuned similarly, the mutual influences of $y_1(\rho,t)$ and $y_2(\rho,t)$ are suppressed.

In other words, the desired sensitivity functions $\mathcal{S}_d$ and $\mathcal{T}_d$ are in diagonal form.

Consider first the tuning of the decoupler $K_{12}(\rho)$. When applying the controller K_0 to the true plant excited by the reference signal $r(t)$, the output $y_1(\rho,t)$ contains the contributions due to the reference signals $r_1(t)$ and $r_2(t)$ and the disturbance $v(t)$. The reference signals $r_1(t)$ and $r_2(t)$ are mutually independent and uncorrelated with $v(t)$. Hence, the idea is to adjust the parameters of $K_{12}(\rho)$ to make the output $y_1(\rho,t)$ uncorrelated with the reference signal $r_2(t)$. The resulting decoupler provides $y_1(\rho,t)$ that contains only the contributions due to $v_1(t)$ and $r_1(t)$, i.e. the influence of $v_2(t)$ and $r_2(t)$ on $y_1(\rho,t)$ is eliminated.

Consider next the tuning of $K_{11}(\rho)$. Again, with K_0 operating in the loop, the observed closed-loop output error $\varepsilon_{oe1}(\rho,t)$ contains a contribution due to the disturbance $v(t)$ and another contribution stemming from the difference between G and G_d that, in turn, has two parts originating from $r_1(t)$ and $r_2(t)$. The idea is to adjust the parameters of $K_{11}(\rho)$ so as to make $\varepsilon_{oe1}(\rho,t)$ uncorrelated with $r_1(t)$. The effect of modeling errors excited by $r_2(t)$ is eliminated by the decoupler $K_{12}(\rho)$. Hence, the resulting controller compensates the effect of modeling errors to the extent that the closed-loop error $\varepsilon_{oe1}(\rho,t)$ contains only the disturbance filtered by the closed-loop system. This way, the output $y_1(\rho,t)$ will achieve the desired output $y_{d1}(t)$.

A similar reasoning follows for $K_{21}(\rho)$ and $K_{22}(\rho)$ that are related to the output $y_2(\rho,t)$.

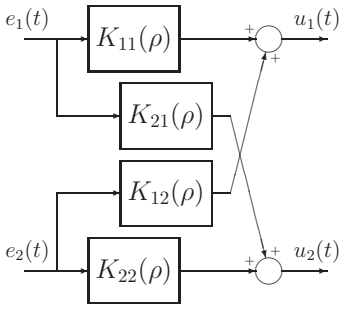

Figure 5.2: Multivariable 2×2 controller

5.3.2 Cross-correlation function

Let the cross-correlation function be defined as follows:

$$F(\rho) \stackrel{\Delta}{=} E\left\{\bar{F}(\rho)\right\} \tag{5.10}$$

where $E\{\cdot\}$ is the mathematical expectation, and the vector $\bar{F}(\rho) \in \mathcal{R}^{n_\rho}$ reads:

$$\bar{F}^T(\rho) = \left[\bar{f}^T_{K_{11}}(\rho), \bar{f}^T_{K_{12}}(\rho), \bar{f}^T_{K_{21}}(\rho), \bar{f}^T_{K_{22}}(\rho)\right] \tag{5.11}$$

with

$$\bar{f}_{K_{jk}}(\rho) = \frac{1}{N}\sum_{t=1}^{N} \zeta_{K_{jk}}(\rho, t)\mathcal{E}_{K_{jk}}(\rho, t) \tag{5.12}$$

where N is the number of data and $\zeta_{K_{jk}}(\rho, t) \in \mathcal{R}^{n_\zeta}$ the vector of instrumental variables associated with the controller $K_{jk}(\rho)$. Note that $n_\zeta = n_r + n_s + 1$, and $n_\rho = 4n_\zeta$. The component $\bar{f}_{K_{jk}}(\rho) \in \mathcal{R}^{n_\zeta}$ corresponds to the controller $K_{jk}(\rho)$. The way $\zeta_{K_{jk}}(\rho, t)$ and the variable $\mathcal{E}_{K_{jk}}(\rho, t) \in \mathcal{R}$ are constructed depends on whether or not the controller $K_{jk}(\rho)$ is on the main diagonal of $K(\rho)$:

- $\underline{j = k}$: $K_{jj}(\rho)$ is tuned so as to reduce the correlation between $\varepsilon_{oej}(\rho, t)$ and $r_j(t)$. Taking into account the fact that the tuning of the controllers $K_{jj}(\rho)$ and the decouplers $K_{jk}(\rho)$ is done simultaneously, the output $y_j(\rho, t)$ will, in the case of perfect decorrelation, follow $y_{dj}(t)$ up to the effect of the disturbance. Thus, the vector of instrumental variables $\zeta_{K_{jj}}(\rho, t)$ should be chosen to be correlated with the reference signal

$r_j(t)$ and independent of the disturbance $v_j(t)$. The variable $\mathcal{E}_{K_{jj}}(\rho, t)$ is chosen as $\varepsilon_{oej}(\rho, t)$.

- $j \neq k$: To eliminate the influence of $r_k(t)$ on $y_j(t)$, it is sufficient to decorrelate these two signals, i.e. $\zeta_{K_{jk}}(\rho, t)$ should be correlated with $r_k(t)$ and $\mathcal{E}_{K_{jk}}(\rho, t) = y_j(\rho, t)$.

Hence, the variable $\mathcal{E}_{K_{jk}}(\rho, t)$ is constructed as follows:

$$\mathcal{E}_{K_{jk}}(\rho, t) = \begin{cases} \varepsilon_{oej}(\rho, t), & j = k \\ y_j(\rho, t), & j \neq k \end{cases} \tag{5.13}$$

and the vector of instrumental variables $\zeta_{K_{jk}}(\rho, t)$ is a function of $r_k(t)$.

The parameters of the controller are computed either by minimization of a norm of the cross-correlation function (5.10) or as the values that make this function equal to zero. Observe that in either case the underlying criterion/equation is nonlinear with respect to the controller parameters. In general, an analytical solution to these problems does not exist and it is necessary to consider iterative numerical methods. Before proceeding further, suppose that Assumptions A1, A2 and A4, introduced in Section 3.2.1, hold. In addition to these, the following assumptions will be needed in the sequel:

(A8) The reference signals $r(t)$ are persistently exciting of sufficiently high order with respect to the number of controller parameters and are uncorrelated with the disturbances $v(t)$. Furthermore, the elements of the reference signal vector $r(t)$ are assumed to be mutually independent.

(A9) The decorrelating controller K° exists, is unique, and belongs to the set of parameterized controllers (the corresponding parameters will be denoted as ρ°).

5.3.3 Decorrelation procedure for MIMO systems

Under Assumption A9, the parameters of the controller that perfectly decorrelates $\zeta_{K_{jk}}(\rho, t)$ from $\mathcal{E}_{K_{jk}}(\rho, t)$ are computed as the solution to the following system of correlation equations:

$$F(\rho) = 0 \tag{5.14}$$

A solution to (5.14) can be found using an iterative stochastic approximation procedure, for example the Robbins-Monro algorithm [70]:

$$\rho_{i+1} = \rho_i - \gamma_i \bar{F}(\rho_i). \tag{5.15}$$

It can be shown using the Theorem 3.1 that, under Assumptions A1, A2, A4, A8 and A9 and assuming that $F(\rho)$ possesses continuous partial derivatives of first and second order with respect to ρ, this scheme converges to a solution of the correlation equations (5.10), provided that $F(\rho)$ is monotonically increasing in the vicinity of the solution ρ°, i.e. the following condition holds:

$$Q(\rho^\circ) = E\left\{ \frac{\partial \bar{F}(\rho)}{\partial \rho}\bigg|_{\rho=\rho^\circ} \right\} > 0. \tag{5.16}$$

Let us investigate the structure of $Q(\rho)$. It follows from (5.3), (5.11), (5.12) and (5.16) that $Q(\rho) \in \mathcal{R}^{n_\rho \times n_\rho}$ can be expressed as:

$$Q(\rho) = \begin{pmatrix} Q_{K_{11}}^{K_{11}} & Q_{K_{11}}^{K_{12}} & Q_{K_{11}}^{K_{21}} & Q_{K_{11}}^{K_{22}} \\ Q_{K_{12}}^{K_{11}} & Q_{K_{12}}^{K_{12}} & Q_{K_{12}}^{K_{21}} & Q_{K_{12}}^{K_{22}} \\ Q_{K_{21}}^{K_{11}} & Q_{K_{21}}^{K_{12}} & Q_{K_{21}}^{K_{21}} & Q_{K_{21}}^{K_{22}} \\ Q_{K_{22}}^{K_{11}} & Q_{K_{22}}^{K_{12}} & Q_{K_{22}}^{K_{21}} & Q_{K_{22}}^{K_{22}} \end{pmatrix} \tag{5.17}$$

where $Q_{K_{mn}}^{K_{jk}} \triangleq E\{\partial \bar{f}_{K_{jk}}(\rho)/\partial \rho_{K_{mn}}\}$ can be expressed as:

$$\begin{aligned} Q_{K_{mn}}^{K_{jk}} &= E\left\{ \frac{1}{N}\sum_{t=1}^{N} \frac{\partial \zeta_{K_{jk}}(\rho,t)}{\partial \rho_{K_{mn}}} \mathcal{E}_{K_{jk}}(\rho,t) \right. \\ &\quad \left. + \frac{\partial \mathcal{E}_{K_{jk}}(\rho,t)}{\partial \rho_{K_{mn}}} \zeta_{K_{jk}}^T(\rho,t) \right\} \end{aligned} \tag{5.18}$$

In the vicinity of the solution, the first term in (5.18) vanishes since the derivative of the instrumental variable vector $\zeta_{K_{jk}}(\rho,t)$ is not correlated with $\mathcal{E}_{K_{jk}}(\rho,t)$. Note that:

$$\frac{\partial \mathcal{E}_{K_{jk}}(\rho,t)}{\partial \rho_{K_{mn}}} = \frac{\partial y_j(\rho,t)}{\partial \rho_{K_{mn}}} \quad \forall j,k. \tag{5.19}$$

At the solution ρ°, (5.5)-(5.8) lead to:

$$\left.\frac{\partial y(\rho,t)}{\partial \rho^{(p)}_{K_{mn}}}\right|_{\rho^\circ_{K_{mn}}} = \mathcal{S}(\rho^\circ) G \left.\frac{\partial K(\rho)}{\partial \rho^{(p)}_{K_{mn}}}\right|_{\rho^\circ_{K_{mn}}} e(\rho^\circ, t) \tag{5.20}$$

where $p = 1, \ldots, n_r + n_s + 1$. Considering that the subvectors $\rho_{K_{mn}}$ are independent, and $\mathcal{S}$ is diagonal at ρ°, it follows from (5.20) and the second equality in (5.6):

$$\left.\frac{\partial y(\rho,t)}{\partial \rho^{(p)}_{K_{mn}}}\right|_{\rho^\circ_{K_{mn}}} \overset{f}{\sim} e_n(\rho^\circ, t) \overset{f}{\sim} r_n(t),\, v_n(t) \tag{5.21}$$

where $\overset{f}{\sim}$ denotes that the signal on the left-hand side of this operator is a function of the right-hand side signal. Furthermore, according to the discussion leading to (5.13), one can write:

$$\zeta_{K_{jk}}(\rho, t) \overset{f}{\sim} r_k(t). \tag{5.22}$$

Using the relationships (5.21) and (5.22), the expression (5.18), and the fact that $r_1(t)$, $r_2(t)$, $v_1(t)$ and $v_2(t)$ are not correlated, it follows that:

$$Q^{K_{jk}}_{K_{mn}} = 0, \quad k \neq n \tag{5.23}$$

i.e. the matrix $Q(\rho^\circ)$ takes the following form:

$$Q(\rho^\circ) = \begin{pmatrix} Q^{K_{11}}_{K_{11}} & 0 & Q^{K_{21}}_{K_{11}} & 0 \\ 0 & Q^{K_{12}}_{K_{12}} & 0 & Q^{K_{22}}_{K_{12}} \\ Q^{K_{11}}_{K_{21}} & 0 & Q^{K_{21}}_{K_{21}} & 0 \\ 0 & Q^{K_{12}}_{K_{22}} & 0 & Q^{K_{22}}_{K_{22}} \end{pmatrix} \tag{5.24}$$

where

$$Q^{K_{jk}}_{K_{mk}} \overset{f}{\sim} r_k(t), v_k(t). \tag{5.25}$$

From (5.18) and (5.24), it is obvious that the choice of the instrumental variables $\zeta_{K_{jk}}$ affects the positive definiteness of $Q(\rho^\circ)$. Hence, it is important to take this fact into account when constructing the instrumental variables. This will be investigated in the following.

Choice of Instrumental Variables

In the case of SISO systems, the typical choice for the instrumental variable vector as a noise-free estimate of the gradient $\partial y_j/\partial \rho_{K_{mn}}$ guarantees the positive definiteness of $Q(\rho^\circ)$. However, in the case of MIMO systems, the choice of $\zeta_{K_{jk}}(\rho,t)$ is less trivial since the aforementioned choice ensures only the positive definiteness of the elements on the principal diagonal of $Q(\rho^\circ)$.

It is clear from (5.22) that the instrumental variables should be chosen as signals obtained by filtering $r_k(t)$. Therefore, the instrumental variables can by generated using the following model structure:

$$\zeta_{K_{jk}}(\rho,t) = \sum_{l=0}^{n_h-1} \left(\mathcal{F}_l(q^{-1}) r_k(t)\right) h^l_{K_{jk}} \tag{5.26}$$

where n_h denotes the model order, $\mathcal{F}_l(q^{-1})$ is the l^{th} element of a set of stable basis transfer functions and $h^l_{K_{jk}}$ the corresponding weighting coefficients. The simplest choice for these functions is $\mathcal{F}_l(q^{-1}) = q^{-l}$. However, in order to reduce the model order, one can adopt

$$\mathcal{F}_l(q^{-1}) = \frac{1}{1-q^{-1}\xi_l} \tag{5.27}$$

where the poles ξ_l are chosen to incorporate some a priori information about the underlying closed-loop dynamics [66]. Another possibility is to use orthonormal basis functions such as Laguerre or Kautz. Since $\zeta_{K_{jk}}(\rho,t)$ and consequently $Q(\rho^\circ)$ are linear with respect to the parameters $h^l_{K_{jk}}$, the problem of obtaining a positive definite matrix $Q(\rho^\circ)$ can be formulated as a convex feasibility problem and solved using Linear Matrix Inequalities (LMIs) [7]. Hence, the choice of the instrumental variables reduces to finding $h^l_{K_{jk}}$ that makes

$$Q(\rho^\circ, h^l_{K_{jk}}) > 0. \tag{5.28}$$

In this feasibility problem, it is necessary to evaluate $Q(\rho^\circ, h^l_{K_{jk}})$ for different values of $h^l_{K_{jk}}$. Plugging (5.18), (5.19), (5.20) and (5.26) in (5.24), it is obvious that $Q(\rho^\circ, h^l_{K_{jk}})$ depends on the derivative $\dfrac{\partial y_j(\rho,t)}{\partial \rho_{K_{mn}}}$ that is unknown. However, this derivative can be estimated using (5.20), where: (i) the transfer function matrix $\mathcal{S}(\rho^\circ)$ is replaced by $\mathcal{S}_d$; (ii) the unknown plant

G is replaced by either G_d or an identified model $\hat{G}$; (iii) the signal $e(\rho^\circ, t)$ is replaced by its estimate $\hat{e}(\rho^\circ, t) = \mathcal{S}_d r(t)$.

In this context, assuming that the conditions for the iterative algorithm (5.15) to converge to ρ° hold, the following question arises: Is the simultaneous excitation of all reference signals advantageous or detrimental to the accuracy of the estimated controller parameters? As a first element of response to this question, the accuracy of the parameter estimates around this solution is investigated as a function of the external reference signals $r_1(t)$ and $r_2(t)$. This is the topic of the next section.

Variance Analysis

From Theorem 3.3 and expression (5.15), the sequence $\sqrt{i}(\rho_i - \rho^\circ)$ converges asymptotically in distribution to a zero-mean normal distribution with covariance

$$V = \alpha^2 \int_0^\infty e^{Dx} P e^{D^T x} dx \tag{5.29}$$

where

$$P = \lim_{i \to \infty} E\left\{ \bar{F}(\rho^\circ) \bar{F}^T(\rho^\circ) \right\}. \tag{5.30}$$

Let us consider the form of the matrices P, D and V. Note that, at $\rho = \rho^\circ$, (5.13) reduces to:

$$\mathcal{E}_{K_{jk}}(\rho, t) = \begin{cases} \mathcal{S}_{jj}(\rho^\circ) v_j(t), & j = k \\ \mathcal{T}_{jj}(\rho^\circ) r_j(t) + \mathcal{S}_{jj}(\rho^\circ) v_j(t), & j \neq k \end{cases} \tag{5.31}$$

Considering that $r_1(t)$, $r_2(t)$, $v_1(t)$ and $v_2(t)$ are independent, and using (5.11), (5.12), (5.30) and (5.31), one gets, after straightforward but tedious calculations:

$$P(\rho^\circ) = \begin{pmatrix} P_{K_{11}}^{K_{11}} & 0 & 0 & 0 \\ 0 & P_{K_{12}}^{K_{12}} & P_{K_{12}}^{K_{21}} & 0 \\ 0 & P_{K_{21}}^{K_{12}} & P_{K_{21}}^{K_{21}} & 0 \\ 0 & 0 & 0 & P_{K_{22}}^{K_{22}} \end{pmatrix} \tag{5.32}$$

where

$$P_{K_{mn}}^{K_{jk}} = E\left\{ \frac{1}{N^2} \sum_{t=1}^{N} \zeta_{K_{jk}}(\rho, t) \mathcal{E}_{K_{jk}}(\rho, t) \times \sum_{s=1}^{N} \zeta_{K_{mn}}^T(\rho, s) \mathcal{E}_{K_{mn}}(\rho, s) \right\}. \tag{5.33}$$

Observe that the matrix $D(\rho^\circ) = I/2 - \alpha Q(\rho^\circ)$ has the same structure as $Q(\rho^\circ)$ in (5.24), and that its elements, due to (5.25), satisfy:

$$D_{K_{mk}}^{K_{jk}} \overset{f}{\sim} r_k(t), v_k(t). \tag{5.34}$$

Finally, note that the covariance matrix V can be partitioned as:

$$V = \begin{pmatrix} V_{K_{11}}^{K_{11}} & V_{K_{11}}^{K_{12}} & V_{K_{11}}^{K_{21}} & V_{K_{11}}^{K_{22}} \\ V_{K_{12}}^{K_{11}} & V_{K_{12}}^{K_{12}} & V_{K_{12}}^{K_{21}} & V_{K_{12}}^{K_{22}} \\ V_{K_{21}}^{K_{11}} & V_{K_{21}}^{K_{12}} & V_{K_{21}}^{K_{21}} & V_{K_{21}}^{K_{22}} \\ V_{K_{22}}^{K_{11}} & V_{K_{22}}^{K_{12}} & V_{K_{22}}^{K_{21}} & V_{K_{22}}^{K_{22}} \end{pmatrix}. \tag{5.35}$$

Next, let us focus on the following two cases:

a) The closed-loop system is excited by a single reference signal, say $r_1(t)$; the corresponding matrices and their elements will carry the subscript "a", for example $V_{a,K_{mn}}^{K_{jk}}$, $j,k,m,n = 1,2$, or D_a.

b) The closed-loop system is excited by both components of $r(t)$; the corresponding matrices and their elements will carry the subscript "b".

When only $r_1(t)$ is excited, it follows from (5.12) and (5.22) that only the controllers $K_{11}(\rho)$ and $K_{21}(\rho)$ can be tuned. Hence, only the variances $V_{K_{11}}^{K_{11}}$ and $V_{K_{21}}^{K_{21}}$ can be compared for the two excitation cases. Furthermore, in order to enforce no signal path between $e_2(t)$ and $u_1(t)$ and $u_2(t)$, $K_{12}(\rho)$ and $K_{22}(\rho)$ are set to zero. This way, similarly to the case where the optimal controllers $K_{12}(\rho^\circ)$ and $K_{22}(\rho^\circ)$ are used, there is no influence of $y_2(t)$ and $v_2(t)$ on $y_1(t)$. Note that, when the MIMO plant to be controlled is not stable, it is not possible to set $K_{12}(\rho)$ and $K_{22}(\rho)$ to zero. In this case, the tuning of the controller $K(\rho)$ can only be performed by exciting both components of $r(t)$.

Next, the following result can be established.

Theorem 5.1 *Consider the tuning of the parameters $\rho_{K_{11}}$ and $\rho_{K_{21}}$ of the controllers $K_{11}(\rho)$ and $K_{21}(\rho)$. Let the components $r_1(t)$ and $r_2(t)$ be independent and persistently exciting of sufficient order. Then, the covariance matrices of the parameter estimates $\hat{\rho}_{K_{11}}$ and $\hat{\rho}_{K_{21}}$ cannot decrease by addi-*

tion of the second excitation $r_2(t)$, i.e.

$$V_{b,K_{11}}^{K_{11}} \geq V_{a,K_{11}}^{K_{11}} \quad \text{and} \quad V_{b,K_{21}}^{K_{21}} \geq V_{a,K_{21}}^{K_{21}} \tag{5.36}$$

Proof. For simplicity, let α in (5.29) be set to 1. Now, observe that the matrices V, D and P are related via the following Lyapunov equation [37]:

$$P + DV + VD^T = 0. \tag{5.37}$$

Due to the specific form of D and P, a straightforward computation of this expression gives the following relation that includes the variances $V_{K_{11}}^{K_{11}}$ and $V_{K_{21}}^{K_{21}}$:

$$\tilde{P} + \tilde{D}\tilde{V} + \tilde{V}\tilde{D}^T = 0, \tag{5.38}$$

where

$$\tilde{P} = \begin{pmatrix} P_{K_{11}}^{K_{11}} & 0 \\ 0 & P_{K_{21}}^{K_{21}} \end{pmatrix}, \quad \tilde{D} = \begin{pmatrix} D_{K_{11}}^{K_{11}} & D_{K_{11}}^{K_{21}} \\ D_{K_{21}}^{K_{11}} & D_{K_{21}}^{K_{21}} \end{pmatrix} \tag{5.39}$$

and

$$\tilde{V} = \begin{pmatrix} V_{K_{11}}^{K_{11}} & V_{K_{11}}^{K_{21}} \\ V_{K_{21}}^{K_{11}} & V_{K_{21}}^{K_{21}} \end{pmatrix}. \tag{5.40}$$

Equation (5.34) indicates that $\tilde{D}$ depends on $r_1(t)$ but not on $r_2(t)$. Therefore, $\tilde{D}$ is identical for both cases of excitation, i.e. $\tilde{D}_a = \tilde{D}_b$. Furthermore, since at the solution the closed-loop system is perfectly decoupled, it follows from (5.22), (5.31) and (5.33) that $P_{K_{11}}^{K_{11}}$ is also identical for both cases of excitation. Let us now consider $P_{K_{21}}^{K_{21}}$. By replacing (5.22) and (5.31) in (5.33), one gets:

$$\begin{aligned} P_{K_{21}}^{K_{21}} \;=\; & E\left\{ \frac{1}{N^2} \sum_{t=1}^{N} \zeta_{K_{21}}(r_1(t), \rho, t) \left\{ \mathcal{T}_{22}(\rho^\circ) r_2(t) \right.\right. \\ & \left. + \mathcal{S}_{22}(\rho^\circ) v_2(t) \right\} \times \sum_{s=1}^{N} \zeta_{K_{21}}^T(r_1(t), \rho, s) \\ & \left.\left. \left\{ \mathcal{T}_{22}(\rho^\circ) r_2(s) + \mathcal{S}_{22}(\rho^\circ) v_2(s) \right\} \right\}. \end{aligned} \tag{5.41}$$

It can be concluded from this expression that the contribution of $r_2(t)$ to $P_{K_{21}}^{K_{21}}$ is positive definite. This contribution will be denoted as $\Delta P_{K_{21}}^{K_{21}}$. There-

fore, one can write:

$$\tilde{P}_b = \tilde{P}_a + \begin{pmatrix} 0 & 0 \\ 0 & \Delta P^{K_{21}}_{K_{21}} \end{pmatrix} \stackrel{\Delta}{=} \tilde{P}_a + \Delta\tilde{P} \tag{5.42}$$

where $\Delta\tilde{P} \geq 0$. Similarly, for the covariance matrices $\tilde{V}_a$ and $\tilde{V}_b$, it can be written $\tilde{V}_b = \tilde{V}_a + \Delta\tilde{V}$, which leads to:

$$\begin{aligned} &\tilde{P}_b + \tilde{D}_b\tilde{V}_b + \tilde{V}_b\tilde{D}_b^T = \\ &\left(\tilde{P}_a + \Delta\tilde{P}\right) + \tilde{D}_b\left(\tilde{V}_a + \Delta\tilde{V}\right) + \left(\tilde{V}_a + \Delta\tilde{V}\right)\tilde{D}_b^T = \\ &\Delta\tilde{P} + \tilde{D}_b\Delta\tilde{V} + \Delta\tilde{V}\tilde{D}_b^T = 0 \end{aligned} \tag{5.43}$$

The last equality can be written more illustratively as:

$$\Delta\tilde{V} = \int_0^\infty e^{\tilde{D}_b x}\,\Delta\tilde{P}\,e^{\tilde{D}_b^T x}dx. \tag{5.44}$$

It is obvious that if $\Delta\tilde{P} \geq 0$ then $\Delta\tilde{V} \geq 0$ [89]. The inequalities (5.36) follow from the fact that any principal submatrix of a positive semi-definite matrix is positive semi-definite. □

Theorem 5.1 states that the presence of the component $r_2(t)$ does not improve the accuracy of the parameters related to the controllers $K_{11}(\rho)$ and $K_{21}(\rho)$. In fact, the accuracy is reduced in most cases. This result is rather interesting taking into account a number of results where, in the cases of open-loop and direct closed-loop identification using prediction error methods, the addition of $r_2(t)$ was shown to almost always improve the variance of the estimated parameters [21, 22, 61].

Remarks:

- This result can be explained intuitively as follows. Consider the instrumental variable method in the field of system identification (see Section 2.4). The expression for the variance of the parameter estimates within this method is as follows [75]:

$$\begin{aligned} P_{IV} \;=\; & \sigma^2 E\left\{\zeta(t)\tilde{\varphi}^T(t)\right\}^{-1} E\left\{[H(q^{-1})\zeta(t)][H(q^{-1})\zeta(t)^T]\right\} \\ & \times E\left\{\zeta(t)\tilde{\varphi}^T(t)\right\}^{-T} = R_{IV}^{-1}P_C R_{IV}^{-T} \end{aligned}$$

where $\tilde{\varphi}(t)$ denotes the noise-free estimate of $\varphi(t)$, $H(q^{-1})$ a noise model, P_C the variance of the criterion, R_{IV} the derivative of the predictor of the output, and σ^2 is the variance of the zero-mean noise. Considering that the instrumental variables are filtered versions of the excitation signal, one can conclude the following. The IV method brings about two opposing effects of the power of the excitation signal on the variance of the parameter estimates: 1) An increase in the power of the excitation signal implies an increase in the variance of the criterion P_C, which in turn increases the variance of the parameter estimates P_{IV}; 2) An increase in the power of the excitation signal induces an increase in the power of the derivatives of the predictor of the output R_{IV}. These derivatives enter inversely in the expression for the variance of the parameter estimates. In general, the overall effect is that the variance of the parameter estimates decreases as the variance of the excitation signal increases. For more details, the reader is referred to [75]. In the case of CbT, due to the decoupling of the outputs $y_1(t)$ and $y_2(t)$, $\tilde{D}$ is insensitive to the changes in $r_2(t)$, and therefore only the first effect is present, i.e. the presence of $r_2(t)$ results in an increase of the variance of the estimated controller parameters.

- Comparison of the case of simultaneous excitation of both components of $r(t)$ with the excitation of these components one-by-one shows that $r_2(t)$ acts as an additional disturbance for the tuning of the decoupler $K_{21}(\rho)$. That is, the addition of this reference deteriorates the signal-to-noise ratio for the estimation of $K_{21}(\rho)$ and, via the covariance matrix, influences negatively the variances of the other elements of the controller transfer function.

- For systems where M_d is not diagonal, i.e. decoupling is not part of the control design specifications, both effects of the variance of the excitation on the variance of estimated controller parameters are present.

In this section, a variance analysis for the parameters of a multivariable controller tuned using the CbT approach has been presented. Two cases of excitation have been considered for 2×2 systems. This analysis indicates that the addition of the second reference signal can worsen the variance of the estimated controller parameters. In fact, there is a user's choice

whether to excite the elements of $\mathbf{r}(t)$ one by one or simultaneously. On the one hand, simultaneous excitation provides smaller experimental cost. On the other hand, the one-by-one excitation implies two experiments per iteration but provides more accurate controller parameters.

5.3.4 Correlation reduction for MIMO systems

In the case of a restricted number of controller parameters, it is not guaranteed that, at the solution ρ^d of (5.14), the variable $\mathcal{E}_{K_{jk}}(\rho^d, t)$, which includes the closed-loop output errors and the outputs, is completely decorrelated from the corresponding reference signals. In other words, if the dimension of the controller parameter vector to be updated is smaller than the dimension of the decorrelating controller parameter vector ρ°), then perfect decorrelation is not attainable. For example, when only one parameter per controller K_{jk} is tuned, $F(\rho)$ represents the cross-correlation between $\mathcal{E}_{K_{jk}}(\rho, t)$ and $r(t-1)$. That is, at the solution of (5.14) these signals are decorrelated only for the delay of 1, and not necessarily for other delays. In other words, the resulting controller does not really decorrelate $\mathcal{E}_{K_{jk}}(\rho^d, t)$ and $r(t)$.

To get a grip on these difficulties, the controller parameters can be computed by minimizing the following correlation criterion:

$$J(\rho) = F^T(\rho)F(\rho) \tag{5.45}$$

with the cross-correlation function $F(\rho)$ defined by (5.10)-(5.12). The variables $\mathcal{E}_{K_{jk}}(\rho, t)$ are chosen as in (5.13). The instrumental variables vector is chosen as a shifted version of the reference signal $r_k(t)$:

$$\zeta_{K_{jk}}^T(t) = [r_k(t+n_z), \ldots, r_k(t), \ldots, r_k(t-n_z)] \tag{5.46}$$

where $2n_z+1 \geq n_r+n_s$. Observe that with this choice of instrumental variables, the number of equations is larger than the number of controller parameters, i.e. the cross-correlation between $\mathcal{E}_{K_{jk}}(\rho, t)$ and $r(t)$ is computed for $2n_z + 1$ delays. This way, the underlying system of cross-correlation equations is a better measure of the cross-correlation between $\mathcal{E}_{K_{jk}}(\rho, t)$ and $r(t)$ and, at the same time, it is independent of the controller order.

Remark: In the case of the decorrelation procedure, the instrumental variables were chosen so as to ensure positive-definiteness of $Q(\rho^\circ)$. In con-

trast, in the case of the correlation reduction, the required condition on positive-definiteness of $\frac{\partial J(\rho)}{\partial \rho}\Big|_{\rho=\rho^\circ}$ is automatically satisfied because $J(\rho)$ is a quadratic criterion. Hence, the instrumental variables with this method can be chosen arbitrarily.

Frequency-domain analysis

In this section, the properties of the achieved closed-loop system are investigated by frequency-domain analysis of the criterion (5.45). It follows from (5.10)-(5.12) and (5.45) that this criterion can be expressed as:

$$J(\rho) = \sum_{j=1}^{2}\sum_{k=1}^{2} E\left\{\bar{f}_{K_{jk}}^{T}\right\} E\left\{\bar{f}_{K_{jk}}\right\} \tag{5.47}$$

Then, by substituting (5.46) in (5.12), (5.47) becomes

$$J(\rho) = \sum_{j=1}^{2}\sum_{k=1}^{2}\sum_{\tau=-n_z}^{\tau=n_z} R_{K_{jk}}^{2}(\tau) \tag{5.48}$$

where the cross-correlation $R_{K_{jk}}(\tau)$ is defined as:

$$R_{K_{jk}}(\tau) = E\left\{\mathcal{E}_{K_{jk}}(\rho,t) r_k(t-\tau)\right\} \tag{5.49}$$

Applying Parseval's formula to (5.48), and letting n_z tend to infinity, one gets

$$\lim_{n_z\to\infty} J(\rho) = \sum_{j=1}^{2}\sum_{k=1}^{2} \frac{1}{2\pi}\int_{-\pi}^{\pi} \left|\mathcal{B}_{jk}(e^{j\omega})\right|^2 \Phi_{r_j}^{2}(\omega) d\omega \tag{5.50}$$

where

$$\mathcal{B}_{jk}(e^{j\omega}) = \mathcal{T}_{jk}(e^{j\omega},\rho) - M_{djk}(e^{j\omega}) \tag{5.51}$$

Now, from (5.50) and (5.51), the following observations can be made:

- Criterion (5.45) is asymptotically unaffected by noise.
- The weighted discrepancy between the achieved $\mathcal{T}$ and desired M_d sensitivity functions is minimized, with the weight being the square of the reference signal power. At frequencies where the reference signal power is large, this discrepancy is small.

- In the ideal case, when the global minimum is reached, $\mathcal{B}_{jk}(e^{j\omega}) = 0$. In other words, since the desired sensitivity function M_d is diagonal, diagonal controllers provide $\mathcal{T}_{jj}(e^{j\omega}, \rho) = M_{djj}(e^{j\omega})$ and decouplers $\mathcal{T}_{jk}(e^{j\omega}, \rho) = 0$, $j \neq k$.

Having analyzed the basic properties of (5.45), the next section presents a method to minimize this criterion.

Minimizing an upper bound of the criterion

Minimization of criterion (5.45) is intractable since it involves the product of expectations that are unknown. Therefore, let us define the following criterion:

$$J_u(\rho) = E\left\{\bar{F}^T(\rho)\bar{F}(\rho)\right\} \tag{5.52}$$

This criterion can be minimized using the stochastic approximation method. It can be shown that $J(\rho) \leq J_u(\rho)$, i.e. by minimizing (5.52) one in fact minimizes an upper bound of (5.45) [45].

A local minimum of (5.52) can be found as the solution to:

$$J_u'(\rho) = E\left\{\frac{\partial \bar{F}(\rho)}{\partial \rho}\bar{F}(\rho)\right\} = 0 \tag{5.53}$$

which can be obtained using the following iterative formula [70]:

$$\rho_{i+1} = \rho_i - \gamma_i \left.\frac{\partial \bar{F}(\rho)}{\partial \rho}\right|_{\rho_i} \bar{F}(\rho_i) \tag{5.54}$$

Under Assumptions A1, A2, A4, and A8, this scheme converges to a local minimum of the criterion as the number of iterations goes to infinity, provided that an unbiased estimate of the gradient $\left.\frac{\partial \bar{F}(\rho)}{\partial \rho}\right|_{\rho_i}$ is available. However, obtaining an unbiased estimate of this gradient for MIMO systems can be very costly. It is proposed here to compute the gradient using an identified MIMO model, which requires only one experiment with the closed-loop system regardless of the number of inputs and outputs. Nevertheless, in this case, local convergence of the algorithm is guaranteed only if an unbiased model can be identified.

In this section, the vector of controller parameters is computed by min-

imizing the cross-correlation criterion (5.52) using the stochastic approximation method. Now, having presented both the decorrelation procedure and the correlation reduction for MIMO systems, it is of interest to compare these two approaches in terms of applicability to practical control situations where one can collect a large number of data. This is discussed next.

5.3.5 Iterative solution using deterministic methods

The stochastic approximation algorithm used in the decorrelation procedure presented in Section 5.3.3 converges to ρ°, under fairly weak conditions. However, the convergence rate could be too slow for industrial applications. If one can collect a large number of data, the influence of noise on $\bar{F}(\rho_i)$ is reduced considerably, and the Newton-Raphson algorithm can be used to compute the controller parameters:

$$\rho_{i+1} = \rho_i - \hat{\bar{Q}}^{-1}(\rho_i)\bar{F}(\rho_i) \tag{5.55}$$

where the elements of the matrix $\hat{\bar{Q}}(\rho_i) = \left(\frac{\partial \hat{\bar{F}}(\rho)}{\partial \rho}\Big|_{\rho_i} \right)$ are:

$$\hat{\bar{Q}}^{K_{jk}}_{K_{mn}}(\rho_i) = \frac{1}{N}\sum_{t=1}^{N} \frac{\partial \hat{y}_j(\rho_i, t)}{\partial \rho_{K_{mn}}} \zeta^T_{K_{jk}}(t). \tag{5.56}$$

The derivatives $\frac{\partial \hat{y}_j(\rho_i,t)}{\partial \rho_{K_{mn}}}$ can be estimated using (5.20), where the transfer function matrix G is typically unknown but can be identified and replaced by its estimate $\hat{G}$. Finally, the estimate $\hat{\mathcal{S}}(\rho_i)$ is calculated using $\hat{G}$ and the current value of the controller $K(\rho_i)$.

Similarly, in the case of correlation reduction, for N sufficiently large, the criterion (5.52) can be considered as deterministic and minimized using the much faster Gauss-Newton iterative algorithm:

$$\rho_{i+1} = \rho_i - H_F(\rho_i)^{-1}\hat{\bar{Q}}(\rho_i)\bar{F}(\rho_i) \tag{5.57}$$

where $H_F(\rho_i)$ is chosen as:

$$H_F(\rho_i) = \hat{\bar{Q}}(\rho_i)\left(\hat{\bar{Q}}(\rho_i)\right)^T \tag{5.58}$$

Observe that the Jacobian estimate $\hat{\bar{Q}}(\rho_i)$ is asymptotically unaffected by noise since the noisy part of $\frac{\partial \hat{y}_j(\rho_i,t)}{\partial \rho_{K_{mn}}}$ is not correlated with $\zeta^T_{K_{jk}}(t)$. However, it is sensitive to modelling errors.

Remark: To tune the decoupler $K_{jk}(\rho)$ by a method that minimizes the 2-norm of the closed-loop output error (such as IFT), it is necessary to excite the component j of the reference signal $r(t)$ while keeping the other components equal to zero and then minimize the 2-norm of $y_j(\rho,t)$. For MIMO systems with a large number of inputs and outputs, this requires a large number of experiments per iteration to tune all decouplers $K_{jk}(\rho)$, $j \neq k$. In contrast, with both decorrelation procedure and correlation reduction, the tuning of all controllers $K_{jk}(\rho)$ is possible with only one experiment per iteration.

5.4 Simulation Results

Two simulation studies are presented in this section. In the first study, the basic features of the decorrelation procedure and correlation-reduction method are investigated, while the second study compares the correlation-reduction method to IFT for MIMO systems. Note that IFT minimizes the sum of squares of the output error:

$$SSOE = \frac{1}{N}\sum_{t=1}^{N} \varepsilon^T_{oe}(\rho,t)\varepsilon_{oe}(\rho,t). \tag{5.59}$$

5.4.1 Decorrelation procedure vs. correlation reduction

Consider the following discrete-time multivariable plant:

$$G(q^{-1}) = \begin{pmatrix} \frac{0.09516q^{-1}}{1-0.9048q^{-1}} & \frac{0.03807q^{-1}}{1-0.9048q^{-1}} \\ \frac{-0.02974q^{-1}}{1-0.9048q^{-1}} & \frac{0.04758q^{-1}}{1-0.9048q^{-1}} \end{pmatrix} \tag{5.60}$$

and let the initial controller for this plant be:

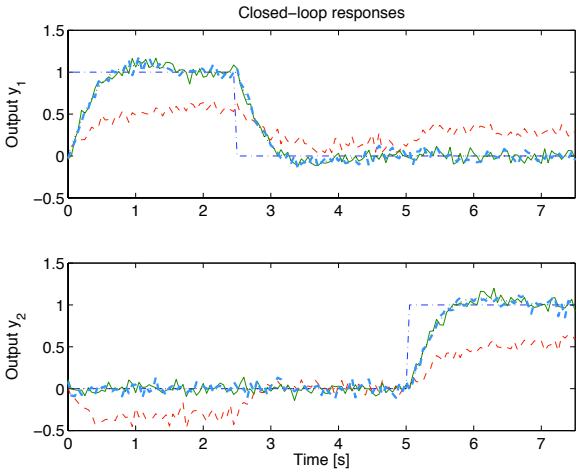

Figure 5.3: Decorrelation procedure vs. correlation reduction. Reference signals (dash-dot) and desired responses (dotted). Achieved responses: the initial controller (dashed), final controller obtained by decorrelation procedure (thin solid line) and final controller obtained by correlation reduction (thick solid line). The references are changed in a step-like manner at 0 and 2.5s (for r_1) and 5s (for r_2).

$$K_0 = \begin{pmatrix} \frac{1-0.99q^{-1}}{1-q^{-1}} & \frac{0.1-0.099q^{-1}}{1-q^{-1}} \\ -\frac{1-0.99q^{-1}}{1-q^{-1}} & \frac{1-0.99q^{-1}}{1-q^{-1}} \end{pmatrix} \tag{5.61}$$

The output of the plant is perturbed by a zero-mean, stationary, white Gaussian sequence $v(t)$ with variance $0.05I$. The reference signals are given in Figure 5.3 (dash-dotted line). The parameters of the controllers $K_{jj}, j = 1, 2$ are tuned to provide the desired closed-loop response with the natural frequency of $3rad/s$ and damping factor of 0.7, while the parameters of $K_{jk}, j \neq k$ are tuned for decoupling. Hence, the corresponding reference model reads:

$$M_{d_1} = \begin{pmatrix} \frac{0.1148q^{-1}-0.0942q^{-2}}{1-1.79q^{-1}+0.8106q^{-2}} & 0 \\ 0 & \frac{0.1148q^{-1}-0.0942q^{-2}}{1-1.79q^{-1}+0.8106q^{-2}} \end{pmatrix} \tag{5.62}$$

The instrumental variables for the decorrelation procedure are computed

using the following Laguerre basis functions:

$$\mathcal{F}_l(q^{-1}) = \left(\frac{\sqrt{1-\xi^2}}{1-\xi q^{-1}}\right)\left(\frac{q^{-1}-\xi}{1-\xi q^{-1}}\right)^l \tag{5.63}$$

where $\xi = 0.895$ is chosen to approximately reflect the closed-loop dynamics, and the model order $l = 2$. The weighting coefficients $h^l_{K_{jk}}$ are obtained by solving the feasibility problem

$$\hat{Q}(\rho^\circ, h^l_{K_{jk}}) > I \tag{5.64}$$

where $\hat{Q}(\rho^\circ, h^l_{K_{jk}})$ is estimated as explained in Section 5.3.3. In the right-hand side of inequality (5.64) the identity matrix I is used instead 0 to ensure the positive definiteness of $Q(\rho^\circ, h^l_{K_{jk}})$. This safety margin is introduced to compensate for differences between $Q(\rho^\circ, h^l_{K_{jk}})$ and its estimate $\hat{Q}(\rho^\circ, h^l_{K_{jk}})$. The following values for the coefficients $h^l_{K_{jk}}$ are obtained using Matlab LMI Control Toolbox: $h^0_{K_{11}} = 200.0328$, $h^1_{K_{11}} = -5.5225$, $h^0_{K_{12}} = 107.4611$, $h^1_{K_{12}} = -352.1068$, $h^0_{K_{21}} = 226.8947$, $h^1_{K_{21}} = -85.2721$, $h^0_{K_{22}} = 234.8072$ and $h^1_{K_{22}} = -371.1253$.

To compare the two CbT methods, the tuning is carried out in 6 iterations, with one experiment per iteration and each experiment is performed with a different realization of the noise. The resulting responses obtained with the initial controller (dashed line), the controller tuned by decorrelation procedure (thin solid line) and that tuned by correlation reduction method (thick solid line) are shown in Fig. 5.3. Both tuned controllers allow following the desired response (dotted line) up to the effect of noise. Observe also that both resulting closed-loop systems are diagonalized. The results are summarized in Table 5.1. Note that the correlation indices are reduced in both cases by 99%, while $SSOE$ index is reduced by 97%.

5.4.2 Correlation-reduction CbT vs. IFT

The aim is to tune a multivariable PI controller for a LV100 gas turbine engine [87]. The simulation conditions are taken from [30]. The plant is represented by a continuous-time state-space model with five states, two inputs and two outputs. The model is discretized using Tustin approximation

Table 5.1: Comparison of CbT variants. The index $||F(\rho_i)||_2$ denotes the 2-norm of $F(\rho_i)$

Iter-	Decorrelation Procedure		Correlation Reduction	
ation	$\|\|F(\rho_i)\|\|_2$	$SSOE$	$J_u(\rho_i)$	$SSOE$
$i=0$	28770.2	34.2411	138.3408	34.2411
$i=6$	335.0878	0.9284	1.2709	0.9352

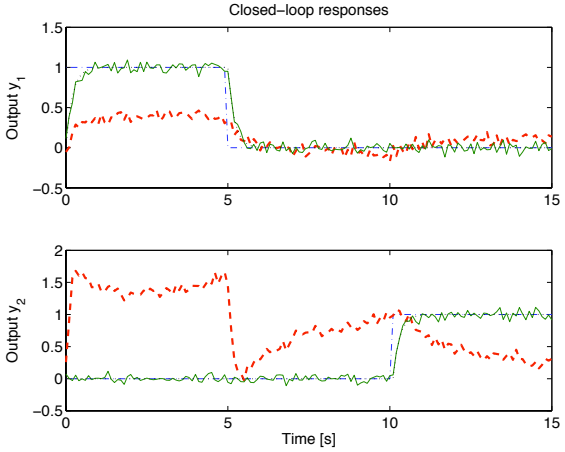

Figure 5.4: Correlation-reduction CbT: Closed-loop responses in a noisy environment. Reference signals (dash-dot), desired responses (dotted), achieved responses with the initial controller (dashed) and final controller (solid). The references are changed in a step-like manner at 0 and 5s (for r_1) and 10s (for r_2).

with the sampling period $T_s = 0.1s$. Each experiment is performed with a different realization of the measurement noise $v(t)$ that is generated as a zero-mean, stationary, white Gaussian sequence with variance $0.0025I$.

The same initial controller K_0 given in (5.61) is used. The responses obtained with this controller are plotted in Fig. 5.4 (dashed line). Eight numerator coefficients are tuned (two for each transfer function element), while the denominators are kept fixed at $1 - q^{-1}$. The following reference model is specified:

$$M_{d_2} = \begin{pmatrix} \frac{0.4q^{-1}}{1-0.6q^{-1}} & 0 \\ 0 & \frac{0.4q^{-1}}{1-0.6q^{-1}} \end{pmatrix} \tag{5.65}$$

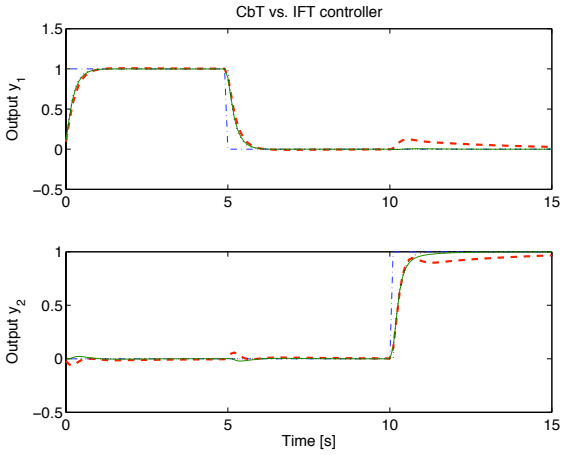

Figure 5.5: Correlation-reduction CbT vs. IFT controller in a noise-free context. Reference signals (dash-dot), desired responses (dotted), closed-loop response with the CbT controller (solid) and IFT controller (dashed)

and the controller parameters are calculated according to (5.57).

A discrete-time state-space model $\hat{G}$ with three states is identified using the acquired closed-loop data. After eight iterations, this procedure provides the closed-loop response shown in Fig. 5.4. A comparison with the desired response (dotted line) shows that the two curves are nearly superposed except for the effect of noise. In addition, changes in the reference signals $r_1(t)$ and $r_2(t)$ do not induce any visible change on the outputs $y_2(t)$ and $y_1(t)$, respectively. In other words, the closed-loop system is almost fully diagonalized. The value of the tuning criterion is reduced by more than 99%. The resulting CbT controller is:

$$K_{CbT} = \begin{pmatrix} \frac{0.3636-0.09866q^{-1}}{1-q^{-1}} & \frac{0.3653-0.2691q^{-1}}{1-q^{-1}} \\ \frac{18.69-18.16q^{-1}}{1-q^{-1}} & \frac{-3.453+2.652q^{-1}}{1-q^{-1}} \end{pmatrix} \tag{5.66}$$

In order to compare the IFT controller provided in [30],

$$K_{IFT} = \begin{pmatrix} \frac{0.248-0.03q^{-1}}{1-q^{-1}} & \frac{0.38-0.199q^{-1}}{1-q^{-1}} \\ \frac{16.47-15.91q^{-1}}{1-q^{-1}} & \frac{0.063+0.054q^{-1}}{1-q^{-1}} \end{pmatrix} \tag{5.67}$$

with the CbT controller, an experiment is performed with the simulation conditions mentioned above. The observed $SSOE$ with the CbT controller is 0.0050, while that with the IFT controller is 0.0082. Since IFT contains a noise-rejection objective, while CbT does not, one would expect IFT to perform better in a noisy situation. However, $SSOE$ obtained with CbT is smaller. The IFT controller did not succeed in (i) fully decoupling the closed-loop system, and (ii) completely satisfying the model-following specification. This indicates that IFT algorithm got stuck in a local minimum. To illustrate this, an additional experiment without noise is performed. The results are shown in Fig. 5.5. The closed-loop response obtained with the CbT controller follows almost perfectly the desired response. In contrast, the closed-loop response obtained with the IFT controller shows some discrepancy in the last 5 seconds of the response. In addition, the influence of the change in the reference signal $r_1(t)$ at the instants 0s and 5s is visible on $y_2(t)$.

In terms of experimental cost, the IFT controller is obtained after 6 iterations (and a total of 30 experiments) compared to 8 iterations (and a total of 8 experiments) with the CbT controller.

5.5 Conclusion

In this chapter, the parameters of a linear time-invariant multivariable controller have been tuned by either solving the correlation equation or minimizing a cross-correlation function. The diagonal controllers are tuned to fulfill the desired output specifications, while the off-diagonal controllers are tuned to decouple the various outputs. In contrast to the approaches where decouplers and diagonal controllers are designed sequentially, the design of decouplers and controllers is done *simultaneously* here. The tuning of all decouplers and controllers can be made by performing only one experiment per iteration regardless of the number of inputs and outputs since all reference signals can be excited simultaneously. This feature represents a major advantage over other data-driven methods such as IFT, where the required number of experiments per iteration increases with the number of inputs and outputs.

The variance of the estimated controller parameters has been compared

for the two cases of simultaneous and sequential excitations. This analysis shows that, due to the fact that decoupling is imposed as a design criterion, simultaneous excitation of all references has a negative impact on the variance of the estimated controller parameters. More accurate estimates require performing n_y experiments per iteration. In fact, one must choose between low experimental cost (simultaneous excitation) and better accuracy of the estimated parameters (sequential excitation). Even in the case of the sequential excitation where CbT requires n_y experiments per iteration, this method is superior in terms of experimental cost to IFT which requires $n_u n_y + 1$ experiments per iteration. The presented theoretical results have been illustrated via two simulation studies.

Chapter 6

Conclusions

6.1 Summary

This thesis presents a novel approach to data-driven controller design labelled "Correlation-based Tuning" (CbT). The underlying idea of this approach, originally intended to address the model-following problem, is to make the closed-loop output error uncorrelated with the excitation signal. Moreover, if it is not possible to decorrelate these two signals, it is proposed to reduce their cross-correlation. The argument behind introducing the correlation criterion is as follows. If the aforementioned signals are uncorrelated, then the closed-loop output error contains no part that originates from the difference between the achieved and designed closed-loop systems. In other words, these closed-loop systems match perfectly, and the closed-loop output error contains only contribution from the noise. Hence, the desired tracking performance can be perfectly met even in the presence of a considerable amount of noise.

Although CbT uses data collected in closed-loop operation to update the controller parameters, it cannot be called a "model-free" approach. For example, in order to reduce the experimental cost, a model is used for gradient computation. Note that a model can be identified from the same data used for controller tuning. This way of computing the gradient allows iterative update of the controller parameters by performing a single experiment per iteration regardless of whether a one-degree-of-freedom or a two-degree-of-freedom controller is tuned.

In the first part of the thesis, it is assumed that there exists a controller that perfectly decorrelates the closed-loop output error and the reference

signal and, furthermore, this controller is in the selected controller class. The features of the decorrelation procedure are investigated for two cases. In the first case, the controller parameters are updated using the Robbins-Monro stochastic approximation method, and it is shown that the algorithm converges to the solution of the correlation equation assuming an appropriate choice of the instrumental variables. Convergence conditions are derived and the accuracy of the updated controller parameters is studied. In the second case, the controller parameters are updated using the deterministic Newton-Raphson method and here the resulting parameter estimates converge toward a region around the decorrelating controller instead of to an unique solution. An asymptotic expression that characterizes this region is given and subsequently used to derive a stopping condition. Excellent performance has been obtained in both simulation and real-time application to a magnetic suspension system.

The correlation-reduction method is presented in the second part of the thesis. Instead of seeking the roots of the correlation equation, the controller parameters are updated by minimizing the two-norm of the cross-correlation function. A frequency-domain analysis of the criterion shows that the achieved closed-loop system approaches the desired one in the two-norm sense. This analysis leads to the formulation of a generalized correlation criterion allowing handling the mixed sensitivity specifications. The possibility of using deterministic algorithms for the correlation-reduction method has also been investigated, and a stopping condition has been introduced. Furthermore, it has been shown that, in the case where the disturbance signal can be measured or it is possible to inject a test disturbance signal, CbT can be adapted to tune the controllers for disturbance rejection. This adaptation is applied to solve a benchmark problem on the design and optimization of restricted-complexity controllers. Very satisfactory results have been obtained. Finally, a very simple choice of the instrumental variables is proposed.

The third part of the thesis treats the possibility of tuning linear time-invariant multivariable controllers using both the decorrelation procedure and the correlation-reduction methods. The CbT criterion allows one to tune simultaneously some elements of the controller transfer function to be decouplers, while the others are tuned to provide good tracking per-

formance. Simultaneous excitation of all reference inputs results in low experimental cost because it is possible to use one experiment per iteration regardless of the number of inputs and outputs of the system. On the other hand, the analysis performed in Section 5 indicates that this way of exciting the reference input has a negative effect on the accuracy of the estimated controller parameters. Therefore, one has to choose whether it is more important to have reduced experimental costs by performing a single experiment per iteration, or it is better to have more accurate controller parameters by exciting one-by-one the reference inputs.

From a practical point of view, the CbT scheme is appealing to control engineers. It works in closed loop and requires a single experiment per iteration. The excitation signal can be constructed as a small variation around the normal operating signal. Although CbT is a time-domain approach, it is possible to handle frequency-domain specifications as well. If needed, certain frequency regions can be emphasized by filtering either the instrumental variables or the reference signals. On the downside, this approach requires a certain engineering effort, in particular in designing the achievable designed closed-loop system.

Last, but not least, this method works well for all types of rational controllers including PID controllers, which makes it well suited for fine-tuning of the already installed industrial loops.

6.2 Perspectives

The concepts presented in this thesis can be extended to several independent research directions. These are briefly presented below.

- Although the cross-correlation function and the correlation equation are used under the assumption that a linear time-invariant (LTI) plant is controlled by an LTI controller, these two approaches are by no means limited to only these classes of systems and controllers. That is, the correlation approach can be used within the context of nonlinear control design as well, which represents a very interesting research area.

- The proposed CbT approach can be used to address the control of slowly time-varying systems. For these systems, the controller param-

eters can be updated in two ways. One possibility is to perform the update recursively. In this case, appropriate recursive on-line algorithms need to be developed. Another possibility is to use again the iterative procedure. However, in this case, the number of data collected in each iteration should be small enough for the process variations to be negligible.

- One of the main features of the correlation approach is that the controller parameters are not affected by measurement noise. Hence, the proposed decorrelation and correlation reduction criteria can be used with methods that update the parameters in high-noise setting. For example, the correlation approach could be used judiciously with the simultaneous perturbation stochastic approximation (SPSA) method. Other examples include iterative learning control (ILC) and virtual reference feedback tuning (VRFT).

- CbT uses the fact that the closed-loop output error contains two parts: the correlated and uncorrelated parts with respect to the excitation signal. The controller tuning objective can be defined as the minimization of the infinity norm of the correlated part. This way, robustness issues of the closed-loop system can be addressed.

- When dealing with a two-degree-of-freedom controller, it may be useful to separately tune the feedback and feedforward controllers. The feedback controller may be tuned first to satisfy a certain performance with respect to disturbance rejection (to obtain some desired sensitivity functions), while the feedforward part is tuned to satisfy some desired tracking performance.

Bibliography

[1] G. W. Anderson, J. A. Aseltine, A. K. Mancini, and C. W. Sarture. A self adjusting system for optimum dynamic performance. *1958 IRE International Convention Record*, 4:182–190, 1958.

[2] K. J. Åström and B. Wittenmark. *Adaptive Control*. Addison-Wesley, 1989.

[3] K.J. Åström and T. Bohlin. Numerical identification of linear dynamic systems from normal operating records. In *Proc. IFAC Symposium on Self-Adaptive Systems*, Teddington, UK, 1965.

[4] K.J. Åström and T. Hägglund. The Future of PID Control. *Control Engineering Practice*, 9(11):1163–1175, 2001.

[5] J.R. Blum. Multidimensional stochastic approximation method. *Ann. Math. Stat.*, 25:737–744, 1954.

[6] H. W. Bode. Feedback amplifier design. *Bell System Technical Journal*, 19:42, 1940.

[7] S. Boyd and L. Vandenberghe. *Convex Optimization*. Cambridge University Press, Cambridge, UK, 2004.

[8] T. F. Brozenec, T. C. Tsao, and M. G. Safonov. Controller validation. *International Journal of Adaptive Control and Signal Processing*, 15:431–444, 2001.

[9] M. C. Campi, A. Lecchini, and S. M. Savaresi. Virtual reference feedback tuning: a direct method for the design of feedback controllers. *Automatica*, 38(8):1337–1346, 2002.

[10] C. Commault, J. Descusse, J. M. Dion, J. F. Lafay, and M. Malabre. New decoupling invariants: The essential orders. *International Journal of Control*, 44(3):689–700, 1986.

[11] J. Descusse and J. M. Dion. On the structure at infinity of linear square decoupled systems. *IEEE Transactions on Automatic Control*, 27(4):971–974, 1982.

[12] P. L. Falb and W. A. Wolovich. Decoupling in design and synthesis of multivariable control systems. *IEEE Transactions on Automatic Control*, AC-12:651–659, 1967.

[13] U. Forssell and L. Ljung. Some results on optimal experiment design. *Automatica*, 36:749–756, 2000.

[14] D. Gabor, W. P. L. Wilby, and R. Woodcock. A universal nonlinear filter, predictor and simulator which optimizes itself by a learning process. *Proc. IEE*, 108(B):422–438, 1961.

[15] L. Gerencsér, Z. Vágó, and H. Hjalmarsson. Randomization methods in optimization and adaptive control. In B. Pasik-Duncan, editor, *Lecture Notes in Control and Information Sciences*, volume 280/2002, pages 137–154. Springer-Verlag, Berlin, Germany, 2002.

[16] L. Gerencsér, Z. Vágó, and H. Hjalmarsson. Randomized iterative feedback tuning. In *15th IFAC World Congress*, Barcelona, Spain, July 2002.

[17] M. Gevers. Identification for control: From the early achievements to the revival of experiment design. *European Journal of Control*, 11(4–5):335–352, 2005.

[18] M. Gevers, X. Bombois, B. Codrons, G. Scorletti, and B.D.O. Anderson. Model validation for control and controller validation in a prediction error identification framework - Part I: theory. *Automatica*, 39(3):403–415, March 2003.

[19] M. Gevers and L. Ljung. Optimal experiment designs with respect to the intended model application. *Automatica*, 22:543–554, 1986.

[20] M. Gevers, L. Ljung, and P.M.J. Van den Hof. Asymptotic variance expressions for closed-loop identification. *Automatica*, 37(5):781–786, May 2001.

[21] M. Gevers, L. Mišković, D. Bonvin, and A. Karimi. Identification of a two-input system: Variance analysis. In *16th IFAC World Congress*, Prague, Czech Republic, July 2005.

[22] M. Gevers, L. Mišković, D. Bonvin, and A. Karimi. Identification of multi-input systems: Variance analysis and input design issues. *submitted to Automatica*, 2005.

[23] G. O. Guardabassi and S. M. Savaresi. Virtual reference direct design method: an off-line approach to data-based control system design. *IEEE Trans. on Automatic Control*, 45(5):954–959, 2000.

[24] S. Gunnarsson, V. Collignon, and O. Rousseaux. Tuning of a decoupling controller for a 2×2 system using iterative feedback tuning. *Control Engineering Practice*, 11(9):1035–1041, 2003.

[25] C. C. Hang, C. C. Lim, and S. H. Soon. A new PID auto-tuner design based on correlation technique. In *2nd Multinational Instrumentation Conference*, pages 844–856, Beijing, China, April 1986.

[26] R. Hildebrand, A. Lecchini, G. Solari, and M. Gevers. A convergence theorem for iterative feedback tuning. Technical Report 2003/17, CESAME, Université Catholique de Louvain, Louvain-la-Neuve, Belgium, 2003.

[27] H. Hjalmarsson. Control of nonlinear systems using iterative feedback tuning. In *Proc. American Control Conference 98*, volume 5, pages 2083–2087, Philadelphia, 1998.

[28] H. Hjalmarsson. Performance analysis of iterative feedback tuning. Technical report, Dept. of Signals, Sensors and Systems, Royal Institute of Technology, Stockholm, Sweden, 1998.

[29] H. Hjalmarsson. Efficient tuning of linear multivariable controllers using Iterative Feedback Tuning. *International Journal of Adaptive Control*, 13:553–572, November 1999.

[30] H. Hjalmarsson. Efficient tuning of linear multivariable controllers using iterative feedback tuning. *International Journal of Adaptive Control and Signal Processing*, 13:553–572, 1999.

[31] H. Hjalmarsson. Iterative feedback tuning – an overview. *International Journal of Adaptive Control and Signal Processing*, 16:373–395, 2002.

[32] H. Hjalmarsson. From experiment design to closed-loop control. *Automatica*, 41:393–438, 2005.

[33] H. Hjalmarsson, M. Gevers, and F. De Bruyne. For model-based control design, closed-loop identification gives better performance. *Automatica*, 32:1659–1673, 1996.

[34] H. Hjalmarsson, M. Gevers, S. Gunnarsson, and O. Lequin. Iterative feedback tuning: Theory and application. *IEEE Control Systems Magazine*, pages 26–41, 1998.

[35] H. Hjalmarsson, S. Gunnarsson, and M. Gevers. A convergent iterative restricted complexity control design scheme. In *33rd IEEE-CDC*, volume 2, pages 1735–1740, December 1994.

[36] H. Hjalmarsson, S. Gunnarsson, and M. Gevers. Optimality and suboptimality of iterative identification and control design schemes. In *Proc. American Control Conference 95*, volume 4, pages 2559–2563, Seattle, Washington, 1995.

[37] R. A. Horn and C. R. Johnson. *Matrix Analysis*. Cambrigde University Press, Cambridge, 1990.

[38] H. Jansson, H. Hjalmarsson, and A. Hansson. On methods for gradient estimation in IFT for MIMO systems. In *15th IFAC World Congress*, Barcelona, Spain, July 2002.

[39] R.E. Kalman. Contributions to the theory of optimal control. *Boletin de la Sociedad Matematica Mexicana*, 5:102–119, 1960.

[40] R.E. Kalman. A new approach to linear filtering and prediction problems. *Transactions ASME, Series D, J. Basic Eng.*, 82:34–45, 1960.

[41] L. C. Kammer, R. R. Bitmead, and P. L. Bartlett. Direct iterative tuning via spectral analysis. *Automatica*, 36(9):1301–1307, 2000.

[42] A. Karimi, L. Mišković, and D. Bonvin. Convergence analysis of an iterative correlation-based controller tuning method. In *15th IFAC World Congress*, Barcelona, Spain, July 2002.

[43] A. Karimi, L. Mišković, and D. Bonvin. Iterative correlation-based controller tuning: Frequency-domain analysis. In *41st IEEE-CDC*, Las Vegas, USA, December 2002.

[44] A. Karimi, L. Mišković, and D. Bonvin. Iterative correlation-based controller tuning with application to a magnetic suspension system. *Control Engineering Practice*, 11(9):1069–1078, 2003.

[45] A. Karimi, L. Mišković, and D. Bonvin. Iterative correlation-based controller tuning. *International Journal of Adaptive Control and Signal Processing*, 18:645–664, 2004.

[46] Y. Kawamura. Direct synthesis of LQ regulator from inner products of response signals. *Proc. 11th IFAC Symp. on System Identification*, 4:1717–1722, 1997.

[47] Y. Kawamura. Direct construction of LQ regulator based on orthogonalization of signals: Dynamical output feedback. *Systems & Control Letters*, 34(1):1–9, 1998.

[48] C. T. Kelley. *Iterative Methods for Linear and Nonlinear Equations*. SIAM, Philadelphia, USA, 1995.

[49] C. T. Kelley. *Iterative Methods for Optimization*. SIAM, Philadelphia, USA, 1999.

[50] R. L. Kosut. Iterative unfalsified adaptive control: analysis of the disturbance-free case. In *American Control Conference*, pages 566–570, San Diego, California, June 1999.

[51] I. D. Landau, A. Karimi, L. Mišković, and H. Prochazka. Control of an active suspension system as a benchmark for design and optimisation of restricted-complexity controllers. *European Journal of Control*, 9(1):3–13, 2003.

[52] F. L. Lewis. *Applied Optimal Control & Estimation: Digital Design & Implementation*. Prentice Hall, Englewood Cliffs, New Jersey 07632, 1992.

[53] L. Ljung. Asymptotic variances of transfer function estimates obtained by the instrumental variable method. In *7th IFAC Symp. on Identification and System Parameter Estimation*, pages 1341–1344, York, UK, 1985.

[54] L. Ljung. *System Identification: Theory for the User, 2nd Edition*. Prentice-Hall, Englewood Cliffs, NJ, 1999.

[55] R. J. McGrath, V. Rajaraman, and V. C. Rideout. A parameter pertubation adaptive control system. *IRE Transactions on Automatic Control*, AC-6:154–161, 1961.

[56] L. Mišković, D. Bonvin, A. Karimi, and M. Gevers. Correlation-based tuning of linear multivariable decoupling controller. In *CDC-ECC 2005*, Sevilla, Spain, Decembre 2005.

[57] L. Mišković, A. Karimi, and D. Bonvin. Correlation-based tuning of a restricted-complexity controller for an active suspension system. *European Journal of Control*, 9(1):77–83, 2003.

[58] L. Mišković, A. Karimi, and D. Bonvin. Iterative controller tuning by minimization of a generalized decorrelation criterion. In *13th IFAC Symp. on System identification*, pages 1177–1182, Rotterdam, The Netherlands, August 2003.

[59] L. Mišković, A. Karimi, and D. Bonvin. Accuracy aspects of iterative correlation-based controller tuning. In *American Control Conference 2004*, pages 4529–4534, Boston, USA, July 2004.

[60] L. Mišković, A. Karimi, D. Bonvin, and M. Gevers. Data-driven correlation-based tuning of decoupling multivariable controllers. *submitted to Automatica*, 2006.

[61] L. Mišković, A. Karimi, D. Bonvin, and M. Gevers. Direct closed-loop identification of 2×2 systems: Variance analysis. In *14th IFAC Symp. on System identification*, Newcastle, Australia, March 2006.

[62] L. Mišković, A. Karimi, D. Bonvin, and M. Gevers. On the input design for data-driven correlation-based tuning of multivariable controllers. In *14th IFAC Symp. on System identification*, Newcastle, Australia, March 2006.

[63] K. S. Narendra and L.E. McBride. Multiparameter self-optimizing systems using correlation techniques. *IEEE Trans. Automatic Control*, pages 31–38, 1964.

[64] K. S. Narendra and D.N. Streeter. An adaptive procedure for controlling undefined linear processes. *IEEE Trans. Automatic Control*, pages 545–548, October 1964.

[65] M. B. Nevelson and R. Z. Khasminskii. Stochastic approximation and recursive estimation. In B. Silver, editor, *Translations of Mathematical Mongraphs*, volume 47. American Mathematical Society, Providence, Rhode Island, 1973.

[66] B. Ninness and F. Gustafsson. A unifying construction of orthonormal bases for system identification. *IEEE Transactions on Automatic Control*, 42(4):515–521, 1997.

[67] H. Nyquist. Regeneration theory. *Bell System Technical Journal*, 11:126, 1932.

[68] B. A. Ogunnaike. A contemporary industrial perspective on process control theory and practice. *Annual Reviews in Control*, 20:1–8, 1996.

[69] P. V. Osburn, H. P. Whitaker, and A. Kezer. New developments in the design of model reference adaptive control systems. *Institute of Aerospace Sciences*, No. 61-39, 1961.

[70] H. Robbins and S. Monro. A stochastic approximation method. *Ann. Math. Stat.*, 22:400–407, 1951.

[71] M. G. Safonov and T-C. Tsao. The unfalsified control concept and learning. *IEEE Trans. on Automatic Control*, 42(6):843–847, 1997.

[72] R. R. Schrama. Accurate identification for control: The necessity of an iterative scheme. *IEEE Transactions on Automatic Control*, 37(7):991–994, July 1990.

[73] S. Skogestad and I. Postlethwaite. *Multivariable Feedback Control - Analysis and Design*. John Wiley & Sons, Chichester, England, 1996.

[74] T. Söderström and P. Stoica. Instrumental variable methods for system identification. In A. V. Balakrishnan and M. Thoma, editors, *Lecture Notes in Control and Information Science*. Springer-Verlag, Berlin, 1983.

[75] T. Söderström and P. Stoica. *System Identification*. Prentice-Hall, U.K., 1989.

[76] G. Solari and M. Gevers. Unbiased estimation of the hessian for iterative feedback tuning (ift). In *CD-ROM Proc. of 43nd IEEE Conference on Decision and Control*, pages 1759–1760, Atlantis, Bahamas, USA, December 2004.

[77] J. C. Spall. Multivariate stochastic approximation using a simultaneous perturbation stochastic approximation. *IEEE Trans. on Automatic Control*, 37(3):332–341, 1992.

[78] J. C. Spall and J. A. Cristion. Model-free control of nonlinear stochastic systems with discrete-time measurements. *IEEE Trans. on Automatic Control*, 43(9):1198–1210, 1998.

[79] Benchmark Specifications. Special Issue of European Journal of Control on "Design and optimization of restricted-complexity controllers", Available: http://iawww.epfl.ch/News/EJC_Benchmark/index.html.

[80] A. I. Talkin. Adaptive servo tracking. *IRE Transactions on Automatic Control*, AC-6:167–172, 1961.

[81] E. Trulsson and L. Ljung. Adaptive control based on explicit criterion minimization. *Automatica*, 21(4):385–399, 1985.

[82] P.M.J. Van den Hof and R.J.P. Schrama. Identification and control - closed-loop issues. *Automatica*, 31:1751–1770, December 1995.

[83] B. L. van der Waerden. *Algebra*. Springer-Verlag, New York, vii edition, 1991.

[84] A. Veres and D. Wall. *Synergy and Duality of Identification and Control*. Taylor and Francis, London, UK, 2000.

[85] B. Wahlberg and L. Ljung. Design variables for bias distribution in transfer function estimation. *IEEE Trans. Automatic Control*, AC-31:134–144, 1986.

[86] M. T. Wasan. On stochastic approximation processes. In *Annals of Mathematical Statistics*, volume 36(3). Inst. Mathematical Statistics, Hayward, California, 1965.

[87] M. Yeddanapudi and A. F. Potvin. *Nonlinear Control Design Blockset: User's Guide*. The Mathworks Inc., Natick, MA, 1997.

[88] Z. D. Yuan and L. Ljung. Black-box identification of multi-variable transfer functions – asymptotic properties and optimal input design. *International Journal of Control*, 40(2):233–256, 1984.

[89] K. Zhou and J. C. Doyle. *Essentials of robust control*. Prentice-Hall, N.Y., 1998.

Curriculum Vitae and List of Publications

Ljubiša Mišković was born in Bor, Serbia and Montenegro. He received his B.Sc. and M.Sc. degrees in Electrical Engineering from the University of Belgrade, Serbia and Montenegro in 1996 and 2000, respectively. In 2000 he joined the Laboratory d'Automatique (LA) at the School of Engineering Sciences & Technology, EPFL. He participated in the Swiss National Science Foundation research project called Controller Design based on Decorrelation, where he made contributions in the field of data-driven control system design. His current research interests include system identification, identification for control, data-based control system design, process control, stochastic processes and estimation theory.

Publications

Journal Articles

1. Mišković, L., A. Karimi, D. Bonvin and M. Gevers, "Data-driven correlation-based tuning of decoupling multivariable controllers", submitted to *Automatica*, 2006.

2. Gevers, M., L. Mišković, A. Karimi and D. Bonvin, "Identification of multi-input systems: variance analysis and input design issues", *Automatica*, Vol. 42, No. 4, pp. 559-572, 2006.

3. Karimi, A., L. Mišković and D. Bonvin, "Iterative correlation-based controller tuning ", *International Journal of Adaptive Control and Signal Processing*, Vol. 18, No. 8, pp. 645–664, 2004.

4. Mišković, L., A. Karimi and D. Bonvin, "Correlation-based tuning of a

restricted-complexity controller for an active suspension system", *European Journal of Control*, Vol. 9, No. 1, pp. 77–83, 2003.

5. Landau, I. D., A. Karimi, L. Mišković and H. Prochazka, "Control for an active suspension system as a benchmark for design and optimisation of restricted-complexity controllers", *European Journal of Control*, Vol. 9, No. 1, pp. 3–12, 2003.

6. Karimi, A., L. Mišković and D. Bonvin, "Iterative correlation-based controller tuning with application to a magnetic suspension system ", *Control Engineering Practice*, Vol. 11, No. 9, pp. 1069–1078, 2003.

7. Mišković, L., Ž. M. Djurović and B. D. Kovačević, Application of the Minimum State Error Variance Approach to Nonlinear System Control, *International Journal of Systems Science*, Vol. 33, No. 5, pp. 359-368, 2002

8. Mišković, L., Ž. M. Djurović and B. D. Kovačević, Nonlinear System Control Using the MSEV Approach, *Control and Intelligent Systems*, Vol. 28, No. 3, pp. 110-117, 2000.

Conference papers

1. Mišković, L., A. Karimi, D. Bonvin, and M. Gevers. "Direct closed-loop identification of 2×2 systems: Variance analysis", In *14th IFAC Symp. on System identification*, Newcastle, Australia, March 2006.

2. Mišković, L., A. Karimi, D. Bonvin, and M. Gevers, "On the input design for data-driven correlation-based tuning of multivariable controllers", In *14th IFAC Symp. on System identification*, Newcastle, Australia, March 2006.

3. Mišković, L., A. Karimi, D. Bonvin and M. Gevers, "Correlation-based tuning of linear multivariable decoupling controller", *CDC-ECC Conference*, Seville, Spain, December 2005.

4. Gevers, M., L. Mišković, A. Karimi and D. Bonvin, "Identification of a two-input system: variance analysis", In *XVI IFAC Congress*, Prague, Czech Republic, July 2005.

5. Mišković, L., A. Karimi, and D. Bonvin,"Accuracy aspects of iterative correlation-based controller tuning", In *American Control Conference 2004*, Boston, USA, June 2004.

6. Mišković, L., A. Karimi, and D. Bonvin,'Iterative controller tuning by minimization of a generalized decorrelation criterion", In *XIII IFAC Symposium on System Identification*, Rotterdam, The Netherlands, pp. 1177-1182, August 2003.

7. Mišković, L., A. Karimi and D. Bonvin,"Correlation-based tuning of a restricted-complexity controller for an active suspension system", *International Workshop on Design and Optimisation of restricted Complexity Controllers*, Grenoble, France, pp. 138–144, January 2003.

8. Landau, I. D., A. Karimi, L. Mišković and H. Prochazka,"Design and optimization of restricted complexity controllers benchmark", *International Workshop on Design and Optimisation of restricted Complexity Controllers*, Grenoble, France, pp. 72–80, January 2003.

9. Karimi, A., L. Mišković and D. Bonvin,"Iterative correlation-based controller tuning: frequency domain analysis ", In *41st IEEE Conference on Decision and Control*, pp.4215–4220, Las Vegas, USA, December 2002.

10. Karimi, A., L. Mišković and D. Bonvin,"Convergence analysis of an iterative correlation-based controller tuning method ", in *XV IFAC Congress*, Barcelona, Spain, July 2002.

11. Djurović, Ž., L. Mišković and B. Kovačević,'Simulation of Air Turbulence Signal and Its Application", In *10th Mediterranean Electrotechnical Conference, MELECON 2000*, Vol. II, pp. 847–850. Cyprus, May 2000.

12. Papić, V., Ž. Djurović, L. Mišković and B. Kovačević,"Velocity tracking based on adaptive Doppler filters", In *4th International Conference on Telecommunications in Modern Satellite, Cable and Broadcasting Services*, Vol. 2, pp. 624–627, Niš, Yugoslavia, October 1999.

13. Mišković, L., Ž. M. Djurović and B.D. Kovačević, "Adaptive MSEV Control of a Nonlinear Nonstationary System" (in Serbian), *Proceedings of XLII ETRAN (Yugoslav Electronics, Communications, Computer Science, Control and Nuclear Science Association) Conference*, Vrnjacka Banja, Yugoslavia, 1998.

14. Djurović, Ž., L. Mišković and B. Kovačević,"Nonlinear Nonstationary Dynamical System Control Using LQG Strategy"(in Serbian), *Proceedings of XLII ETRAN Conference*, Vrnjacka Banja, Yugoslavia, 1998.

15. Mišković, L., and S. Stanković, "Intelligent Vehicle Highway Systems (IVHS): Platoon Control Strategy" (in Serbian), *SinfoN97 Conference*, Zlatibor, Yugoslavia, 1997 (best student paper award).